The Contribution of Syntrophic Fatty-Acid Degrading Microbial Communities to Anaerobic Digester Function and Stability

Prince Peter Mathai
Marquette University

THE CONTRIBUTION OF SYNTROPHIC FATTY-ACID DEGRADING MICROBIAL COMMUNITIES TO ANAEROBIC DIGESTER FUNCTION AND STABILITY

by

Prince Peter Mathai, B.Tech.

A Dissertation submitted to the Faculty of the Graduate School,
Marquette University,
in Partial Fulfillment of the Requirement for
the Degree of Doctor of Philosophy

Milwaukee, Wisconsin

December 2015

ABSTRACT
THE CONTRIBUTION OF SYNTROPHIC FATTY-ACID DEGRADING MICROBIAL COMMUNITIES TO ANAEROBIC DIGESTER FUNCTION AND STABILITY

Prince Peter Mathai, B.Tech.

Marquette University, 2015

Anaerobic digestion (AD), the conversion of complex organic matter to methane, occurs through a series of reactions mediated by different guilds of microorganisms. AD process imbalances, such as organic overload or high organic loading rates (OLR), can result in the accumulation of volatile fatty acids (VFA) e.g., propionate, which must be degraded to maintain stable reactor function. VFAs are metabolized by syntrophic fatty-acid degrading bacteria (SFAB) in association with methanogenic archaea (collectively, syntrophic microbial communities, SMC). Despite their indispensable role in AD, little is known about the ecology of SFAB, especially under stressed conditions. To facilitate ecological studies, four quantitative PCR assays, targeting propionate- and butyrate-degraders were developed, and applied to a variety of methanogenic environments. The highest SFAB abundance was observed in propionate enrichment cultures and anaerobic reactors. In addition, SFAB and methanogen abundance varied with reactor configuration and substrate identity. The contribution of SMC to AD function and stability was investigated in lab-scale reactors exposed to two forms of disturbance: shock overload (pulse disturbance) and increased OLR (press disturbance). SMC dynamics were linked to AD function using physicochemical and molecular techniques. The first experiment examined the effect of shock overloads on SMC structure and function. Results showed that functional resilience to the pulse disturbance in reactors was linked to the abundance of propionate-degraders and Methanosarcinaceae. Reactors with reduced numbers of these microorganisms displayed increased VFA buildup, however, there was a subsequent increase in the abundance of propionate-degraders and Methanosarcinaceae which improved the functional resilience in these reactors to the next perturbation. The second experiment examined the effect of increased OLRs on SMC structure and function. SMC decreased in abundance with increasing OLR. Prior to system collapse, a decrease in acetoclastic methanogens corresponded with an increase in syntrophic acetate oxidizers and hydrogenotrophic methanogens. In summary, this work demonstrates that an increased abundance of syntrophic fatty acid degrading microbial communities are essential in AD during stressed conditions, such as organic overload and high OLRs. These results could change how digesters are monitored and aid in the design of better anaerobic treatment processes.

ACKNOWLEDGMENTS

Prince Peter Mathai, B.Tech.

First and foremost, I would like to thank my mentor, Dr. James Maki, for his support, encouragement and incredible patience. I have learnt a lot from him and he has played a tremendous role in my growth as a scientist. He has always made time for me and has been very supportive in my research endeavors.

I am also grateful to my committee members, Dr. James Courtright, Dr. Dale Noel, Dr. Charles Wimpee, and Dr. Daniel Zitomer, for their guidance and helpful comments. I would also like to thank Dr. Krassimira Hristova for her valuable suggestions.

I would like to thank former members of the Maki lab: Dr. Rachel Morris and Keerthi Cherukuri for being wonderful colleagues, and all the undergraduates, especially, Melinda Martin, many of whom I have mentored for the past several years.

I gratefully acknowledge all faculty, staff and colleagues at the Department of Biological Sciences, especially, Deb Weaver, Kirsten Boeh, Patti Colloton, Janell Romatowski, Tom Dunk and Dan Holbus for their help. Special thanks goes to Dr. Anthony Kappell, Dr. Deepa Valsangkar and Jerrin Cherian for their friendship.

I am thankful to the current and former members of the Zitomer lab: Mike Dollhopf, Dr. Vaibhav Tale, Dr. Ujwal Bhattad, Dr. Nava Navaratnam, Dr. Ben Bocher, Kaushik Venkiteshwaran and Matt Seib for their help and collaboration.

No words can express my heartfelt gratitude towards my parents for their steadfast love and continuous support. They have always been, and will continue to be, my source of inspiration. Thank you for always being there for me. This dissertation is dedicated to both of you. I am also thankful to my sister and brother for their support.

TABLE OF CONTENTS

LIST OF TABLES

LIST OF FIGURES

ABBREVIATIONS

AD: Anaerobic digestion

COD: Chemical oxygen demand

CSTR: Continuously stirred tank reactor

DGGE: Denaturing gradient gel electrophoresis

FISH: Fluorescence *in-situ* hybridization

HRT: Hydraulic retention time

LB: Luria broth

MBT: Methanobacteriales

MMB: Methanomicrobiales

MMC: Methylmalonyl-CoA

MSC: Methanosarcinaceae

MST: Methanosaetaceae

OLR: Organic loading rate

OTU: Operational taxonomic unit

PCR: Polymerase chain reaction

PEL: *Pelotomaculum*

qPCR: Quantitative polymerase chain reaction

RDP: Ribosomal database project

SBC: *Syntrophobacter*

SCOD: Soluble chemical oxygen demand

SFAB: Syntrophic fatty-acid degrading bacteria

SIP: Stable isotope probing

SMA: Specific methanogenic activity

SMI: *Smithella*

SMS: *Syntrophomonas*

SPOB: Syntrophic propionate oxidizing bacteria

T-RFLP: Terminal restriction fragment length polymorphism

TAN: Total ammonia nitrogen

UASB: Upflow anaerobic sludge blanket

VFA: Volatile fatty acids

CHAPTER I

BACKGROUND

1.1 Anaerobic Digestion

Anaerobic digestion (AD) is a popular wastewater treatment approach that converts complex organic matter to biogas, containing methane, under anaerobic conditions. Advantages of this process include a high degree of waste stabilization, odor reduction, pathogen treatment and reduction in greenhouse gas emissions. In addition, the methane-rich biogas produced is combustible and can be used to generate heat and electricity. The complete conversion of organic matter under methanogenic conditions is a result of the concerted action of different physiological groups of microorganisms (Fig. 1.1). AD follows four major steps: (1) hydrolysis, (2) acidogenesis, (3) acetogenesis and (4) methanogenesis. To start with, complex polymeric substances like lipids, cellulose and proteins are broken down to their corresponding monomers such as glucose and amino acids. Subsequently, these monomers are fermented to reduced organic compounds which include fatty acids such as propionate and butyrate. The reduced products are syntrophically degraded to the methanogenic substrates - hydrogen, formate and acetate, which are finally metabolized to carbon dioxide and methane.

1.2 Volatile Fatty Acids in Anaerobic Digestion

Propionate is an important intermediate during AD, and can account for between 6%-35% of the total methane produced (Glissmann and Conrad, 2000). VFA buildup is hardly observed in high performance reactors as their degradation and production rates are proportional to each other (Li et al., 2012). However, substrate overload, toxicity and

fluctuations in process parameters disturb the AD process and cause instability, which generally results in VFA accumulation (Pullammanppallil et al., 2001; Shah et al., 2009; Liu et al., 2010). Several studies have described the toxic effects of VFAs at very high concentrations in AD (Barredo and Evison, 1991; Pullammanppallil et al., 2001; Han et al., 2005; Gallert and Winter, 2008). Propionate degradation is often considered as a rate-limiting step in anaerobic digestion (Amani et al., 2011). Furthermore, fermentation may cease at high propionate concentrations (Boone and Xun, 1987). An increase in propionate levels is often observed before process failure (Kaspar and Wuhrmann, 1978). Wang et al. (2009) showed that propionate had a greater inhibitory effect on methanogens when compared to acetate and butyrate. The tolerable concentrations of butyrate was reported to

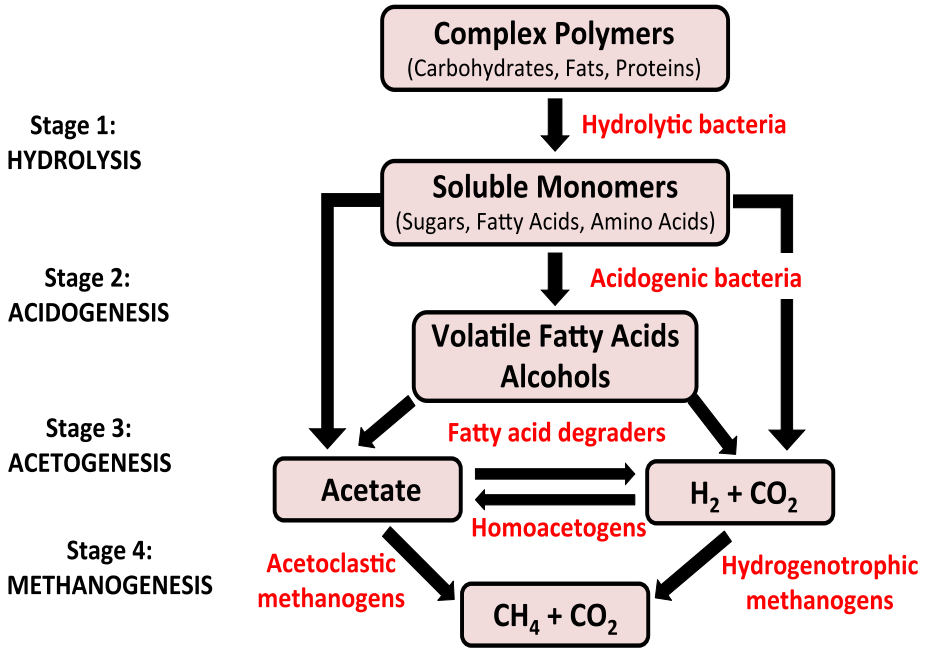

Figure 1.1: The key process stages of anaerobic digestion

be 10-times higher than that of propionate (McCarty and Brosseau, 1963). Barredo and Evison (1991) demonstrated that methanogen abundance was affected at propionate concentrations around 1.5 g L^{-1} while it declined 100-fold when it crossed 6 g L^{-1}. Hajarins and Ranade (1994) showed that methane production decreased more than 60% at neutral pH when propionate concentrations reached 5 g L^{-1}. Moreover, the extent of inhibition increased at lower pH, which indicated that undissociated propionate was more toxic. Dhaked et al. (2003) reported that the addition of 15 g L^{-1} propionate resulted in a 100-fold reduction in methanogen counts and methane content.

1.3 Factors Affecting VFA Degradation

1.3.1 H_2 Partial Pressure: VFAs are converted into acetate and H_2/CO_2 that are utilized by methanogens. It is well documented that high H_2 partial pressure negatively affects anaerobic digestion (Boone, 1982). Very low H_2 partial pressure (10^{-6} to 10^{-4} atm) has to be maintained to ensure propionate and butyrate degradation (Lier et al., 1993; Wang et al., 1999; Fukuzaki et al., 1990; Schmidt and Ahring, 1993; Kaspar and Wuhrmann, 1978; Wu et al., 1996; Labib et al., 1992; Ahring and Westermann, 1988).

1.3.2 Volatile Fatty Acids: Propionate degradation can be inhibited at elevated VFA concentrations (Siegert and Banks, 2005). For example, acetate levels ranging from 2 to 5 g L^{-1} have been shown to inhibit the breakdown of propionate (Mawson et al., 1991; Lier et al., 1993; Kaspar and Wuhrmann, 1978; Wang et al., 1999; Labib et al., 1992; Ahring and Westermann, 1988; Amani et al., 2011). Fukuzaki et al. (1990) reported that an increase in the undissociated acid forms of acetate and propionate contributed to the inhibition of

propionate degradation.

1.3.3 pH: Boone and Xun (1987) reported that the fastest growth of propionate oxidizers occurred between pH 6.8 and 8.5. Along similar lines, Dhaked et al. (2003) showed that propionate degradation was much faster at neutral or weak alkaline pH (7-8) than at weak acidic pH.

1.3.4 Nutrients: Several studies have shown that addition of metals such as iron, cobalt, nickel, molybdenum, calcium and magnesium resulted in enhanced propionate degradation (Espinosa et al., 1995; Boonyakitsombut et al., 2002).

1.4 Syntrophic Fatty Acid Degradation

Bacteria involved in anaerobic propionate and butyrate fermentation have to cope with the unfavorable energetics of the conversion process (Table 1.1). It is clear that these bacteria can obtain energy for growth only when product (esp., H_2) concentrations are kept low, which is possible via obligate dependence (aka syntrophy) on methanogenic archaea. These obligately syntrophic communities have several unique characteristics: (1) fatty acid degradation is coupled to growth, these compounds cannot be metabolized by the bacterium or the methanogen alone, (2) distance between the two partners in the syntrophy influence the fatty-acid degradation rates and microbial specific growth rates, which encourages the formation of bacterial and archaeal aggregates (granules and biofilms), (3) syntrophic growth occurs in conditions close to thermodynamic equilibrium, and (4) both types of microorganisms have evolved mechanisms that allow sharing of energy (Stams and Plugge, 2009; reviewed in Stams et al., 2012 a, b).

Table 1.1: Energetics of syntrophic growth on propionate and butyrate

Reactions	$\Delta G^{0'}$ (kJ/mol)	$\Delta G'$ (kJ/mol)
Proton-reducing bacteria		
$Propionate^- + 2H_2O \rightarrow Acetate^- + CO_2 + 3H_2$	+76	-21
$Butyrate^- + 2H_2O \rightarrow 2\ Acetate^- + H^+ + 2H_2$	+48	-22
Methanogens		
$4H_2 + CO_2 \rightarrow CH_4 + 2H_2O$	-131	-15
$Acetate^- + H^+ \rightarrow CO_2 + CH_4$	-36	-36

$\Delta G^{0'}$ (standard Gibbs free energy change) is calculated for H_2 in the gaseous state at 1 Pa, and CH_4 and CO_2 in the gaseous state at 10^4 Pa. All other compounds are calculated at 10 mM. Adapted from Stams and Plugge (2009).

1.5 Syntrophic Propionate Degrading Bacteria

Boone and Bryant (1980) were the first to isolate and describe a propionate-degrading bacterium, named *Syntrophobacter wolinii*, which grew in syntrophic association with either methanogens or sulfate-reducers. A number of additional mesophilic and thermophilic bacteria that degraded propionate and grew in syntrophy with methanogens have been described since then (Table 1.2). These include *Syntrophobacter*, *Smithella*, *Pelotomaculum*, and *Desulfotomaculum*. All four genera are phylogenetically related to sulfate-reducing bacteria and species within *Syntrophobacter* and *Desulfotomaculum* are able to reduce sulfate. Most syntrophic propionate degrading bacteria have the ability to also grow by fermentation of fumarate or pyruvate, which along with sulfate-dependent growth, have been used to obtain these bacteria in pure culture. The only exceptions are *Pelotomaculum schinkii* (de Bok et al., 2005) and *Pelotomaculum propionicum* (Imachi et al., 2007) which are the only obligately 'true' propionate-degrading syntrophs. Two thermophilic species have been identified (*Pelotomaculum thermopropionicum*, *Desulftomaculum thermobenzoicum* subsp. thermopropionicum), which grow in syntrophy with thermophilic methanogens (Imachi et

al., 2002; Plugge et al., 2002).

Propionate is degraded either via the methylmalonyl-CoA (MMC) or dismutation pathway (reviewed in Sieber et al, 2010; Stams et al (2012 a, b). The MMC pathway (Fig. 1.2 A) is found in all known propionate-degraders (*Syntrophobacter* spp., *Pelotomaculum* spp.) with the exception of *Smithella propionica*. In this pathway, propionate is activated to propionyl-CoA, which is then carboxylated to MMC (Houwen et al., 1990). MMC is rearranged to form succinyl-CoA, which is converted to succinate. Succinate is oxidized to fumurate, which is hydrated to malate and then oxidized to oxaloacetate. Pyruvate is formed via decarboxylation and is further oxidized to acetyl-CoA and finally to acetate. In contrast, *S. propionica* utilizes a dismutation pathway (Fig. 1.2 B) which involves the condensation of two molecules of propionate to produce a six-carbon intermediate, which is ultimately cleaved to form acetate and butyrate (Liu et al., 1999; de Bok et al., 2001). The intermediates and enzymes involved in this pathway are not known yet.

Table 1.2: Characteristics of propionate degrading bacteria

Species	Cell width	Cell length	Motility	Spore formation	pH range	Temp. range (°C)	Substrates used in co-culture	Syntrophic partner	Reference
Syntrophobacter fumaroxidans	1.1-1.6	1.8-2.5	-	-	6.0-8.0 (7-7.6)	20-40 (37)	C3	*Methanospirillum hungatei*	Harmsen et al. (1998)
Syntrophobacter pfennigii	1.0-1.2	2.2-3.0	+	-	6.2-8.0 (7.0-7.3)	20-37 (37)	C3, lactate, propanol	*Methanospirillum hungatei*	Wallrabenstein et al. (1995)
Syntrophobacter sulfatireducens	1.0-1.3	1.8-2.2	-	-	6.2-8.8 (7.0-7.6)	20-48 (37)	C3	*Methanospirillum hungatei*	Chen et al. (2005)
Syntrophobacter wolinii	0.6-1.0	1.0-4.5	-	-	5.5-7.7 (6.9)	23-40 (35)	C3	*Methanospirillum hungatei Desulfovibrio sp.*	Boone and Bryant (1980)
Pelotomaculum schinkii	1.0	2.0-2.5	-	+	ND	ND	C3	*Methanospirillum hungatei*	de Bok et al. (2005)
Pelotomaculum thermopropionicum	0.7-0.8	1.7-2.8	-	+	6.5-8.0 (7.0)	45-65 (55)	C3, lactate, various alcohols	*Methanothermobacter thermoautotrophicus*	Imachi et al. (2002)
Pelotomaculum propionicum	1.0	2.0-4.0	ND	+	6.5-7.5 (6.5-7.2)	25-45 (37)	C3	*Methanospirillum hungatei*	Imachi et al. (2007)
Smithella propionica	0.5	3.0-10	+	-	6.3-7.8 (7)	23-40 (33)	C3, C4, malate, fumarate	*Methanospirillum hungatei Methanogenium sp.*	Liu et al. (1999)
Desulfotomaculum thermobenzoicum subsp. thermosyntrophicum	1.0	3.0-11	+	+	6-8 (7.0-7.5)	45-62 (55)	C3, C4, benzoate	*Methanothermobacter thermoautotrophicus*	Plugge et al. (2002)
Desulfotomaculum thermocisternum	0.7-1.0	2.0-5.2	+	+	6.2-8.9 (6.7)	41-75 (62)	C3, C4	*Methanothermobacter thermolithotrophicus*	Nilsen et al. (1996)

*Adapted and modified from Stams et al (2012 a)

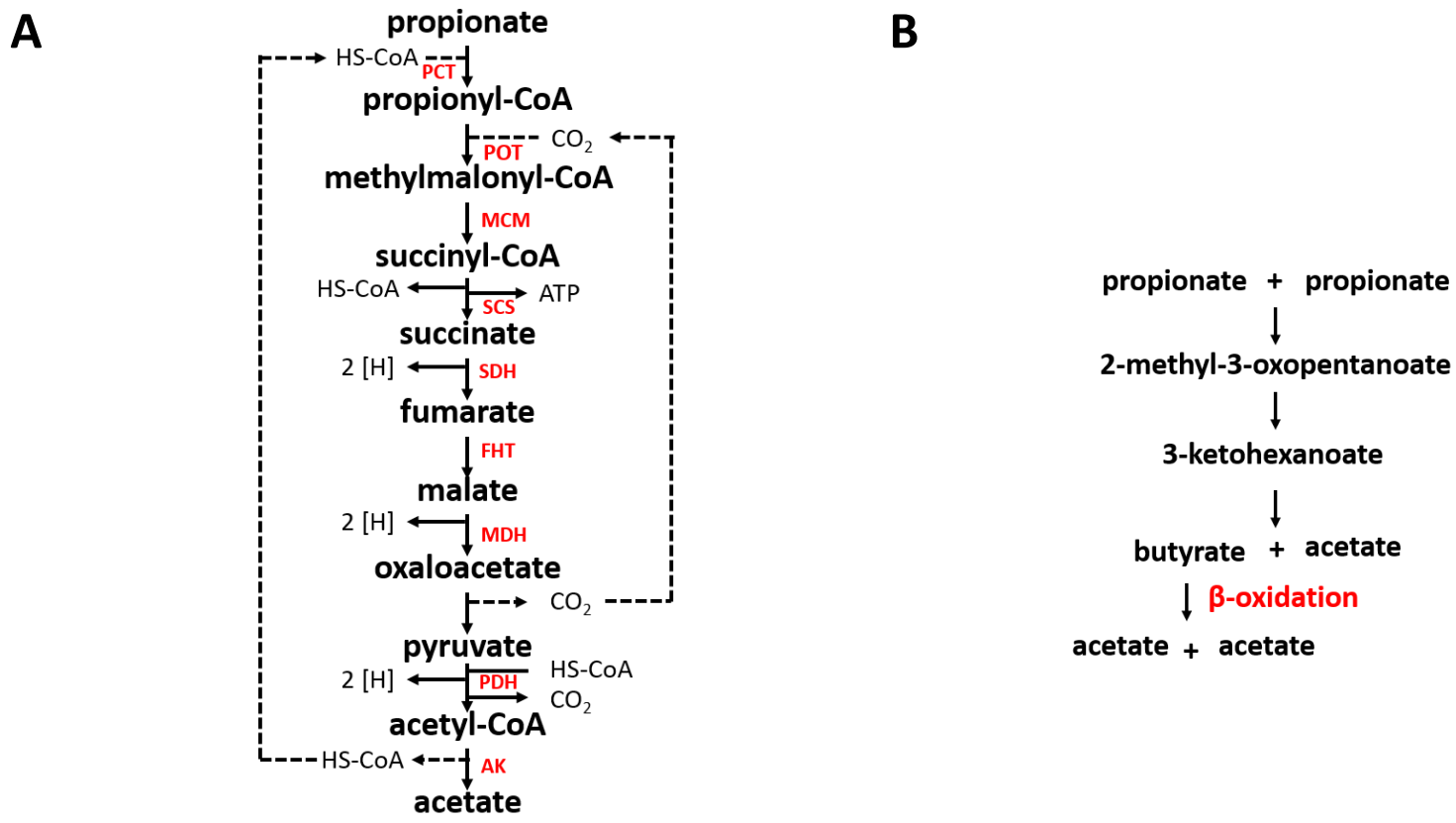

Figure 1.2: Pathways of propionate metabolism. A: The methylmalonyl-CoA pathway for propionate metabolism: Enzymes involved: PCT: propionate CoA transferase, POT propionyl-CoA: oxaloacetate transcarboxylase; MCM: methylmalonyl-CoA mutase; SCS: succinyl-CoA synthetase; SDH: succinate dehydrogenase; FHT: fumurate hydratase; MDH: malate dehydrogenase; PDH: pyruvate dehydrogenase; AK: acetate kinase. Adapted from Kosaka et al. (2006), Stams et al. (2012 a,b) and Sieber et al. (2010). **B:** The dismutation pathway for the metabolism of propionate by *Smithella propionica*. The enzymes involved in this pathway have yet to be described. This figure was adapted from de Bok et al. (2001).

1.6 Syntrophic Butyrate Degrading Bacteria

McInerney et al. (1981a) described *Syntrophomonas wolfei*, a butyrate and higher fatty-acid degrading bacterium that grows in syntrophic association with methanogens. Several other mesophilic and thermophilic butyrate-degrading bacteria that grow in syntrophy with methanogens or sulfate-reducers have been described since then (Table 1.3; McInerney et al., 2008; Sousa et al., 2009; Stams et al, 2012 a,b). All mesophilic bacterial species capable of butyrate utilization are placed within the genus *Syntrophomonas*, with the exception of *Syntrophus aciditrophicus* (Jackson et al., 1999). In addition, three thermophilic: *Thermosyntropha lipolytica* (Svetlitshnyi et al., 1996), *Thermosyntropha tengcongensis* (Zhang et al., 2012) and *Syntrophothermus lipocalidus* (Sekiguchi et al., 2000), and one psychrophilic: *Algorimarina butyrica* (Kendall et al., 2006) species have been described that degrade butyrate. The majority of butyrate-degraders are able to ferment crotonate, with the exception of *Syntrophomonas sapovorans* and *Syntrophomonas zehnderi*, which are only available as co-cultures (Roy et al., 1986; Sousa et al., 2007). Butyrate-degraders involved in sulfate-reduction have not been identified to date.

Butyrate and higher fatty acids are degraded via beta-oxidation (Fig. 1.3) (Wofford et al, 1986; Stams et al, 2012 a, b; Sieber et al, 2010). In this pathway, butyrate is first activated to butyryl-CoA, which is dehydrogenated to crotonyl-CoA. After hydrolysis, the 3-hydroxybutyryl-CoA formed is dehydrogenated to acetoacetyl-CoA, which is further cleaved into two acetyl-CoA molecules. One of these is used to activate butyrate, while the other one is used to produce ATP via phosphotransacetylase and acetate kinase reactions.

Table 1.3: Characteristics of butyrate degrading bacteria

Species	Cell width	Cell length	Motility	Spore formation	pH range	Temp. range (°C)	Substrates used in co-culture	Syntrophic partner	Reference
Syntrophomonas bryantii	0.4	4.5-6.0	-	+	6.5-7.5	28-34	C4-C11	*Methanospirillum hungatei Desulfovibrio sp. E70*	Stieb and Schink (1985)
Syntrophomonas wolfei subsp. wolfei	0.5-1.0	2.0-7.0	+	-	ND	(35-37)	C4-C8	*Methanospirillum hungatei Desulfovibrio sp. G11*	McInerney et al. (1981a)
Syntrophomonas wolfei subsp. saponavida	0.4-0.6	2.0-4.0	+	-	ND	ND	C4-C18	*Methanospirillum hungatei Desulfovibrio sp. G11*	Lorowitz et al. (1989)
Syntrophomonas sapovorans	0.5	2.5	+	-	6.3-8.1 (7.3)	25-45 (35)	C4-C18, C16:1, C18:1, C18:2	*Methanospirillum hungatii*	Roy et al. (1986)
Syntrophomonas wolfei subsp. methylbutyratica	0.4-0.5	3.0-6.0	-	-	6.5-8.5 (7.0-7.6)	25-45 (37-40)	C4-C8	*Methanobacterium formicicum*	Wu et al. (2007)
Syntrophomonas curvata	0.5-0.7	2.3-4.0	+	-	6.3-8.4 (7.5)	20-42 (35-37)	C4-C18, C18:1	*Methanobacterium formicicum*	Zhang et al. (2004)
Syntrophomonas erecta subsp. sporosyntropha	0.5-0.7	4.0-14.0	+	+	5.5-8.4 (7.0)	20-48 (35-37)	C4-C8	*Methanobacterium formicicum*	Wu et al. (2006)
Syntrophomonas erecta subsp. erecta	0.6-0.9	2.0-8.0	+	-	(7.8)	(37-40)	C4-C8	*Methanospirillum hungatii*	Zhang et al. (2005)
Syntrophomonas zehnderi	0.4-0.7	2.0-4.0	+	+	ND	25-40 (37)	C4-C18, C16:1, C18:1, C18:2	*Methanobacterium formicicum*	Sousa et al. (2007a)
Syntrophomonas cellicola	0.4-0.5	3.0-10.0	+	+	6.5-8.5 (7.0-7.5)	25-45 (37)	C4-C8, C10	*Methanobacterium formicicum Desulfovibrio sp. G11*	Wu et al. (2006)
Syntrophomonas palmitatica	0.4-0.6	1.5-4.0	-	-	6.5-8.0 (7.0)	30-50 (37)	C4-C18	*Methanobacterium formicicum*	Hatamoto et al. (2007a)
Thermosyntropha lipolytica	0.3-0.4	2.0-3.5	-	-	7.5-9.5 (8.1-8.9)	52-70 (60-66)	C4-C18, C18:1, C18:2, triglycerides	*Methanobacterium strain JW/VS-M29*	Svetlitshnyi et al. (1996)
Thermosyntropha tengcongensis	0.3-0.4	4.5-5.0	-	-	7.0-9.3 (8.2)	55-70 (60)	C4-C18, C18:1, C18:2	*Methanothermobacter thermoautotrophicus*	Zhang et al. (2012)

Syntrophothermus lipocalidus	0.4-0.5	2.0-4.0	+	-	6.5-7.0	45-60 (55)	C4-C10, isobutyrate	*Methanobacterium thermoautotrophicum*	Sekiguchi et al. (2000)
Algorimarina butyrica	ND	ND	+	-	6.2-7.1	10-25 (15)	C4, isobutyrate	*Methanogenium sp.*	Kendall et al. (2006)
Syntrophus aciditrophicus	0.5-0.7	1.0-1.6	-	-	ND	25-42 (35)	C4-C8, C16, C18	*Methanospirillum hungatei Desulfovibrio sp. G11*	Jackson et al. (1999)

*Modified from Sousa et al (2009), Stams et al (2012 a,b).

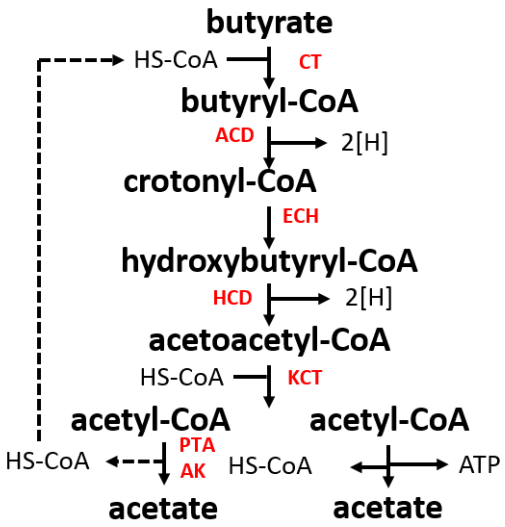

Figure 1.3: Pathway of butyrate metabolism: The beta-oxidation pathway for butyrate metabolism in *Syntrophomonas wolfei*, The enzymes involved are: CT: CoA transferase, ACD: acyl-CoA dehydrogenase, ECL: enoyl-CoA hydratase, HCD: 3-hydroxybutyrl-CoA dehydrogenase, KCT: 3-ketoacyl-CoA thiolase, PTA: phosphotransacetylase, AK: acetate kinase. Adapted from Wofford et al. (1986), Stams et al. (2012 a,b) Sieber et al. (2010)

1.7 Identification of Propionate- and Butyrate-Degrading Bacteria Using Cultivation-Independent Molecular Approaches

1.7.1 Stable Isotope Probing (SIP)

Using terminal restriction fragment length polymorphism (T-RFLP) and clone library analyses, Leuders et al. (2004) showed that *Syntrophobacter* spp., *Smithella* spp. and *Pelotomaculum* spp. dominated the 'heavy' ^{13}C-labelled bacterial rRNA, which clearly showed that these microorganisms were actively involved in syntrophic propionate oxidation in anoxic paddy soil. Moreover, *Syntrophomonas* spp. were detected in low frequency. Similar results were reported by Gan et al. (2012) in anoxic soil slurries at 30°C. They also reported that *Syntrophobacter* spp. were more active at 15°C, while *Pelotomaculum* spp. showed reduced activity. SIP analysis of paddy soil identified

Syntrophomonadaceae spp. as the active butyrate-utilizers (Liu et al., 2011). Chauhan and Ogram (2006) investigated soils collected from a nutrient gradient in the Florida Everglades. In the propionate microcosms, clone libraries from eutrophic and transition sites were dominated by *Pelotomaculum* spp. and *Syntrophobacter* spp.. In the butyrate microcosms, *Syntrophospora* spp. and *Syntrophomonas* spp., and *Pelospora* spp., dominated the eutrophic and transition sites, respectively. Butyrate-based SIP analysis of four methanogenic sludges revealed that *Syntrophoceae* spp., *Tepidanaerobacter* spp. and *Clostridium* spp. dominated the ^{13}C-labeled rRNA fraction (Hatamoto et al., 2008).

1.7.2 Enrichment Culturing

Clone library analysis and denaturing gradient gel electrophoresis (DGGE) revealed that *Syntrophobacter* spp. predominated propionate-fed chemostats maintained at low dilution rate, while *Pelotomaculum* spp. dominated at higher dilution rates (Shigematsu et al., 2006). Tang et al. (2007) showed that bacteria associated with Syntrophaceae dominated at low dilution rate, while those affiliated with Firmicutes, including *Syntrophomonas*, and Candidate division OP3 dominated at high dilution rates. A 454-pyrosequencing analysis of enrichment cultures revealed that propionate enrichments were dominated by *Syntrophobacter sulfatireducens* and *Syntrophobacter fumaroxidans*, while butyrate enrichments were dominated by *Syntrophomonas palmitatica* and *Syntrophomonas cellicola* (Narihiro et al., 2015).

1.8 Quantitative Detection and Structure-Function Analysis of Syntrophic Fatty Acid Degraders

Several 16S rRNA-targeted (hybridization-based) oligonucleotide probes have been designed to estimate the abundance of syntrophic propionate and butyrate degraders (Table 1.4). However, most probes either lacked specificity or were not broad enough to target at the genus level. Out of them, only five probes exist that target at least 50% of 16S rRNA gene sequences, deposited within the Ribosomal Database Project, within their respective genus: Synm700 (*Syntrophomonas*; Hansen et al., 1999), SYN835 (*Syntrophobacter*; Scheid and Stubner, 2001), GIh821m (*Pelotomaculum*; Imachi et al., 2006), Synbac824 (*Syntrophobacter*; Ariesyady et al., 2007a) and GSYM1240 (*Pelotomaculum*; Narihiro et al., 2012). Hybridization-based techniques such as fluorescence *in-situ* hybridization (FISH) are labor-intensive and often display reduced sensitivity, which is a major drawback when attempting to detect microbial populations present in low numbers (Bouvier and Giorgio, 2003).

Previous studies in which syntrophic fatty acid degraders have been detected (using hybridization-based techniques) are summarized in Table 1.5. Though syntrophic fatty-acid degrading bacteria (SFAB) have been detected in numerous studies, only one exists where a detailed analysis has been performed (McMahon et al., 2004). These authors reported that digesters with a history of poor performance better tolerated a severe organic overload than those that had performed well, which led them to hypothesize that higher abundance of fatty acid degraders and methanogenic partners in previously unstable reactors were responsible for this behavior.

Table 1.4: List of previously designed 16S rRNA-based probes for hybridization-based studies:

Study	Probe name	Sequence (5'-3')	Target group (Family /Genus/ Species)	Genus coverage*	Non-target hits*
Harmsen et al. (1995)	MPOB2m	CCGTCAGCCATGAAGCTTAT	*S. fumaroxidans*	13/115	0
	KOP1m	TCAAGTCCCCAGTCTCTTCGAC	*S. pfennigii*	1/115	0
Harmsen et al. (1996b)	S223m	ACGCAGACTCATCCCCGTGC	*S. wolinii*	1/115	1
Hansen et al. (1999)	S.wol180	ACATGCGTATTGTACAGCTTA	*S. wolfei*	10/234	0
	Synm700	ACTGGTRTTCCTTCCTGATTTCTA	*Syntrophomonas*	137/234	23
	Syn126	CGCTTATGGGTAGGTTGCC	*Syntrophomonas*	24/234	0
Scheid and Stubner (2001)	SYN835	GCAGGAATGAGTACCCGC	*Syntrophobacter*	102/115	21
McMahon et al. (2004)	GSM443m	GCCACTATGCATTTCTTCCCGC	*Smithella*	10/122	1
Imachi et al. (2006)	GIh821m	ACCTCCTACACCTAGCACCC	*Pelotomaculum*	123/142	55
Menes and Traves (2006)	Butox	CCTCTCCTGCCCTCAAGATG	Syntrophomonadaceae	7/234	7
Ariesyady et al. (2007a)	Synbac824	GTACCCGCTACACCTAGT	*Syntrophobacter*	103/115	13
	SmiSR354	CGCAATATTCCTCACTGC	*Smithella* sp. short rod	68/115	11024
	SmiLR150	CCTTTCGGCACGTTATTC	*Smithella* sp. long rod	9/122	7
Narihiro et al. (2012)	GSYM1240	TCGCTGCTCTCTGTACCATCCA	*Syntrophomonas*	141/234	41
	SPTS637	CCCTCAAGTCCCTCAGTTTCAA	*P. thermopropionicum*	4/142	0

*Based on RDP Release 11, Update 4

Table 1.5: Previous studies in which syntrophic fatty-acid degrading bacteria have been detected

Reactor type	Reactor influent/feed	Target group (Probe used)	Relative abundance (%)	Reference
Mesophilic full-scale continuous stirred tank reactor (CSTR)	Swine manure + cattle manure + variety of industrial organic waste streams	*Syntrophomonas* (Synm700)	0.2–1	Hansen et al. (1999)
Mesophilic lab-scale CSTR	Glucose	*S. wolfei* (Synb835) + *S. fumaroxidans* (Synm700)	2.0-4.0	Fernandez et al. (2000)
Mesophilic lab-scale reactors	Organic fraction of municipal solid waste + primary sludge + waste activated sludge	*S. fumaroxidans* (MPOB2m) *S. pfennigii* (KOP1m) *S. wolinii* (S223m) *S. propionica* (GSM443m) *Syntrophomonas* (Synm700)	<0.4 <0.5 <0.5 <0.3 <1.8	McMahon et al. (2001)
Mesophilic lab-scale anaerobic migrating blanket reactor (AMBR)	Synthetic wastewater	*Syntrophobacter* (Synb838)+ *Syntrophomonas* (Synm700)	<3.5	Angenent et al. (2002)
Mesophilic lab-scale reactors	Synthetic organic fraction of municipal solid waste + primary sludge + waste activated sludge	*S. fumaroxidans* (MPOB2m) *S. pfennigii* (KOP1m) *S. wolinii* (S223m) *S. propionica* (GSM443m) *Syntrophomonas* (Synm700)	<1.5 <0.9 <0.6 <0.6 <2.0	McMahon et al. (2004)
Mesophilic full-scale anaerobic contact reactor	Edible tallow refinery wastewater	*Syntrophomonas* (Butox)	3.0	Menes and Travers (2006)
Thermophilic lab-scale upflow sludge blanket (UASB) reactor Thermophilic lab-scale reactor Mesophilic lab-scale UASB reactor	Synthetic wastewater Clear liquor manufacture wastewater Synthetic wastewater	*Pelotomaculum* (GIh821m)	0.5 4.1 <0.1	Imachi et al. (2006)
Mesophilic full-scale two-phase reactor	Domestic wastewater	*Smithella* (SmiSR354) *Syntrophobacter* (Syn835)	2.0 0.5	Ariesyady et al. (2007a)

		Syntrophomonas (Synm700)	1.5	
Mesophilic lab-scale reactor	Synthetic wastewater	*Syntrophobacter* (Synbac824) + *Smithella* (SmiSR354, SmiLR150)	2.7-7.3	Ariesyady et al. (2007b)
Mesophilic lab-scale UASB reactor	Brewery wastewater	*Syntrophobacter* (Syn835)	5-10	Fernandez et al. (2008)
Mesophilic full-scale UASB reactor	Sugar processing wastewater	*Syntrophobacter* (Syn835)	3.0	Narihiro et al. (2012)
Mesophilic full-scale UASB reactor	Amino acid processing wastewater	*Syntrophobacter* (Syn835)	3.9	
Thermophilic pilot-scale UASB reactor	Alcohol processing wastewater	*Pelotomaculum* (GIh821m)	3.5	
Mesophilic lab-scale UASB reactor	Alcohol processing wastewater	*Smithella* (GSM443m)	3.4	
Mesophilic lab-scale reactor	Synthetic wastewater	*Syntrophobacter* (Synbac824) + *Smithella* (SmiSR354, SmiLR150)	<2.0	Ito et al. (2012)
Acidogenic two-stage reactor (upflow mode)	Synthetic wastewater	*Syntrophomonas* (Synm700) + *S. wolinii* (S223m) + *S. fumaroxidans* (MPOB2m)	19.8	Liu et al. (2012)
Mesophilic full-scale Mesophilic full-scale Mesophilic full-scale Mesophilic full-scale Mesophilic full-scale Mesophilic full-scale Mesophilic lab-scale	Sewage sludge wastewater Brewery wastewater Dairy wastewater Dairy and fish waste Sugar industry wastewater Yeast industry wastewater Slaughterhouse waste + pig manure + glycerin	*Syntrophomonas* (Synm700)	2.4-4.0 7.0–8.4 2.0–4.0 6.0–7.2 2.7–3.6 6.8–8.5 6.3–8.1	Regueiro et al. (2012)
Thermophilic single-phase lab-scale CSTR	Industrial organic fraction of municipal solid waste	*Syntrophobacter* (Synbac824) *Syntrophomonas* (Synm700)	6.1-15.1 8.7-10.3	Zahedi et al. (2013a)
Thermophilic two-phase lab-scale CSTR	Industrial organic fraction of municipal solid waste	*Syntrophobacter* (Synbac824) *Syntrophomonas* (Synm700)	8-17; 11-27 8-16; 18-37	Zahedi et al. (2013b)
Mesophilic lab-scale anaerobic baffled reactor (ABR)	Synthetic wastewater	*Syntrophomonas* (Synm700) *S. wolinii* (S223m)	7.2; 2.6 13.0; 4.0	Peng et al. (2013)

Mesophilic lab-scale CSTR	Hydro pulper disintegrated biowaste	*Syntrophobacter* (Synbac824) + *Smithella* (SmiSR354, SmiLR150) + *Pelotomaculum* (GIh821m)	<5.1	Moertelmaier et al. (2014)
Thermophilic lab-scale CSTR	Organic fraction of municipal solid waste	*Syntrophobacter* (Synbac824) *Syntrophomonas* (Synm700)	4.0-17.0 6.0-16.0	Zahedi et al. (2014)
Mesophilic lab-scale UASB	Dairy wastewater	*Syntrophomonas* (Synm700)	<0.2	Couras et al. (2014)
Mesophilic dry anaerobic digestion (DAD) reactors	Fresh biowaste + solids residues of digested biowaste suspension	*Pelotomaculum* (GIh821m) *Syntrophobacter* (Synbac824)	<4.0 <2.5	Li et al. (2014)
Mesophilic lab-scale reactor (upflow mode)	Biowaste Biowaste + Wheat bread Biowaste + Rye bread	*Syntrophobacter* (Synbac824) + *Smithella* (SmiSR354, SmiLR150) + *Pelotomaculum* (GIh821m)	2.3 1.6 1.2	Li et al. (2015)
Mesophilic lab-scale ABR	Synthetic wastewater	*Syntrophomonas* (Synm700) + *S. wolinii* (S223m)	<1.2	Peng et al. (2015)

1.9 Aims of the Dissertation

The accumulation of VFA, especially propionate, is a common reason for process deterioration in anaerobic digesters. Despite their indispensable role in VFA degradation, little information exists on the microbial communities involved. A detailed insight on structure-function relationships of syntrophic microbial communities is essential to better comprehend AD processes. The overall goal of this dissertation was to understand the contribution of syntrophic fatty acid degrading microbial communities to anaerobic digester function and process stability.

Chapter 2 describes the development of novel culture-independent molecular tools targeting syntrophic propionate- and butyrate-degraders and their application to a wide variety of methanogenic environments. These tools were further applied to gain insight into the ecology of syntrophic microbial communities in anaerobic digesters, especially under stressed conditions. Two kinds of disturbance, i.e., pulse and press, were applied to evaluate the role of syntrophic microbial communities in process stability during stable and perturbed conditions. In Chapter 3, the contribution of syntrophic microbial communities to functional resilience of anaerobic reactors exposed to shock organic overload perturbations (pulse disturbance) was investigated. In Chapter 4, the effect of different organic loading rates (press disturbance) on reactor stability and microbial structure was examined.

CHAPTER II

QUANTITATIVE DETECTION OF SYNTROPHIC FATTY ACID DEGRADING BACTERIAL COMMUNITIES IN METHANOGENIC ENVIRONMENTS[1]

2.1 Introduction

Microbial degradation of complex organic matter to biogas, which contains methane and carbon dioxide, occurs in anaerobic environments that are low in external electron acceptors (Schink, 1997). Volatile fatty acids (VFA), e.g., propionate and butyrate, are major intermediates in this process and can account for a significant proportion of the total methane produced (Gujer and Zehnder, 1983). However, fatty acid degradation is highly endergonic under standard conditions (propionate: $\Delta G^{\circ\prime} = +72$ kJ; butyrate: $\Delta G^{\circ\prime} = +48$ kJ) (Thauer et al., 1977). Nevertheless, under methanogenic conditions, these reactions can proceed via cooperation between syntrophic fatty acid degrading bacteria (SFAB) and methanogenic archaea, which keep the end products of VFA degradation (especially, H_2 and formate) at low concentrations (Schink and Stams, 2002). These syntrophic partnerships occur in methanogenic habitats such as anaerobic digesters, rice paddy fields, freshwater sediments and wetlands.

Due to the fastidious nature of syntrophic metabolism and slow growth rates, current knowledge of SFAB is extremely limited and is based on a few pure- and co-cultures (Stams et al., 2012a). To date, seven mesophilic species within three genera have been reported to degrade propionate: *Syntrophobacter* (*S. fumaroxidans*, *S. sulfatireducens*, *S. pfennigii* and *S. wolinii*), *Smithella* (*S. propionica*) and *Pelotomaculum* (*P. schinkii* and *P. propionicum*) while

[1] This chapter has been published as Mathai PP, Zitomer DH, Maki JS (2015) Quantitative detection of syntrophic fatty acid degrading bacterial communities in methanogenic environments. *Microbiol* 161:1169-1177.

eight mesophilic species within *Syntrophomonas* (*S. bryantii*, *S. cellicola*, *S. curvata*, *S. erecta*, *S. palmitatica*, *S. sapnovida*, *S. wolfei* and *S. zehnderi*) have been reported to degrade butyrate and higher fatty acids (McInerney et al., 2008). Additionally, six thermophilic and one psychrophilic species involved in VFA degradation have been isolated (McInerney et al., 2008).

The application of molecular techniques to environmental samples has enabled the analysis of microorganisms that are difficult to culture. Microbial diversity studies in different methanogenic habitats, based on stable isotope probing (Lueders et al., 2004; Chauhan and Ogram, 2006; Hatamoto et al., 2007; Liu et al., 2011; Gan et al., 2012) and enrichment culturing (Shigematsu et al., 2006; Sousa et al., 2007b; Tang et al., 2007; Narihiro et al., 2015), have confirmed *Syntrophobacter*, *Smithella*, *Pelotomaculum*, and *Syntrophomonas* to be the major bacterial genera involved in VFA degradation under mesophilic conditions. While it is important to understand SFAB diversity, it would be extremely beneficial to measure their abundance in methanogenic habitats. This is particularly important in anaerobic digesters where process upsets (e.g., substrate overload) and operational problems often cause VFA accumulation, which, in most cases, result in digester malfunction and lowered methane output (McCarty and Smith, 1986). VFA (especially propionate) degradation has been considered to be a rate-limiting step in anaerobic digestion (e.g., Ito et al., 2012). Despite their indispensable role in VFA degradation, little is known about the quantitative significance of SFAB, which might be a critical factor to ensure reactor stability. Therefore, monitoring the abundance of these microorganisms would provide a much-detailed insight into reactor performance during stable and perturbed states.

Previously, probe-based molecular techniques such as membrane hybridization (Harmsen et al., 1995; Hansen et al., 1999; Scheid and Stubner, 2001; McMahon et al., 2004),

fluorescence in situ hybridization (FISH) (Imachi et al., 2006; Ariesyady et al., 2007a) and the cleavage method with ribonuclease H (Narihiro et al., 2012) have been used to quantify SFAB, primarily at the species level. However, only using cultured species as targets is not ideal because known isolates only represent a fraction of all 16S rRNA gene sequences deposited within a genus in Ribosomal Database Project (Cole et al., 2014). Therefore, targeting these microorganisms at the genus level would potentially be more inclusive. Moreover, hybridization-based techniques such as FISH are labor-intensive and often display reduced sensitivity, which is a major drawback when detecting microbial populations present in low numbers (Bouvier and Giorgio, 2003).

Quantitative PCR (qPCR) is a powerful technique that allows rapid, reproducible and sensitive detection of specific microbial populations in complex ecosystems (Smith and Osborn, 2009). From a practical standpoint, this technique has been successfully used in combination with analytical methods to relate methanogen abundance and dynamics to digester function (Hori et al., 2006; Yu et al., 2006; Morris et al., 2014). In this study, we report the development of four genus-specific qPCR assays, based on the 16S rRNA gene, for the quantification of known SFAB within the genera *Syntrophobacter*, *Smithella*, *Pelotomaculum*, and *Syntrophomonas*. After validation, these novel qPCR assays were used to measure SFAB abundance in biomass samples obtained from a variety of methanogenic environments.

2.2 Materials and Methods

2.2.1 Sample Collection

Fourteen methanogenic biomass samples (nine engineered and five natural

environments) were collected and analyzed in this study. Samples from engineered habitats included one propionate enrichment culture, one pilot-scale and seven full-scale reactors. The enrichment culture was established using seed biomass from brewery sludge as described previously (Tale et al., 2011). The culture was fed calcium propionate (0.25 g COD/L-day) and basal nutrient medium (Schauer-Gimenez et al., 2010), once a day, continuously stirred at 35±1°C and maintained at a 15-day hydraulic retention time (HRT). After 5.5 years of operation, the feed concentration was increased from 0.25- to 1.04 g COD/L-day and feeding frequency was modified from once a day to once an hour. Biomass samples were collected at T = 0 (seed inoculum), 2.5 and 6 years post start-up. The pilot-scale reactor was fed daily with non-fat dry milk (2.5 g COD/L-day) and basal nutrient medium, continuously stirred at 35±1°C and maintained at a 15-day HRT. Full-scale samples were obtained from seven mesophilic municipal and industrial reactors, which included four upflow anaerobic sludge blanket (UASB) reactors (UASB-1: soft-drink bottling waste; UASB-2: food flavoring waste; UASB-3 & 4: brewery waste) and three continuous stirred-tank reactors (CSTR) (CSTR-1 & 2: municipal waste; CSTR-3: cheese processing waste). Specific methanogenic activity (SMA) tests, using propionate as sole carbon substrate, were performed as described by Sorensen and Ahring (1993). In addition, five samples were collected from natural methanogenic habitats including cow rumen (East Lansing, MI), horse feces (Camp Lake, WI), an experimental rice paddy soil (Milwaukee, WI), a bog stream (Cedarburg Bog, WI) and swamp sediments (Woods Hole, MA). All samples for DNA extraction were stored at -20°C immediately upon receipt.

2.2.2 DNA Extraction

DNA extraction was performed on biomass samples (0.25 g wet pellet weight) using

the PowerSoil® DNA Isolation Kit according to manufacturer's instructions (MO BIO, Carlsbad, CA). DNA integrity was confirmed on 0.8% agarose gels stained with ethidium bromide (10 μg/mL). DNA extracts were purified using the PowerClean® DNA Clean-Up Kit according to manufacturer's instructions (MO BIO) and quantified spectrophotometrically (Nanodrop ND-1000; ThermoScientific, Waltham, MA). The purified DNA was stored in 10 mM Tris buffer (pH: 8) at -80°C until subsequent analysis.

2.2.3 Primer Design and *In-Silico* Validation

For each genus of interest, full-length or partial 16S rRNA gene sequences (≥1200 bp) were retrieved from the Ribosomal Database Project (RDP) – Release 11, Update 1 (Cole et al., 2014), aligned using ClustalW2 (Larkin et al., 2007) and manually examined for genus-specific oligonucleotides. Probe Match function (RDP) was used to determine genus specificity and coverage of each newly designed oligonucleotide and probes previously used for hybridization-based studies. Oligonucleotides that qualified as potential primer sets (based on probe length: 18-25 bases, melting temperature: 50-65°C, GC content: 40-65%, low possibility of hairpin and self/hetero-dimer formation and product size: 75-300 bp) were selected for qPCR-based applications.

2.2.4 Experimental Validation

Primer set specificity was evaluated using target and non-target bacterial DNA. Five positive DNA controls were obtained from Deutsche Sammlung von Mikroorganismen und Zellkulturen (DSMZ): *S. fumaroxidans* (DSM 10017), *S. sulfatireducens* (DSM 16706), *P. thermopropionicum* (DSM 13744), *S. curvata* (DSM 15682) and *S. zehnderi* (DSM 17840). Genomic DNA extracts of *S. fumaroxidans* and *S. wolfei* were kindly provided by C.M. Plugge

(Wageningen University, Netherlands) and M.J. McInerney (University of Oklahoma, USA), respectively. For *Smithella*, an environmental clone (EMBL accession number: LN650407), displaying 100% sequence similarity to *S. propionica*, was obtained from the propionate enrichment culture using primers designed in this study. To check for non-specific amplification, each primer set was tested against 28 non-target bacterial DNA with varying degrees of primer mismatches. Each PCR mixture (50 µl) contained 100 nM of each primer, 0.2 mM dNTPs, 50 ng template DNA, 1X Standard *Taq* Reaction Buffer (New England BioLabs; Ipswich, MA) and 1.25U *Taq* Polymerase (New England BioLabs). PCR conditions were as follows: initial denaturation at 95°C for 5 min, followed by 35 cycles of denaturation at 95°C for 30 s, annealing at either 55°C (*Pelotomaculum*) or 60°C (all others) for 30 s and extension at 72°C for 1 min, and a final extension at 72°C for 7 min. PCR products were examined in 2% agarose gels to confirm product presence and size.

To further verify primer set specificity, clone libraries were constructed for each genus using PCR products from DNA extracted from anaerobic biomass. PCR products were generated as described above and purified with the Ultra-Clean PCR Clean-Up Kit (MO BIO). PCR products were cloned into pCR®4-TOPO® plasmid vector and transformed into One Shot TOP10 Chemically Competent *E. coli* cells using TOPO TA Cloning Kit according to manufacturer's instructions (Invitrogen; Carlsbad, CA). Cells were spread onto LB agar plates containing ampicillin (50 µg/mL) and grown overnight at 37°C. Positive transformants were randomly selected and colony PCR was performed with vector-specific primers PUC-F (5'-GTAAAACGACGGCCAG-3') and PUC-R (5'-CAGGAAACAGCTATGAC-3') (Invitrogen). PCR conditions were as follows: initial denaturation at 95°C for 5 min, followed by 35 cycles of denaturation at 95°C for 1 min, annealing at 55°C for 1 min and extension at 72°C for 1 min, and a final extension at 72°C

for 10 min. For each genus, 47-50 clones with insert DNA were identified and further purified. The clones were sequenced at the DNA Sequencing and Genotyping Facility - University of Chicago Comprehensive Cancer Center (Chicago, IL). Taxonomic assignments (up to genus level) were performed for all 16S rRNA gene sequences using the Classifier function (bootstrap cutoff: 50%) at the RDP (Wang et al., 2007). One hundred and ninety three 16S rRNA gene sequences, representing four clone libraries were deposited in the European Nucleotide Archive (see below).

2.2.5 Standard Curve Construction

Standard curves were constructed using 16S rRNA gene-based PCR products, derived from either pure culture DNA or environmental clones, using the genus-specific primers designed in this study. PCR amplification and cloning was performed as described above. Positive transformants were grown overnight at 37°C in LB broth with ampicillin (100 μg/ml). Plasmids were purified with a Plasmid Mini-Prep Kit according to manufacturer's instructions (Qiagen; Valencia, CA) and quantified as described above. Plasmids were sequenced (as described above) to confirm presence of the correct insert. Plasmid DNA was normalized to 10^{10} copies per μl and diluted ten-fold to obtain a dilution series ranging from 10^{0} to 10^{10} copies per μl. This dilution series was used to determine the linear dynamic range for each assay developed in this study.

2.2.6 Quantitative PCR

Quantitative PCR (qPCR), based on SYBR Green chemistry, was carried out in triplicate on a CFX Connect Real-Time PCR Detection System (Bio-Rad) according to the recommendations of Smith et al. (2006) and Smith and Osborn (2009). Minimum

Information for Publication of Quantitative Real-Time PCR Experiments (MIQE) guidelines (Bustin et al., 2009), as applicable to environmental samples, were followed while optimizing qPCR protocols. qPCRs were performed in triplicate in a reaction volume of 20 µl and the final mixture contained: 1× iTaq™ Universal SYBR® Green Supermix (Bio-Rad), 500 nM of each primer, 10 ng of template DNA and PCR-grade sterile water. Each qPCR run included a no-template control. Amplification was performed as a two-step cycling procedure: initial denaturation at 95°C for 3 min, followed by 40 cycles at 95°C for 10 s and at 55°C (*Pelotomaculum*) or 60°C (all others) for 30 s. Melt-curve analysis was performed after each run to confirm reaction specificity. Baseline and threshold calculations were determined with CFX Manager™ software (Bio-Rad). Total Bacterial and Archaeal 16S rRNA gene copies were quantified using domain-specific primers (341F-518R and 915F-1059R, respectively) as described previously (Muyzer et al., 1993; Yu et al., 2005). In addition, methanogen-specific methyl coenzyme M reductase alpha-subunit, (*mcrA*), gene copies were quantified as described by Morris et al. (2014).

2.2.7 Nucleotide Sequence Accession Numbers

The 16S rRNA gene sequences reported in this study have been deposited in the EMBL database under accession numbers LN650256 to LN650448.

2.3 Results and Discussion

2.3.1 Primer Design and *In-silico* Validation

Four genus-specific primer sets were designed (Table 2.1) based on 16S rRNA gene sequences retrieved from Ribosomal Database Project (Release 11, update 1). *In-silico* analysis

using the RDP Probe Match function revealed that each primer set: SBC, SMI, PEL, and SMS, targeted 91, 67, 84, and 83% of all sequences (≥1200 bp) in the database within the genera *Syntrophobacter*, *Smithella*, *Pelotomaculum*, and *Syntrophomonas*, respectively. Importantly, these primer sets displayed either comparable or greater coverage than genus-specific probes previously designed for hybridization-based studies: SYN835 (*Syntrophobacter*: 89%; Scheid and Stubner, 2001), Synbac824 (*Syntrophobacter*: 90%; Ariesyady et al., 2007a), GIh821m (*Pelotomaculum*: 86%; Imachi et al., 2006), Synm700 (*Syntrophomonas*: 59%; Hansen et al., 1999), and GSYM1240 (*Syntrophomonas*: 60%; Narihiro et al., 2012). Additionally, all SFAB species type strains within target genera: *Syntrophobacter* (*S. fumaroxidans*, *S. pfennigii*, *S. sulfatireducens*, *S. wolinii*), *Smithella* (*S. propionica*), *Pelotomaculum* (*P. propionicum, P. schinkii*, *P. thermopropionicum*) and *Syntrophomonas* (*S. cellicola*, *S. erecta*, *S. palmitatica*, *S. sapovorans*, *S. wolfei*, *S. zehnderi*, except *S. curvata*) were detected using the respective primer sets. Primer set mismatches with all closely related non-target species type strains (within target family) are illustrated in Table 2.2.

2.3.2 Experimental Validation

Primer set specificity was experimentally verified using DNA extracts or environmental clones representing 34 bacterial species. PCR products of expected size (SBC: 150 bp, SMI: 100 bp, PEL: 257 bp, SMS: 121 bp) were obtained from all target DNA (Fig. 2.1), whereas no amplification was observed with non-target DNA (data not shown). To further confirm primer set specificity, four clone libraries (47-50 clones per genus) were constructed from DNA extracted from anaerobic biomass using the genus-specific primers designed in this study. Classifier function (RDP) designated 100, 93, 98, and 52% of the clones as *Syntrophobacter*, *Smithella*, *Pelotomaculum*, and *Syntrophomonas*, respectively. The remaining clones were below the recommended confidence threshold (bootstrap cutoff:

50%). Though all SMS-specific clones were placed within the target family, only 52% of the total clones could be classified down to the genus level. *In-silico* analysis using pre-classified SMS-specific 16S rRNA gene sequences, retrieved from the RDP, revealed that the SMS-specific primers amplified a 121-bp region (*E. coli* positions 637-757) that exhibited low taxonomic resolution, which thereby did not allow accurate classification beyond the family level.

2.3.3 Standard Curves

Standard curves, constructed from a series of 10-fold plasmid DNA dilutions, displayed a linear dynamic range spanning eight orders of magnitude (10^9 to 10^2 copies) and a lower detection limit of 100 copies per reaction (Table 2.3; Fig. 2.2). The regression coefficient (R^2) of each standard curve was always above 0.99. High C_T values were observed for no-template controls. Melt-curve analysis displayed a single observable peak for each genus (SBC: 82°C, SMI: 79.5°C, PEL: 84.5°C, and SMS: 81.5°C) (Fig. 2.3). Peaks indicative of non-specific amplification were not observed.

Table 2.1: Characteristics of the16S rRNA gene-targeted qPCR primer sets designed in this study

Target Genus	Primer[#]	Sequence[*] (5'-3')	*E. coli* Position	T_m (^oC)	GC (%)	Coverage[§] (%)	Product Size (bp)	Annealing Temp (^oC)
Syntrophobacter	SBC-695F	ATTCGTAGAGATCGGGAGGAATACC	695-719	57.4	48.0	94.8	150	60
	SBC-844R	TGRKTACCCGCTACACCTAGTGMTC	820-844	60.6	54.0	94.0		
Smithella	SMI-732F	GRCTTTCTGGCCCDATACTGAC	732-753	57.2	53.8	86.4	100	60
	SMI-831R	CACCTAGTGAACATCGTTTACA	810-831	52.4	40.9	77.3		
Pelotomaculum	PEL-622F	CYSDBRGMSTRCCTBWGAAACYG	622-644	60.0	57.2	96.2	257	55
	PEL-877R	GGTGCTTATTGYGTTARCTAC	857-877	51.5	42.9	87.2		
Syntrophomonas	SMS-637F	TGAAACTGDDDDTCTTGAGGGCAG	637-660	57.8	47.2	89.2	121	60
	SMS-757R	CAGCGTCAGGGDCAGTCCAGDMA	735-757	63.4	61.6	93.6		

[#] F = Forward Primer, R = Reverse Primer

[*] R=A/G, K=G/T, M=A/C, D=A/G/T, Y=C/T, S=G/C, B=C/G/T, W=A/T

[§] Ratio (%) of number of sequence hits within target group to the total number of target sequences

Table 2.2: Partial 16S rRNA gene sequences of non-target bacteria, which includes all isolated type strains within same family of interest as target genus.

Organism (Type Strain)	Strain Used	Forward Primer*	Reverse Primer*
***Syntrophobacter*-Specific Primers**		5′ ATTCGTAGAGATCGGGAGGAATACC 3′	3′ CTMGTGATCCACATCGCCCATKRGT 5′
Target site		5′ ATTCGTAGAGATCGGGAGGAATACC 3′	5′ GAKCACTAGGTGTAGCGGGTAMYCA 3′
Desulfacinum hydrothermale	DSM 13146	--G------T---------------	-G----------C--------T-G-
Desulfacinum infernum	DSM 9756	--G------T---------------	-G-------------------T-G-
Desulfoglaeba alkanexedens	DSM 18185	--G----------------------	-G-------------------T-G-
Desulforhabdus amnigena	DSM 10338	----------------------T-	-------G----------------
Desulfosoma caldarium	DSM 22027	--G------T---------------	-G-------------------T-G-
Desulfovirga adipica	DSM 12016	--------------------C---	-------G-------T---------
Thermodesulforhabdus norvegica	DSM 9990	--G------T---------------	-G-AC-------GT------T--A-
***Smithella*-Specific Primers**		5′ GRCTTTCTGGCCCDATACTGAC 3′	3′ ACATTTGCTACAAGTGATCCAC 5′
Target site		5′ GRCTTTCTGGCCCDATACTGAC 3′	5′ TGTAAACGATGTTCACTAGGTG 3′
Desulfobacca acetoxidans	DSM 11109	----------A----C------	----------GG---------
Desulfomonile limimaris	ATCC 700979	-----C----A----------	C-------G--AG---------
Desulfomonile tiedjei	DSM 6799	-----C----A----------	C-------G--AG---------
Syntrophus aciditrophicus	DSM 26646	-----C----T----------	C----------------------
Syntrophus buswellii	DSM 2612	-----C----T----------	C----------------------
Syntrophus gentianae	DSM 8423	-----C----T----------	C----------------------
***Pelotomaculum*-Specific Primers**		5′ CYSDBRGMSTRCCTBWGAAACYG 3′	3′ CATCRATTGYGTTATTCGTGG 5′
Target site		5′ CYSDBRGMSTRCCTBWGAAACYG 3′	5′ GTAGYTAACRCAATAAGCACC 3′
Cryptanaerobacter phenolicus	DSM 15808	----------------------	----------------------
Desulfotomaculum acetoxidans	DSM 771	--T---------T----------	AC------------------T
Desulfotomaculum aeronauticum	DSM 10349	---C-T--T---------T----	--------------------T
Desulfotomaculum alcoholivorax	DSM 16058	--------T---TA---------	-G------------------
Desulfotomaculum alkaliphilum	DSM 12257	--T-----T--------------	----------GC-------T
Desulfotomaculum arcticum	DSM 17038	--------TG--TAAG-------	----------------------
Desulfotomaculum australicum	DSM 11792	---C---G-----A--------A	----------------------
Desulfotomaculum carboxydivorans	DSM 14880	---C-T--T---------T----	-C---A--------------T
Desulfotomaculum geothermicum	DSM 3669	---C----TG--T----------	-C-------------------
Desulfotomaculum gibsoniae	DSM 7213	----------T---A------	-C-------------------
Desulfotomaculum halophilum	DSM 11559	------AGT-------A------	-C------------------T
Desulfotomaculum hydrothermale	DSM 18033	---C-T--T---------T----	-C------------------T
Desulfotomaculum kuznetsovii	DSM 6115	---C---G-------------A	-----A---------------
Desulfotomaculum nigrificans	DSM 574	-----T--T---------T----	-C---A--------------T
Desulfotomaculum putei	DSM 12395	---C----T---------T----	--------------------T
Desulfotomaculum ruminis	DSM 2154	---C-T-----------T----	--------------------T
Desulfotomaculum sapomandens	DSM 3223	---C----TG--GA--------A	-C------------------T
Desulfotomaculum solfataricum	DSM 14956	---C---G-------------A	-----A---------------
Desulfotomaculum thermoacetoxidans	DSM 5813	---C---G-------------A	-----A---------------
Desulfotomaculum thermobenzoicum	DSM 6193	---C---G-------------A	-----A---------------
Desulfotomaculum thermocisternum	DSM 10259	---C---G-----A--------A	----------------------
Desulfotomaculum thermosapovorans	DSM 6562	---C----TG--GA---------	-C----------C--------
Desulfotomaculum thermosubterraneum	DSM 16957	---C---G-------------A	-----A---------------
Desulfurispora thermophila	DSM 16022	--TC--------T--C------A	----------------------
Sporotomaculum hydroxybenzoicum	DSM 5475	--------TGT-GA---------	-C----------C--------
***Syntrophomonas*-Specific Primers**		5′ TGAAACTGDDDDTCTTGAGGGCAG 3′	3′ AMDGACCTGACDGGGACTGCGAC 5′
Target Site		5′ TGAAACTGDDDDTCTTGAGGGCAG 3′	5′ TKHCTGGACTGHCCCTGACGCTG 3′
Pelospora glutarica	DSM 6652	A----------------------	----------------------
Syntrophothermus lipocalidus	DSM 12680	---T------C-------------	-----------G----------
Thermohydrogenium kirishiense	DSM 11055	-------G----G------TCA--	-C----------A---------
Thermosyntropha lipolytica	DSM 11003	---T------C-------------	----------------------

* Nucleotides that differ from target sequences are shown

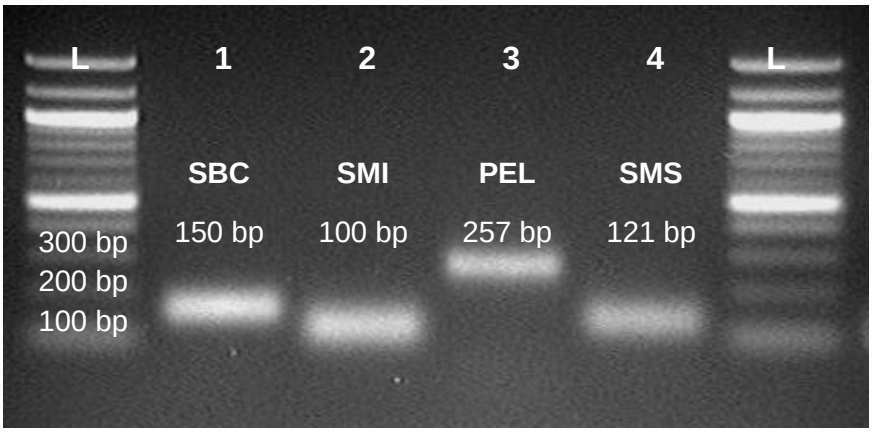

Figure 2.1: Gel electrophoresis analysis of PCR products obtained with genus-specific primers. Lane descriptions: L=100 bp ladder, 1=*Syntrophobacter*, 2=*Smithella*, 3=*Pelotomaculum*, and 4=*Syntrophomonas*.

Table 2.3: Characteristics of standard curves constructed in this study

Assay	Target Genus	Linear range (copies/μl)	Slope	Efficiency (%)	R^2	y-intercept	Clone used as standard (GenBank / EMBL accession no.)
SBC	*Syntrophobacter*	10^2 - 10^9	-3.177	106.4	0.999	37.083	*S. fumaroxidans* (X82874)
SMI	*Smithella*	10^2 - 10^9	-3.217	104.6	0.997	37.518	Clone SMI06 (LN650407)
PEL	*Pelotomaculum*	10^2 - 10^9	-3.362	98.3	0.999	39.245	*P. thermopropionicum* (AB035723)
SMS	*Syntrophomonas*	10^2 - 10^9	-3.301	100.9	0.998	39.414	*S. wolfei* (M26492)

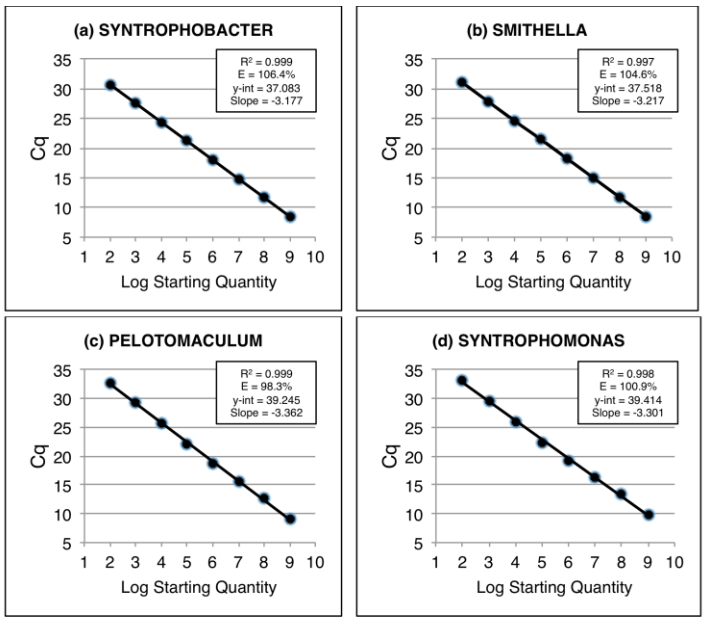

Figure 2.2: Standard curves for four qPCR assays developed in this study

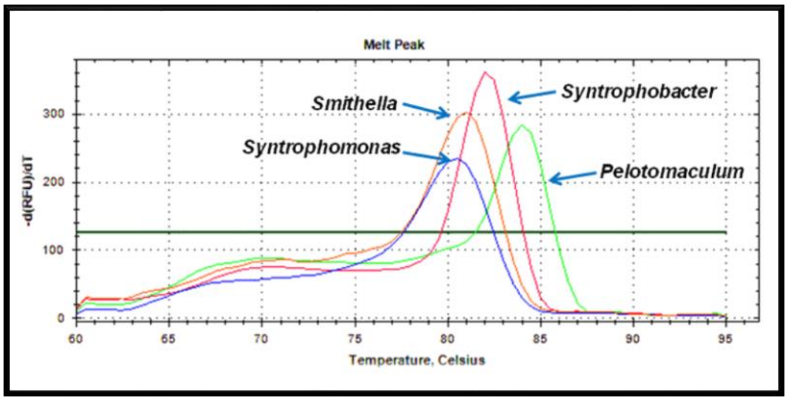

Figure 2.3: Melt-curve profiles of qPCR products obtained with genus-specific primers

2.3.4 Quantification of Microbial Communities

The novel qPCR assays were applied to quantify 16S rRNA gene copies of SFAB in biomass samples obtained from a variety of mesophilic methanogenic habitats. Biomass samples were determined to be methanogenic based upon the demonstration of methane

production when fed propionate (SMA test; data not shown) and/or detection of the *mcrA* gene, which encodes the alpha-subunit of 'methyl coenzyme M reductase' an enzyme that catalyzes the terminal step in methanogenesis (Fig. 2.4). Using the new primer sets, each SFAB genus was detected in all samples, though their abundance (Fig. 2.5) varied up to four orders of magnitude. In general, total SFAB were at least an order of magnitude more abundant in anaerobic reactor samples (10^5 - 10^6 16S rRNA gene copies ng^{-1} DNA) when compared to samples obtained from natural environments (10^2 - 10^4 gene copies ng^{-1} DNA) (Figs. 2.5 & 2.6). These results are in agreement with previous high-throughput sequencing- (Sundberg et al., 2013) and hybridization-based studies (Harmsen et al., 1996a; Hansen et al., 1999; McMahon et al., 2004; Ariesyady et al., 2007a; Narihiro et al., 2012) that estimated SFAB to generally constitute only a fraction (<2%) of the total microbial community in anaerobic digesters. When viewed in total, the data from this and the previous studies suggest that SFAB constitute a 'keystone' guild, i.e., organisms whose impact on community structure and function is far greater than what their abundance would suggest (Power et al., 1996). A loss of SFAB function, i.e., VFA degradation, would lower pH and negatively impact the entire microbial consortia and could trigger system collapse. Moreover, Tale et al. (2011) reported enhanced recovery of upset digesters when augmented with a propionate enrichment culture, which in this study was shown to contain high numbers of known syntrophic propionate-degraders (see Fig. 2.7; T = 2.5 years).

2.3.4.1 Engineered Environments

Among the full-scale reactor samples, reactor configuration and substrate identity appeared to influence SFAB and methanogen abundance. UASB reactors harbored at least 10-fold more propionate degraders than CSTR digesters (Figs. 2.5 & 2.6). This result could

be because UASB configuration promotes granule formation that brings SFAB and methanogens within close physical proximity, thereby facilitating efficient fatty acid degradation (Schink and Thauer, 1988). It is also noteworthy that the majority of currently identified SFAB have been isolated from full-scale UASB reactors (Stams et al., 2012a). Interestingly, in municipal reactors, numbers of *Syntrophobacter* were reduced while those of *Pelotomaculum* were increased when compared to industrial reactors (Fig. 2.5). In addition, municipal reactors also displayed the lowest abundance of methanogens (Fig. 2.4) amongst all full-scale reactors. Differences in waste composition and nutrient levels may explain these observations. Industrial sludge samples have been reported to display higher methane production rates against propionate than those obtained from municipal sludge (Tale et al., 2011).

An analysis of the enrichment culture over time revealed a 20- and 534-fold increase in the abundance of total propionate-degraders (*Syntrophobacter* + *Smithella* + *Pelotomaculum*), at 2.5 and 6 years post start-up, respectively, when compared to the seed inoculum (Fig. 2.7). The increase in substrate concentration from 0.25 to 1.04 g COD/L-day resulted in a 27-fold increase in the abundance of total propionate-degraders. The abundance of *Syntrophobacter* and *Pelotomaculum* increased 41- and 18-fold, respectively, while that of *Smithella* decreased 28-fold in the culture after 6 years when compared to the enrichment at 2.5 years (Fig. 2.7). After 6 years, *Syntrophobacter* dominated the microbial community with 51% of the total 16S rRNA gene sequences detected (Fig. 2.6). This result is comparable to those from a recent high-throughput sequencing study where *Syntrophobacter* accounted for up to 88% and 52% of the total bacterial 16S rRNA gene sequences in propionate enrichment cultures seeded with sludge and swine manure, respectively (Narihiro et al., 2015). The presence of *Syntrophomonas*, a butyrate-degrader, in the propionate enrichment culture may be due to the

presence of *Smithella*, which utilizes a non-randomizing pathway where propionate is first dismutated to acetate and butyrate. The butyrate then becomes available to *Syntrophomonas*, which syntrophically metabolizes it to acetate via beta-oxidation (de Bok et al., 2001). Previously, stable isotope probing based studies, using ^{13}C-labeled propionate, identified that *Syntrophomonas*, in addition to *Syntrophobacter*, *Smithella*, and *Pelotomaculum*, was enriched in the 'heavy' ^{13}C-labeled DNA fractions (Leuders et al., 2004; Chauhan and Ogram, 2006; Gan et al., 2012) supporting the presence of these bacteria in the propionate enrichment.

Previous studies, in agreement with my findings, have reported differences in the structure of propionate degrading bacterial communities in (a) anaerobic sludge samples incubated at different propionate concentrations (Ariesyady et al., 2007b) and (b) propionate fed chemostats maintained at different hydraulic retention times (Shigematsu et al., 2006). It has been suggested that the coexistence of phylogenetically diverse but functionally redundant microbial communities (i.e., parallel substrate processing) is essential to maintain stable ecosystem function under fluctuating environmental conditions (Fernandez et al., 2000; Hashsham et al., 2000). These conditions are frequently observed in full-scale digesters where perturbations such as substrate overload often result in VFA accumulation. Hence, as observed within acetoclastic methanogens (Yu et al., 2006), it is plausible that differences in growth rates and substrate affinities within members of these microbial groups help maintain low propionate concentrations.

2.3.4.2 Natural Environments

Within natural samples, the highest numbers of SFAB were observed in the swamp sediment and bog samples (Figs. 2.5 & 2.6). Previous studies have reported syntrophic fatty acid degradation in freshwater sediments (Lovley and Klug, 1982; Scholten and Stams, 1995)

and wetlands (Chauhan et al., 2004; Juottonen et al., 2005). In contrast, relatively lower numbers of SFAB were detected in the experimental rice paddy soil (Figs. 2.5 & 2.6). This result was unexpected because high propionate turnover rates have been reported in anoxic paddy field soil (Krylova et al., 1997; Glissmann and Conrad, 2000). This anomaly could be attributed to the fact that soil samples analyzed in this study were obtained from an open experimental flooded rice plot maintained in a temperate region. Amongst all the samples analyzed, the lowest abundance of SFAB were detected in cow rumen and horse feces (Figs. 2.5 & 2.6). These animals use microbes to ferment cellulose to VFA, the cow in the rumen (Russell and Hespell, 1981) and the monogastric horse in its hindgut (Mackie and Wilkins, 1988). Results from the current study may not be unusual because both animals absorb VFA via their intestinal epithelium as a major source of energy and these acids would, therefore, not be as readily available to support SFAB growth (Bergman, 1990). Moreover, it has been suggested that SFAB, with long generation times, cannot maintain stable populations in habitats (e.g., cow rumen) that have short retention times (McInerney et al., 1981b).

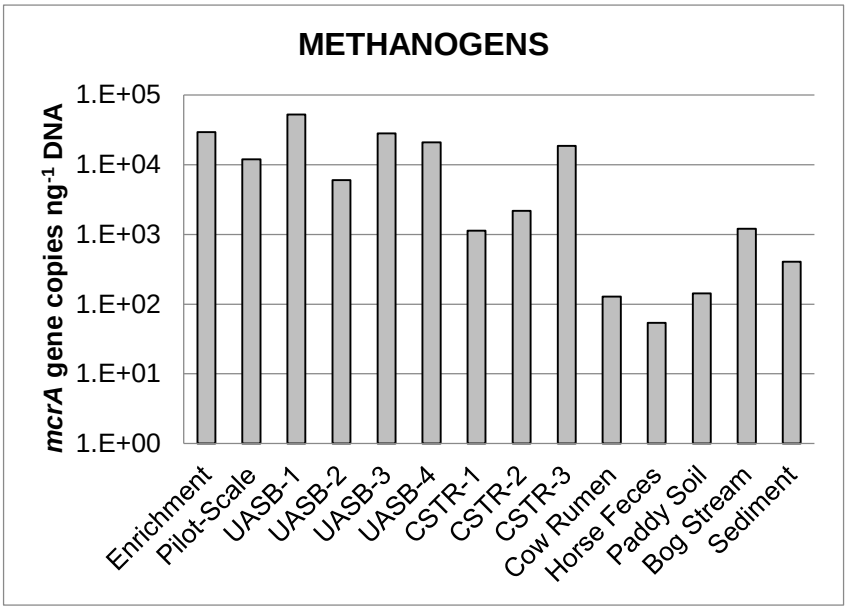

Figure 2.4: Mean *mcrA* gene copies ng^{-1} DNA in biomass samples from different methanogenic environments. Enrichment: 6 years post start-up. UASB: upflow anaerobic sludge blanket reactor; CSTR: continuously stirred tank reactor. UASB-1: soft-drink bottling waste; UASB-2: food flavoring waste; UASB-3 & 4: brewery waste; CSTR 1 & 2: municipal waste; CSTR-3: cheese processing waste. Standard error less than 10% for all samples.

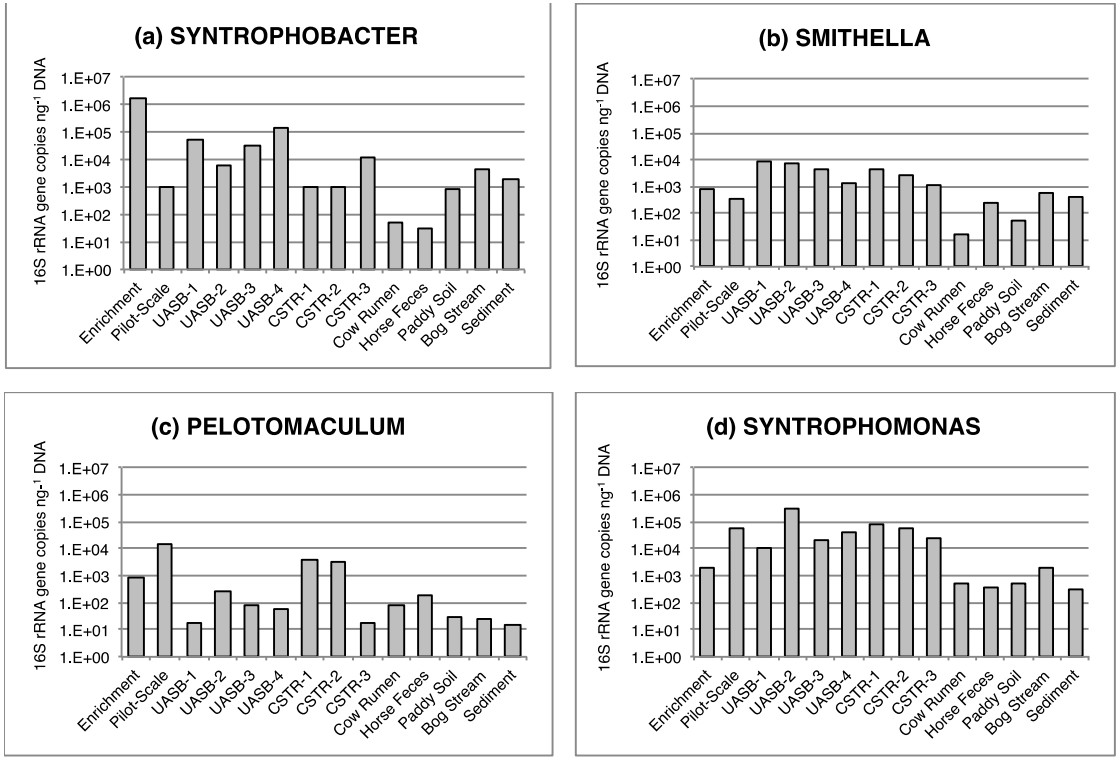

Figure 2.5: Quantification of syntrophic fatty acid degraders in biomass samples from different methanogenic environments showing mean number of 16S rRNA gene copies ng^{-1} DNA. Enrichment: 6 years post start-up. UASB: upflow anaerobic sludge blanket reactor; CSTR: continuously stirred tank reactor. UASB-1: soft-drink bottling waste; UASB-2: food flavoring waste; UASB-3 & 4: brewery waste; CSTR 1 & 2: municipal waste; CSTR-3: cheese processing waste. Standard error less than 10% for all samples.

	Archaea	SBC	SMI	PEL	SMS
Enrichment	17.517	50.920	0.023	0.025	0.067
UASB-1	7.575	0.877	0.141	0.000	0.162
UASB-3	5.909	0.720	0.102	0.002	0.475
UASB-4	4.649	2.460	0.022	0.001	0.668
Pilot-Scale	3.955	0.016	0.005	0.235	0.954
UASB-2	3.758	0.147	0.163	0.006	7.017
Bog Stream	1.984	0.155	0.021	0.001	0.071
Sediment	1.829	0.194	0.045	0.001	0.031
CSTR-2	1.634	0.029	0.080	0.103	1.895
CSTR-3	1.526	0.174	0.017	0.000	0.370
CSTR-1	0.773	0.017	0.076	0.065	1.320
Paddy Soil	0.206	0.033	0.002	0.001	0.017
Cow Rumen	0.099	0.001	0.000	0.001	0.007
Horse Feces	0.098	0.001	0.009	0.007	0.014

Figure 2.6: Heat map displaying relative abundance (%) of various microbial groups in biomass samples from different methanogenic environments. Enrichment: 6 years post start-up. Relative abundance = [Target group abundance/(Bacteria+Archaea abundance)] x 100. SBC: *Syntrophobacter*, SMI: *Smithella*, PEL: *Pelotomaculum*, SMS: *Syntrophomonas*. Samples ordered according to archaeal relative abundance.

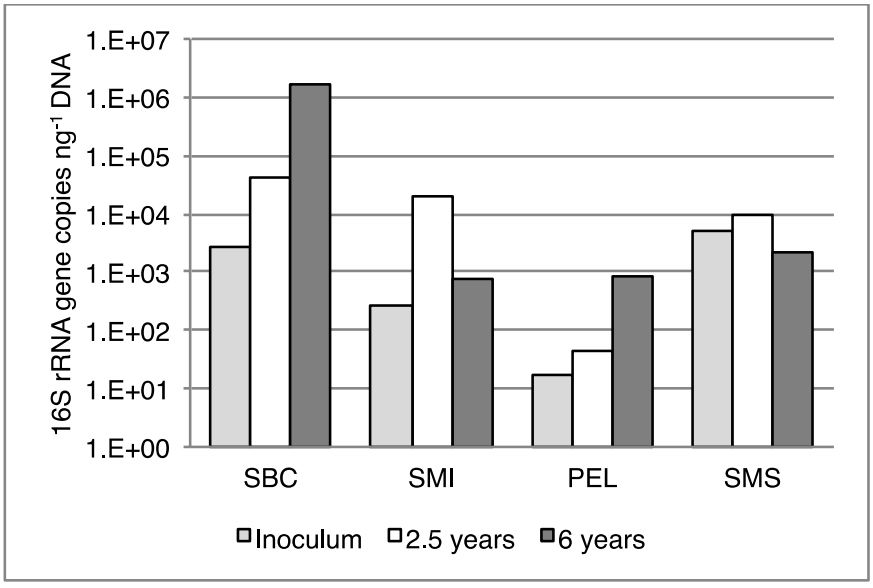

Figure 2.7: Effect of the addition of propionate on the abundance of syntrophic fatty acid degraders in a long-term enrichment culture. SBC: *Syntrophobacter*, SMI: *Smithella*, PEL: *Pelotomaculum*, SMS: *Syntrophomonas*. Standard error less than 10% for all samples.

2.4 Conclusion

This study provides a suite of validated assays that were successfully used to quantify SFAB in biomass samples obtained from a variety of methanogenic habitats. To the best of our knowledge, this is the first qPCR-based study to detect SFAB at the genus level, and the first, using a targeted approach, to quantify these bacteria in natural environments. Our data confirms that SFAB constitute only a fraction of the total microbial community, and that anaerobic reactors harbored higher numbers of SFAB when compared to natural methanogenic habitats. In addition, within full-scale reactors, we report that SFAB and methanogen abundance varied with reactor configuration and substrate identity. Future studies must be performed to understand how different anaerobic digester process parameters (e.g., substrate composition, temperature, retention time and organic loading rate) affect SFAB and methanogen community dynamics. A better understanding of syntrophic microbial communities will help optimize digester technologies for enhanced biogas production and efficient waste treatment.

CHAPTER III

DETERMINE THE CONTRIBUTION OF SYNTROPHIC MICROBIAL COMMUNITIES TO THE FUNCTIONAL STABILITY OF ANAEROBIC DIGESTERS EXPOSED TO ORGANIC OVERLOAD PERTURBATIONS

3.1 Introduction

Anaerobic digestion (AD) is an effective method to treat high-strength industrial wastes. Its advantages over aerobic process include lower energy requirement, lower sludge generation, pathogen reduction and production of methane that can be used as fuel. In AD, complex organic matter is hydrolyzed and fermented to volatile fatty acids (VFA), which are converted by syntrophic fatty acid degraders to produce acetate, H_2 and CO_2. These intermediates are in turn consumed by methanogens to produce methane (Schink, 1997). Despite its benefits, AD is underutilized and existing industrial installations have not been optimized due to stability issues with the microbial mediated process that can be sensitive to disturbances. Because of the dynamic nature of waste production, the composition and volume of digester influent may change regularly. Shock overloading may cause process instability and even failure when VFA production exceeds its degradation (due to kinetic uncoupling), leading to reactor acidification (Borja and Banks, 1995; Dupla et al., 2004). Improving AD process stability is important when influent substrate composition or concentration rapidly change. Process stability could be improved by developing a greater understanding of the dynamics of the key microbial players involved in fatty acid degradation when faced with a shock overload.

Few studies have looked into the effect of organic shock overload on microbial communities in methanogenic reactors and these have focused on analyzing the entire

community or specifically on the methanogens. Xing et al. (1997a; 1997b) showed that the community involved in AD was able to adapt to periodic substrate (glucose) perturbation through a long-term change in its structure. Two studies reported that parallel substrate processing conferred greater functional stability in response to a substrate (glucose) perturbation and that reactors with an inflexible community structure were associated with greater functional instability (Hashsham et al., 2000; Fernandez et al., 2000).

The effect of reactor acidification on methanogens has been previously studied. Delbes et al. (2001) reported a major shift in archaeal populations from hydrogenotrophic to acetoclastic methanogens during a period of elevated acetate levels with a corresponding decrease in pH. In reactors dominated by acetoclastic methanogens, one with *Methanosarcina* as the primary methanogen survived an organic loading rate (OLR) increase causing a shift in pH, while another with *Methanosaeta* failed (McMahon et al., 2004). Hori et al. (2006) observed a shift in predominant hydrogenotrophic methanogens (*Methanoculleus* to *Methanothermobacter*) and an increase in the acetoclastic methanogen *Methanosarcina* concurrent with increases in VFA concentration and lower pH in a lab-scale reactor. Process stability in an acidified lab-scale reactor was linked to the disappearance of methanogens in the family Methanosaetaceae (Blume et al., 2010). In a comparison between acidic bog sediments and municipal sludge, Steinberg and Regan (2011) reported that the lab-scale reactor inoculated with the former survived a glucose shock while a reactor inoculated with the latter did not. The contribution of syntrophic propionate- and butyrate-degraders to reactor stability during shock overload perturbations has not been studied to the author's knowledge, despite the fact that propionate and butyrate contribute up to 35% of the total methane produced (Gujer & Zehnder, 1983). Syntrophic propionate- and butyrate-degraders are functional specialists and constitute only a fraction of the total AD microbial community structure (see

Chapter 2 and Mathai et al., 2015).

The objective of this study was to investigate the contribution of syntrophic microbial communities to the functional stability of lab-scale reactors exposed to organic overload perturbations. To test this, six lab-scale reactor sets, inoculated from different sources, were subjected to organic overloads and monitored for recovery. Reactor function and microbial structure were monitored using a combination of physicochemical and molecular techniques. The results indicate that syntrophic microbial communities play a crucial role in reactor functional resilience when exposed to shock overload perturbations.

3.2 Materials and Methods

3.2.1 Reactor Setup and Operation

Six anaerobic reactor sets were established in triplicate in 160 ml serum bottles (working volume: 60 ml) and incubated on a shaker table (100 rpm) at 37±1°C. Each reactor set was started with an inoculum obtained from a different, existing anaerobic reactor treating a specific waste: Set A (food and beverage waste), Set B (ethanol waste), Set C (yogurt waste), Set D (brewery waste), Set E (non-fat dry milk) and Set F (municipal waste). Different seed inoculum were used to obtain different starting microbial communities. Before startup, the inoculum for reactor sets C were acclimatized to non-fat dry milk and operating conditions for 2 months. All reactors were sparged with N_2:CO_2 gas mixture (7:3 ratio v/v) and fed synthetic industrial waste composed of non-fat dry milk (Roundy's; Milwaukee, WI) in basal nutrient medium (Speece, 2008). Biogas production was measured daily (24±1 h cycle) using a glass syringe. Each day, 4 ml of effluent was discarded and

replaced with 4 ml of feed to maintain a 15-day hydraulic retention time (HRT). The organic loading rate (OLR) was 2 g COD $L_R^{-1}day^{-1}$ except on days 45 and 90 when the reactors were shock overloaded with feed at a ten-times greater organic strength (20 g COD $L_R^{-1}day^{-1}$). Two ecological parameters (i.e., resistance and resilience) were used to measure reactor stability (Grimm et al, 1997; Neubert and Caswell, 1997; Hashsham et al, 2000). Resistance is defined as the maximum accumulation of the intermediate product, while resilience is defined as the time taken by the accumulated intermediate product to return to its referential state (Hashsham et al., 2000). Baseline values used to define both start up times and reactor recovery were: acetate (<200 mg L^{-1}), propionate (<100 mg L^{-1}), butyrate (<100 mg L^{-1}), pH (>7.3) and methane (>60%).

3.2.2 Analytical Methods

Effluent samples for physicochemical analyses were collected as follows: Phase 1 (days 6, 13, 20, 27, 34, 41, 43 and 45), Phase 2 (days 46, 47, 48, 49, 50, 52, 53, 57, 60, 64, 67, 73, 77, 83 and 90) and Phase 3 (days 91, 92, 93, 94, 95, 96, 100, 103, 106 and 115). Samples for volatile fatty acids (VFA) (acetic acid, propionic acid, iso-butyric acid, butyric acid, iso-valeric acid and valeric acid) and soluble COD (SCOD) concentration analysis were centrifuged at 10,000 g for 10 minutes. The supernatant was filtered through a 0.45 μM syringe filter (Bonna-Agela Technologies Inc., DE, USA) and immediately acidified with phosphoric acid (1%) for VFA analysis. VFA concentrations were measured using a gas chromatograph (7890A GC system; Agilent Technologies, CA, USA) equipped with a flame ionization detector (FID). SCOD was measured in the filtrate as described in Standard Methods (APHA et al., 1998). Biogas methane content was measured using a GC equipped with a thermal conductivity detector (TCD). Effluent pH was measured using a bench-top

pH meter and a general-purpose pH electrode (Orion; Thermo Fisher Scientific, Inc, Waltham, MA) as described in Standard Methods (APHA et al., 1998).

3.2.3 Molecular Analysis

3.2.3.1 DNA Extraction

Effluent samples for DNA extraction were collected as follows: Phase 1 (days 0 and 45), Phase 2 (days 52, 59, 66, 73, 80 and 90) and Phase 3 (days 97 and 104). DNA was extracted from 1 ml effluent sample with the PowerSoil Total RNA Isolation Kit (steps 1-10; MO BIO, Carlsbad, CA) followed by the PowerSoil DNA Isolation Kit (steps 8-13; MO BIO). DNA integrity was confirmed on 0.8% agarose gels stained with ethidium bromide (10 μg/mL) and quantified using a Nanodrop (ND-1000; ThermoScientific, Waltham, MA). The extracted DNA was stored in 10 mM Tris buffer (pH: 8) at -80°C until subsequent analysis.

3.2.3.2 Quantitative PCR

Quantitative PCR (qPCR) was carried out on a CFX Connect Real-Time PCR Detection System (Bio-Rad) according to the recommendations of Smith et al. (2006) and Smith and Osborn (2009). Minimum Information for Publication of Quantitative Real-Time PCR Experiments (MIQE) guidelines (Bustin et al., 2009) as applicable to environmental samples were followed. Target microbial groups including SFAB and methanogens included are listed in Table 3.1: hydrogenotrophic- (orders: Methanobacteriales and Methanomicrobiales) and acetoclastic- (families: Methanosarcinaceae and Methanosaetaceae) methanogens, and syntrophic propionate- (genera: *Syntrophobacter*, *Smithella*, and

Pelotomaculum), and butyrate- (genus: *Syntrophomonas*) degraders (Table 3.1). Standard curves (linear dynamic range: 10^2-10^8 gene copies per reaction) were constructed for each target group using 16S rRNA gene-based PCR products, derived from either pure culture DNA or environmental clones, using the group-specific primers used in this study (Table 3.1). qPCRs were performed in duplicate in a total volume of 20 µl and the final reaction mixture contained: 1× iTaq Universal SYBR Green Supermix (Bio-Rad), 500 nM of each primer, 1:10 dilution of extracted DNA and PCR-grade water. Each qPCR run included no-template controls. Amplification was performed as a two-step cycling procedure: initial denaturation at 95°C for 3 min, followed by 40 cycles at 95°C for 10 s and 55-60°C for 30 s (Table 3.1). Melt-curve analysis was performed after each run to confirm reaction specificity. Baseline and threshold calculations were determined with CFX Manager™ software (Bio-Rad).

Table 3.1: Primer sets used for quantification purposes in this study

Target Group	Primer	Sequence (5'-3')	T_m (°C)	Reference
Syntrophobacter (SBC)	SBC-695F SBC-844R	ATTCGTAGAGATCGGGAGGAATACC TGRKTACCCGCTACACCTAGTGMTC	60	Chapter 2 Mathai et al. (2015)
Smithella (SMI)	SMI-732F SMI-831R	GRCTTTCTGGCCCDATACTGAC CACCTAGTGAACATCGTTTACA	60	
Pelotomaculum (PEL)	PEL-622F PEL-877R	CYSDBRGMSTRCCTBWGAAACYG GGTGCTTATTGYGTTARCTAC	55	
Syntrophomonas (SMS)	SMS-637F SMS-757R	TGAAACTGDDDDTCTTGAGGGCAG CAGCGTCAGGGDCAGTCCAGDMA	60	
Methanobacteriales (MBT)	MBT857F MBT1196R	CGWAGGGAAGCTGTTAAGT TACCGTCGTCCACTCCTT	60	Yu et al. (2005)
Methanomicrobiales (MMB)	MMB282F MMB832R	ATCGRTACGGGTTGTGGG CACCTAACGCRCATHGTTTAC	60	
Methanosarcinaceae (MSC)	Msc380F Msc828R	GAAACCGYGATAAGGGGA TAGCGARCATCGTTTACG	60	
Methanosaetaceae (MST)	Mst702F Mst862R	TAATCCTYGARGGACCACCA CCTACGGCACCRACMAC	60	

3.3 Results

3.3.1 Phase 1: Reactor Startup (1-45 d)

3.3.1.1 Reactor Function

Six triplicate reactor sets (A-F) were established with seed biomass from different lab- and full-scale reactors. Reactor sets C and E displayed much faster startup times (less than a week) with no VFAs detected, in addition to high reactor pH and methane content (Fig. 3.1-3.6). Maximum VFA concentrations (g L^{-1}) in other reactor sets during this phase ranged from 0.4 to 5.7 (acetate), 2.3 to 4.8 (propionate) and 0.0 to 3.2 (butyrate). VFAs were subsequently degraded in all reactor sets, except in Set A, where propionate levels increased from 2.0 g L^{-1} (6 d) to 5.7 g L^{-1} (45 d). Increased acetate utilization between days 20 and 40 resulted in higher reactor pH and methane content (Fig. 3.3).

3.3.1.2 Microbial Dynamics

Three HRTs (i.e., 45 days) post startup, total SPOB (i.e., *Syntrophobacter* + *Smithella* + *Pelotomaculum*) abundance remained similar to that of the source inoculum for all reactor sets except Sets A and D, in which a 13- and 17-fold decrease was observed, respectively. Total SPOB (gene copies mL^{-1}) were least abundant in Set A (1.1×10^{7}) and Set F (1.9×10^{7}) (Fig. 3.8). In addition, the relative abundance of propionate degraders shifted during this period. *Syntrophomonas* (SMS) abundance increased ~12 fold in reactor sets A and F (Fig. 3.9). Methansarcinaceae (MSC) replaced Methanosaetaceae (MST) as the dominant acetoclast in four reactor sets [A, B, D and F] where its abundance increased 15, 5, 18 and 1200000-fold, respectively (Fig. 3.10). MST remained dominant in reactor sets C and E.

3.3.2 Phase 2: First Shock Overload (46-90 d)

3.3.2.1 Reactor Function

The shock overload resulted in a dramatic increase in VFA concentrations (Fig. 3.1-3.3). Moreover, pH and methane content dropped to their lowest concentrations in all reactors within two days of the shock overload (Fig. 3.4, 3.6). In most reactors, VFAs returned to baseline levels (acetate: 200 mg L^{-1}, propionate: 100 mg L^{-1}, butyrate: 100 mg L^{-1}) within 14 days post overload, except in Set A, Set B, C6 and Set F (Fig. 3.1-3.3). Reactor pH reached 7.3 in all reactors within 7 days, except for Set A, C5, C6 and Set D (Fig. 3.4). Methane content reached 60% within 7 days of the overload in most reactors, except for Set A, Set B, C5 and C6 (Fig. 3.6). Subsequent VFA buildup was observed: acetate (C4, C6, E4, E5, E6, F4, F5), propionate (C6, E6) and butyrate (C4, C6, E6) (Fig. 3.1-3.3). Prior to the second overload (90 d), elevated VFA concentrations were observed: acetate (C4, E5, E6, F4, F5), propionate (C6, E6) and butyrate (C4) (Fig. 3.1-3.3). A drastic decline in pH and methane content was observed in reactors C4, C6 and E6, of which only C6 recovered prior to the second overload (Fig. 3.4, 3.6).

3.3.2.2 Microbial Dynamics

Reactors [A5, A6, B4, F5 and F6] with a lower pre-overload SPOB abundance (~10^7 gene copies ml^{-1}) took 3-4 times longer to degrade propionate than those with higher numbers ($\geq 10^8$ gene copies ml^{-1}) (Fig. 3.8). A subsequent increase in SPOB abundance within these reactors was correlated with a decrease in propionate. After propionate was completely degraded, a fluctuation in SPOB numbers resulted in its buildup as observed within reactors C4, C6, E5 and E6 (Fig. 3.8). An increase in SPOB abundance post decline

restored function in reactor C6. A gradual decline in SMS numbers was observed in reactor sets A and F during this phase with no corresponding increase in butyrate (Fig 3.9). In contrast, a decline in SMS numbers in C6 resulted in butyrate buildup whereas a subsequent increase resulted in gain of function. In addition, SMS abundance increased in E5 and E6 (Fig 3.9). The shock overload resulted in a shift from MST to MSC in Set C and Set E; except C5. MST decreased in reactors C4, C6, E5, E6, F4, F5 and F6 (Fig. 3.10). Increased acetate utilization occurred after MSC increased in abundance: C6, E4, E5 and E6 (Fig. 3.10). A drop in MSC numbers, post recovery, was observed in B5 and B6.

3.3.3 Phase 3: Second Shock Overload (91-120 d)

3.3.3.1 Reactor Function

Reactor sets [A, B, D and F] were either more or equally resistant to the second shock overload when compared to the first (Fig. 3.1-3.6). In contrast, variability in resistance profiles was observed within replicates of Set C and Set E (Fig. 3.1-3.6). Reactor C6 was much more resistant to VFA buildup whereas reactors C4, E5 and E6 were more prone to VFA accumulation. Increased resilience to propionate was observed in reactors A5 A6, B4, C6, F5 and F6 when compared to the first shock overload (Fig. 3.1). Similarly, reactors A5, A6, B4 and C6 displayed improved resilience to acetate and butyrate (Fig. 3.2, 3.3). In contrast, process deterioration (e.g., VFA buildup) occurred in reactors C4, E5 and E6 (Fig. 3.1-3.7). Functional parameters in these reactors did not reach baseline levels within 25 days post second overload.

3.3.3.2 Microbial Dynamics

Total SPOB numbers were stable in all reactors except C4, E5 and E6 where they declined and resulted in a corresponding propionate buildup (Fig. 3.1, 3.8). An increase in SMS abundance post overload in C4 and Set E enhanced butyrate utilization (Fig 3.2, Fig 3.9). Increases in MSC numbers in C4 and C6 helped reduce acetate concentrations (Fig. 3.3, 3.10). Increased acetate levels triggered MSC growth in reactors E5 and E6. Increases in MSC corresponded with loss of MST within reactor sets C and E. Methanomicrobiales (MMB) was linked to reactor instability as they drastically increased in abundance in reactors C4, E5 and E6 (Fig. 3.11).

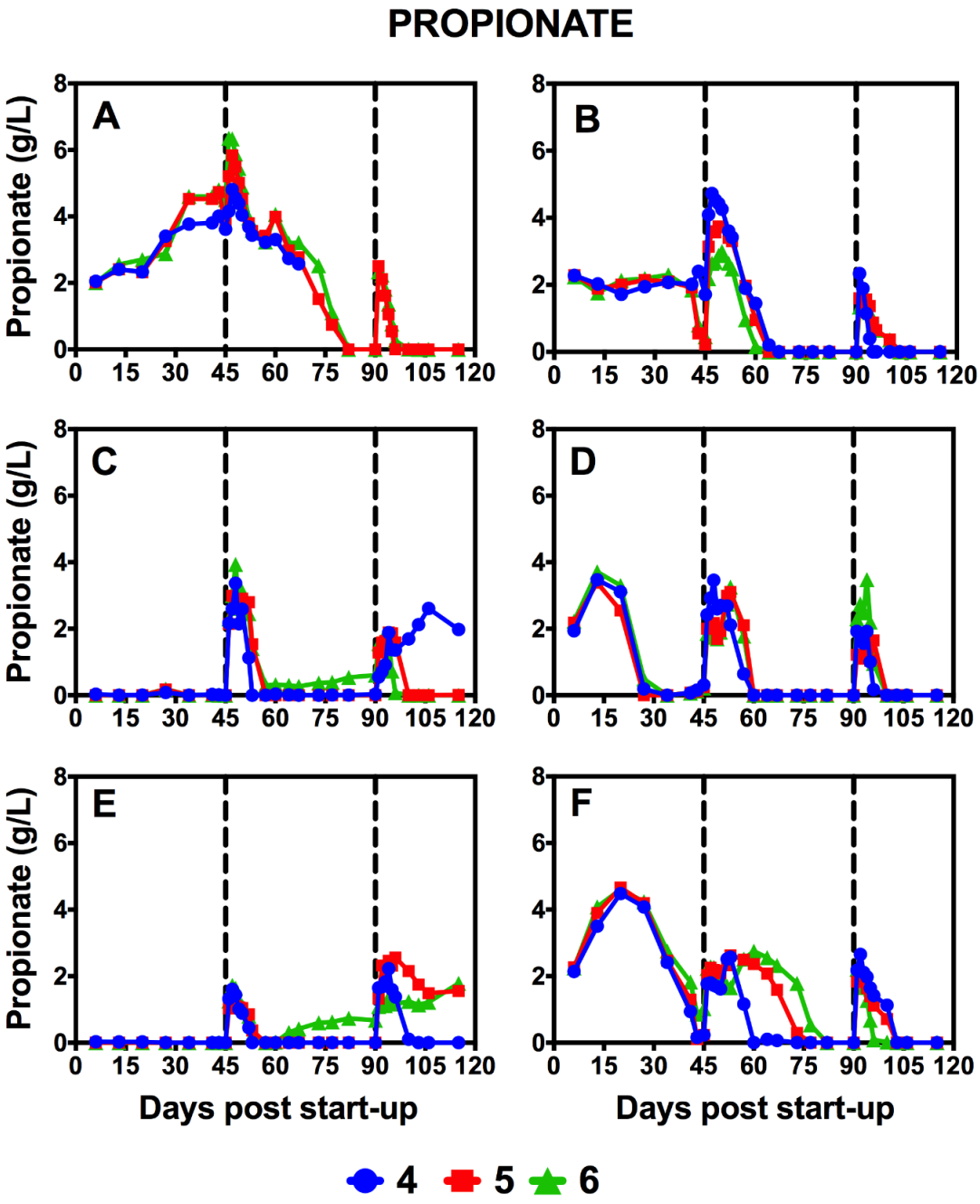

Figure 3.1: Propionate concentration in six different reactor sets: (A): Set A, (B): Set B, (C): Set C, (D): Set D, (E): Set E, and (F): Set F. Triplicate reactors within each set are shown in blue, red and green.

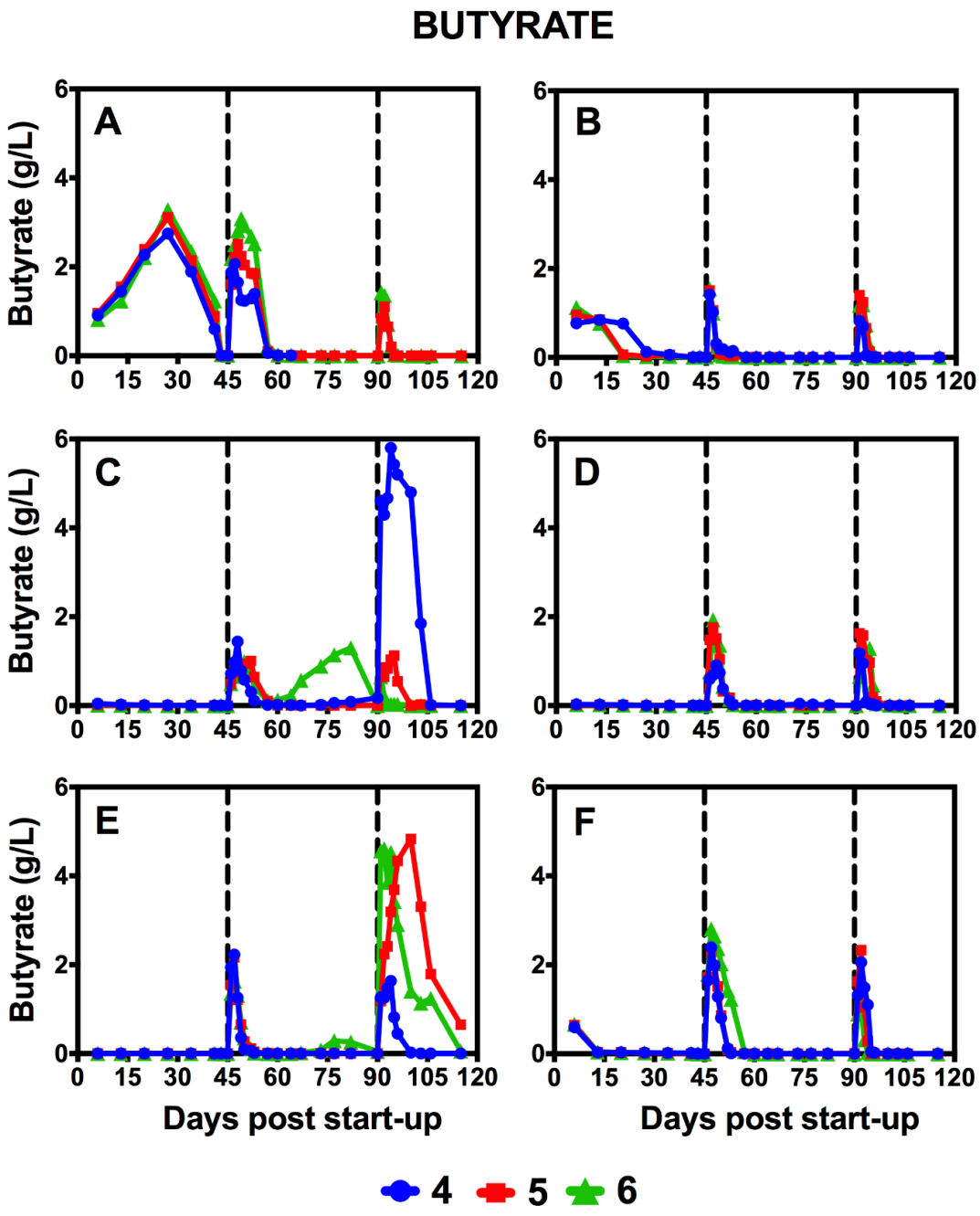

Figure 3.2: Butyrate concentration in six different reactor sets: (A): Set A, (B): Set B, (C): Set C, (D): Set D, (E): Set E, and (F): Set F. Triplicate reactors within each set are shown in blue, red and green.

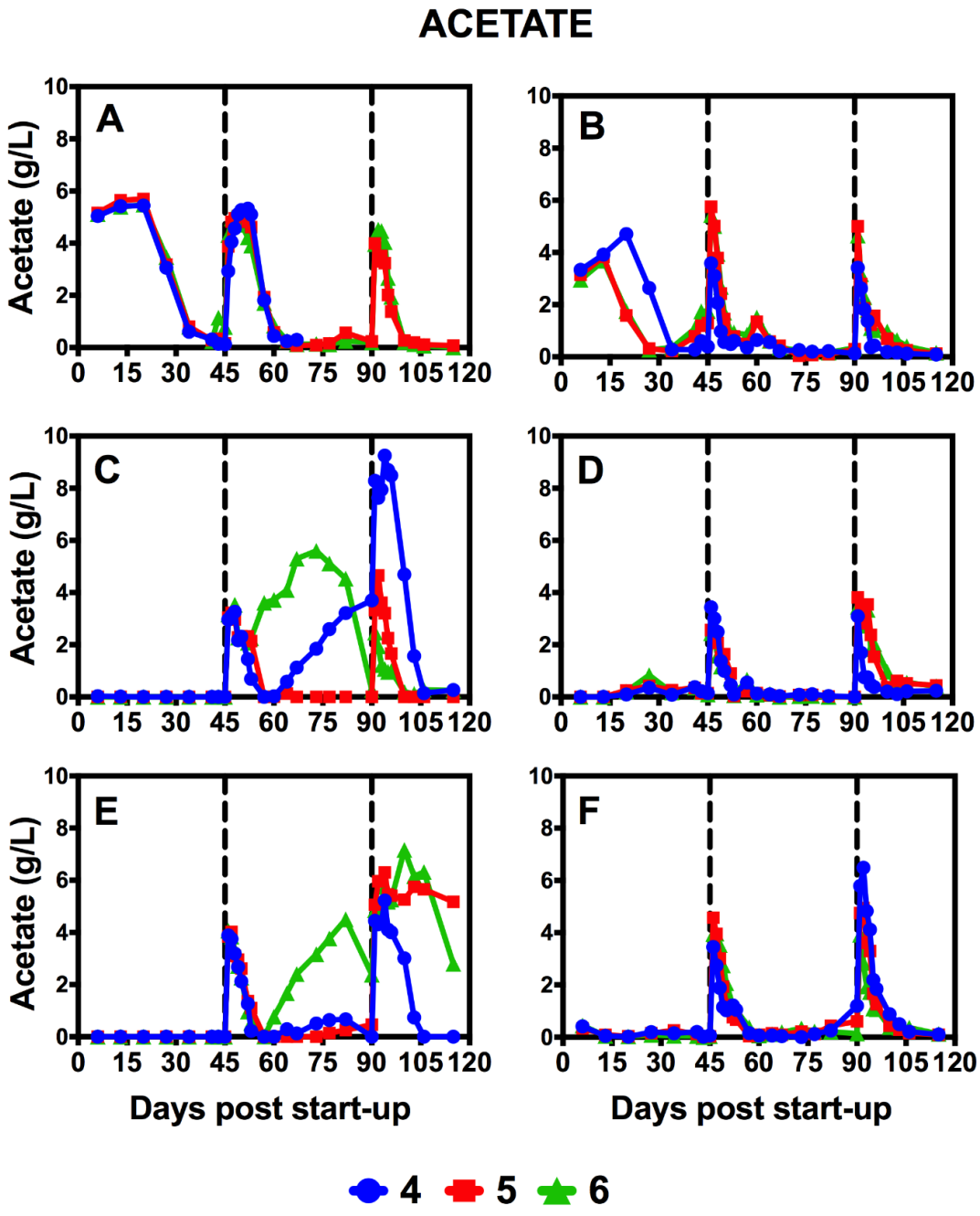

Figure 3.3: Acetate concentration in six different reactor sets: (A): Set A, (B): Set B, (C): Set C, (D): Set D, (E): Set E, and (F): Set F. Triplicate reactors within each set are shown in blue, red and green.

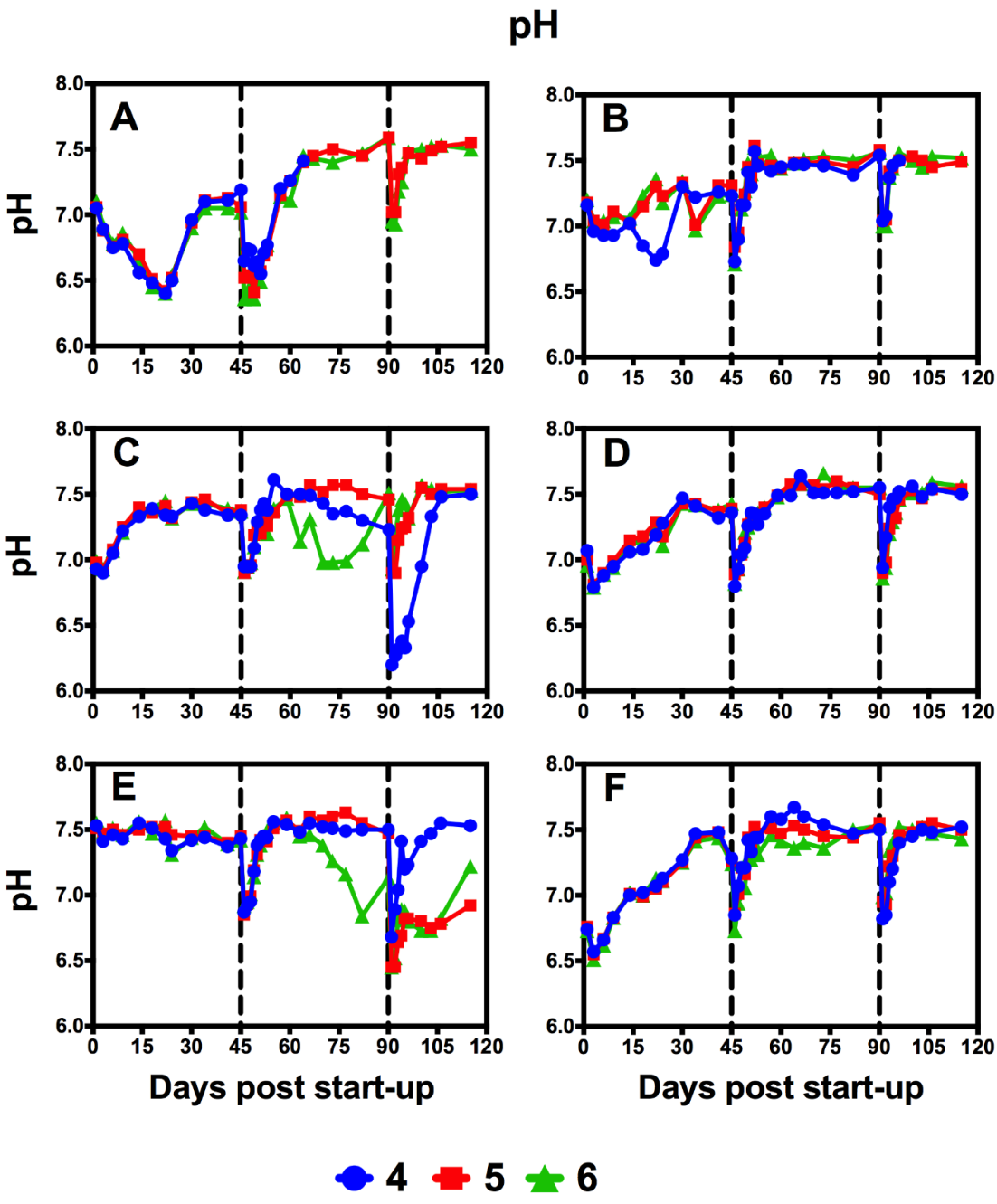

Figure 3.4: pH in six different reactor sets: (A): Set A, (B): Set B, (C): Set C, (D): Set D, (E): Set E, and (F): Set F. Triplicate reactors within each set are shown in blue, red and green

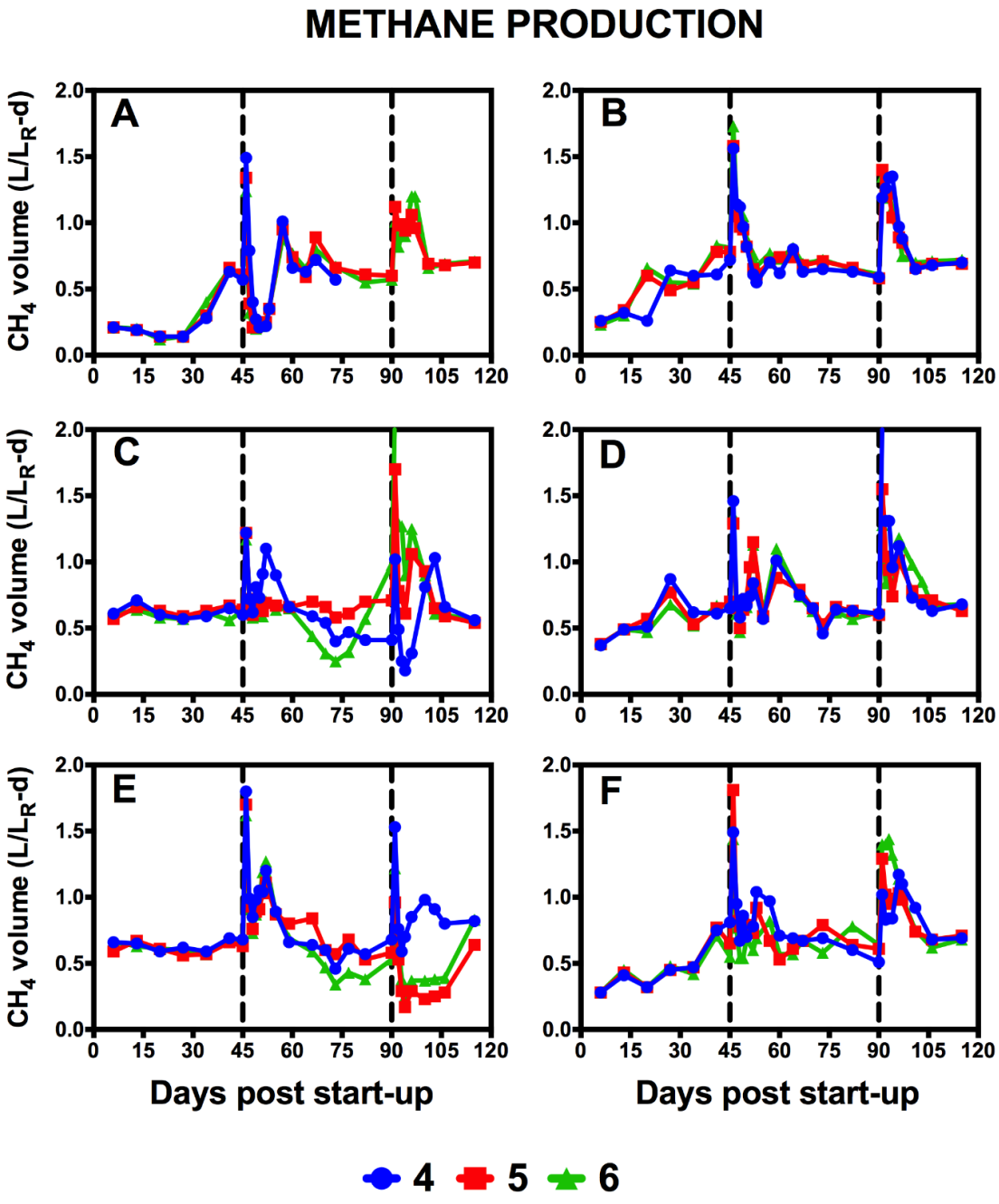

Figure 3.5: Methane production in six different reactor sets: (A): Set A, (B): Set B, (C): Set C, (D): Set D, (E): Set E, and (F): Set F. Triplicate reactors within each set are shown in blue, red and green

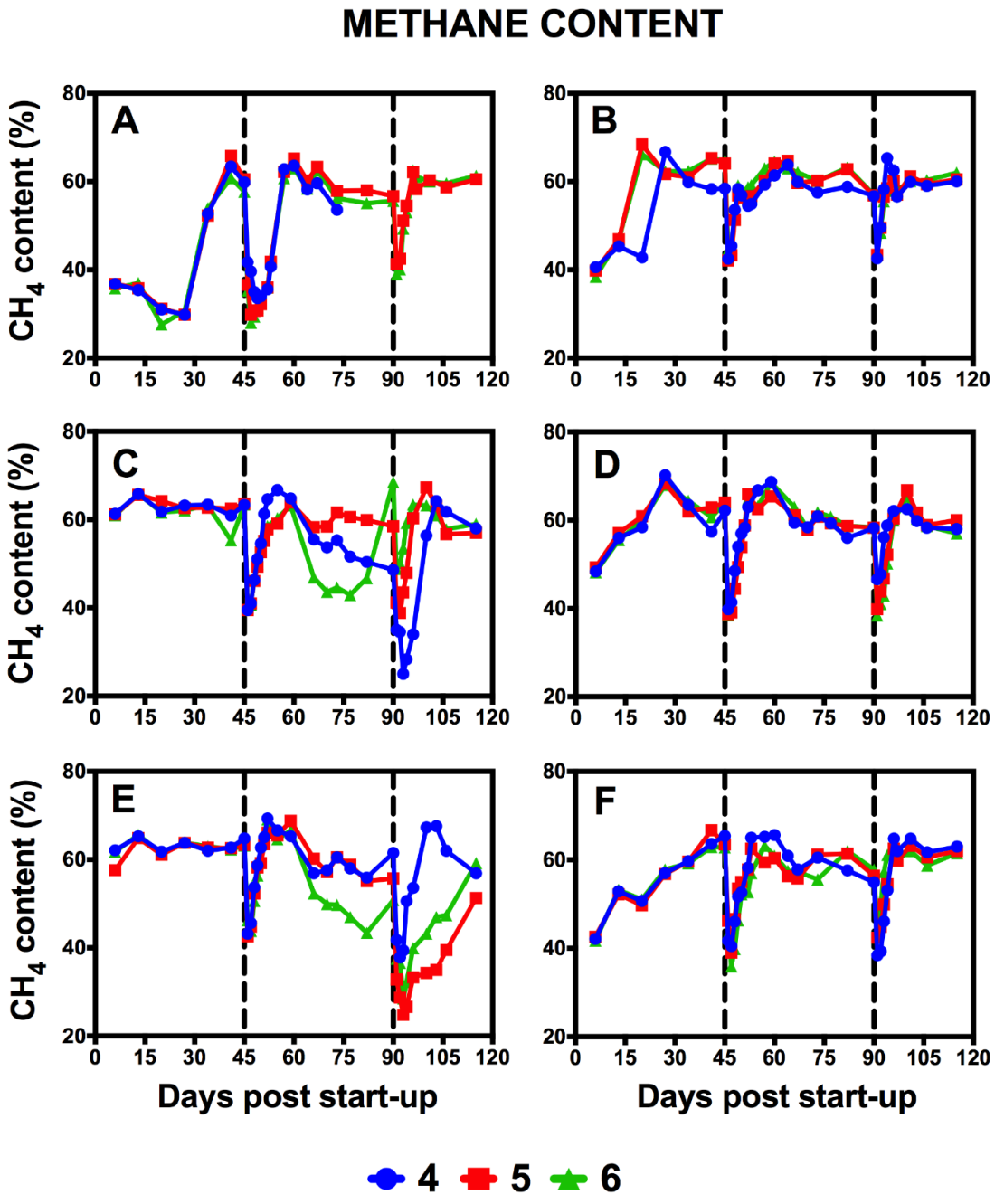

Figure 3.6: Methane content (%) in six different reactor sets: (A): Set A, (B): Set B, (C): Set C, (D): Set D, (E): Set E, and (F): Set F. Triplicate reactors within each set are shown in blue, red and green

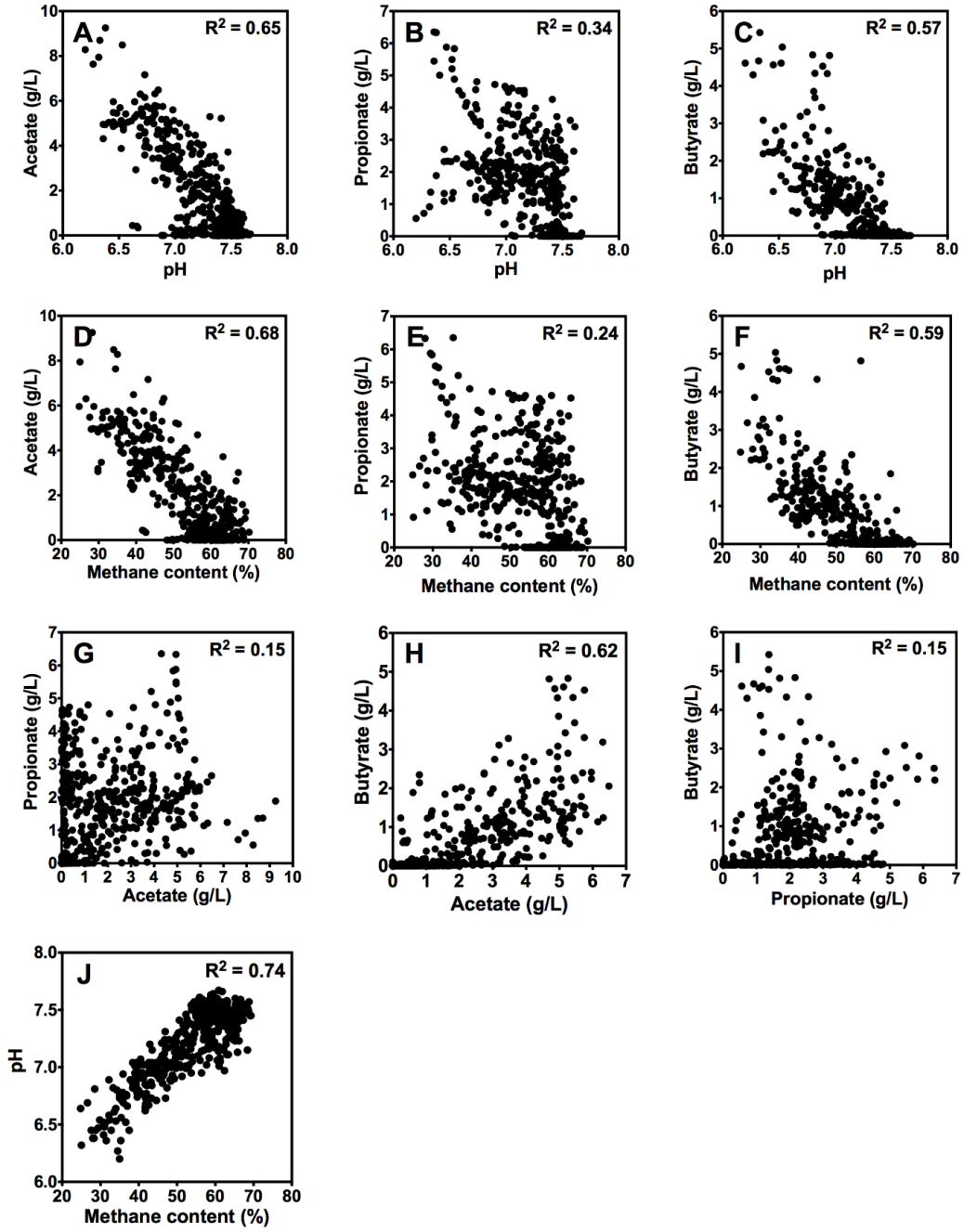

Figure. 3.7: Coefficient of determination analyses between different physicochemical parameters

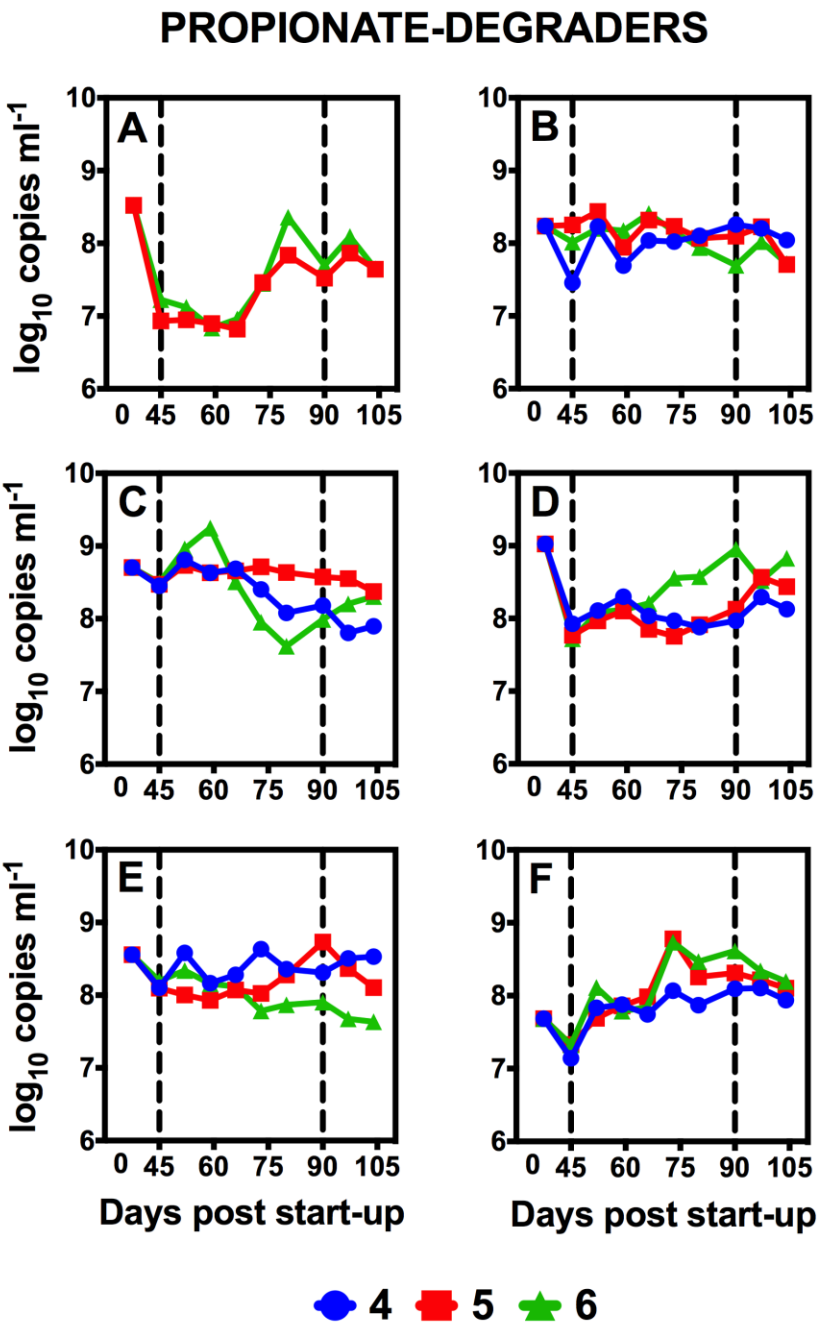

Figure 3.8: Quantification of total propionate-degraders (SBC+SMI+PEL) in six different reactor sets: (A): Set A, (B): Set B, (C): Set C, (D): Set D, (E): Set E, and (F): Set F. Triplicate reactors within each set are shown in blue, red and green

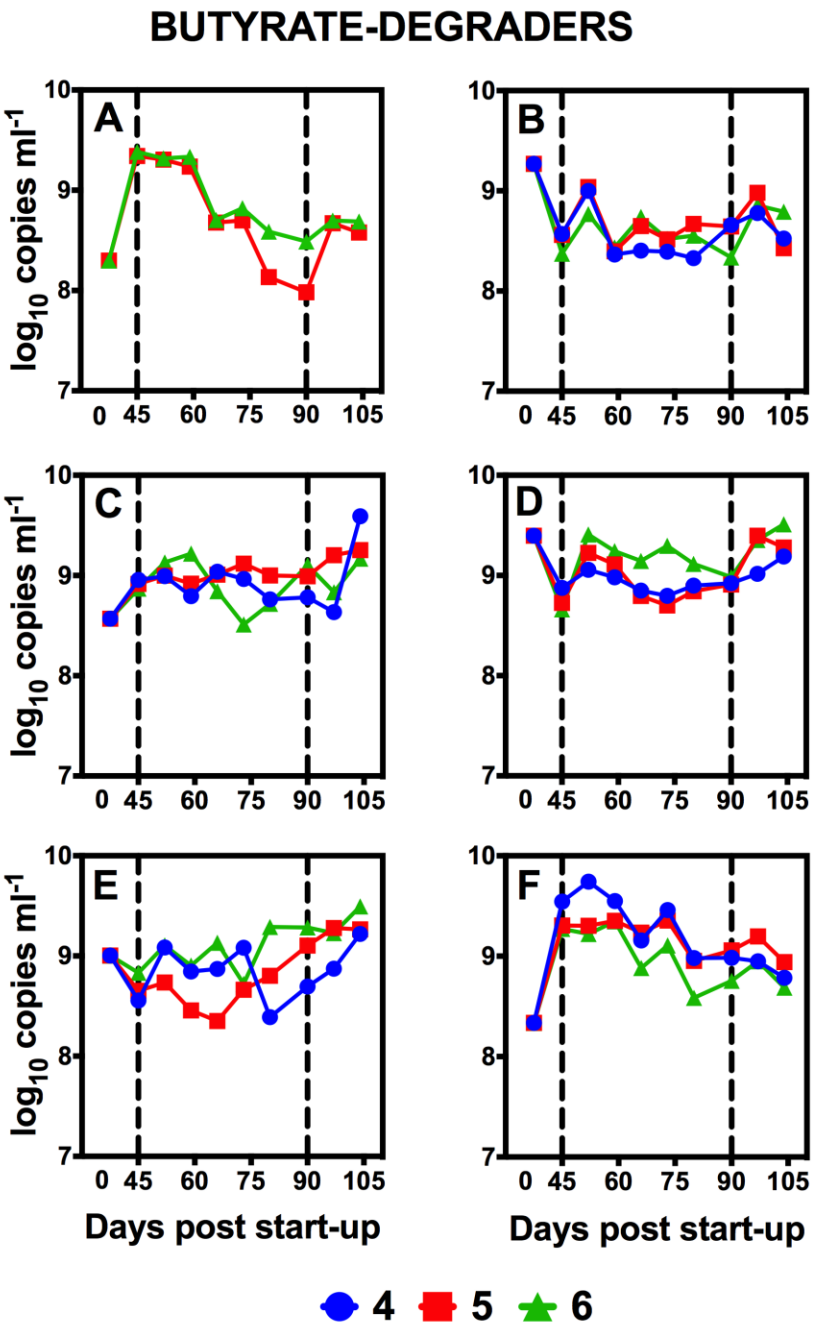

Figure 3.9: Quantification of butyrate-degraders in six different reactor sets: : (A): Set A, (B): Set B, (C): Set C, (D): Set D, (E): Set E, and (F): Set F. Triplicate reactors within each set are shown in blue, red and green

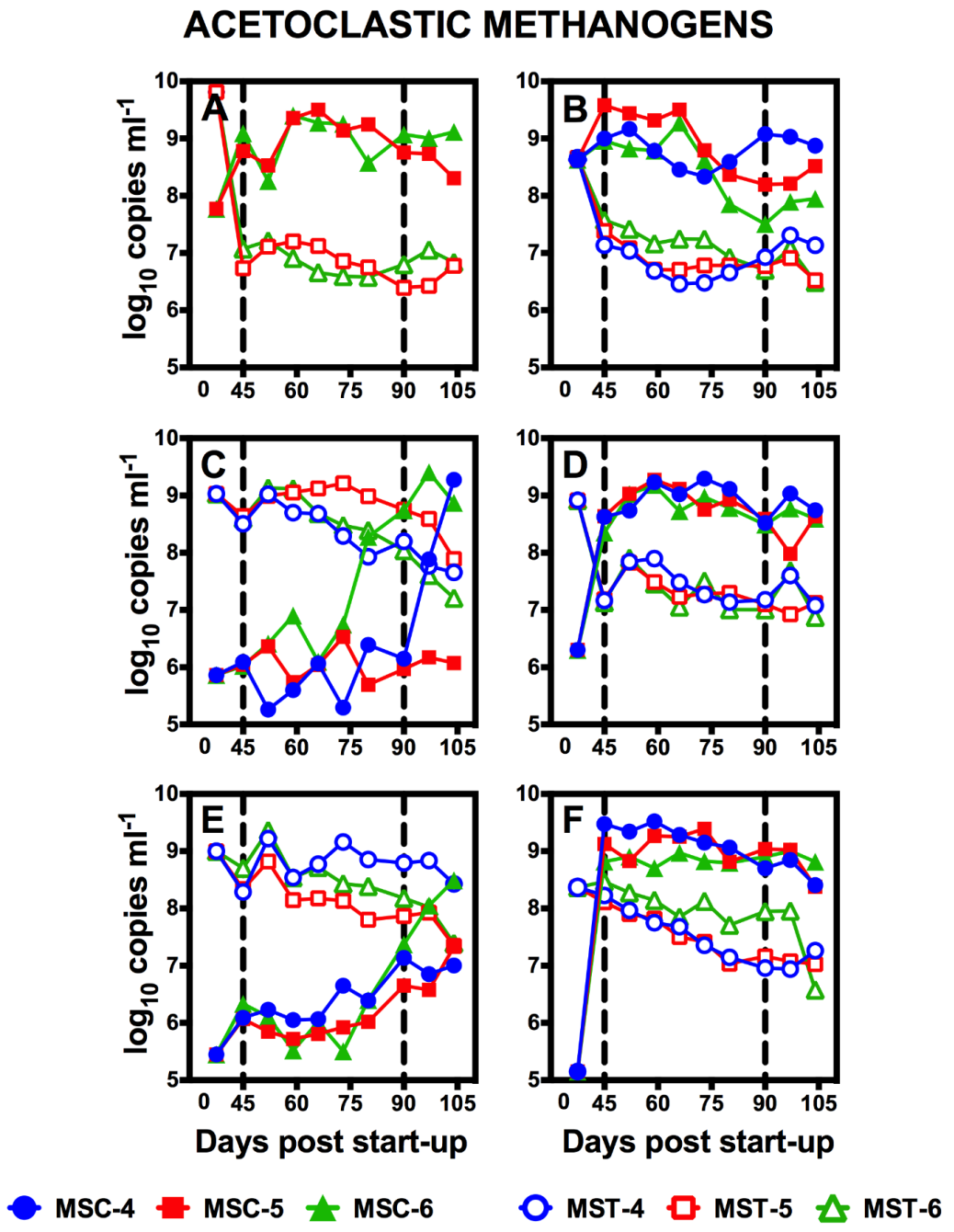

Figure 3.10: Quantification of acetoclastic methanogens in six different reactor sets. : (A): Set A, (B): Set B, (C): Set C, (D): Set D, (E): Set E, and (F): Set F. Triplicate reactors within each set are shown in blue, red and green. MSC= Methanosarcinaceae, MST= Methanosaetaceae

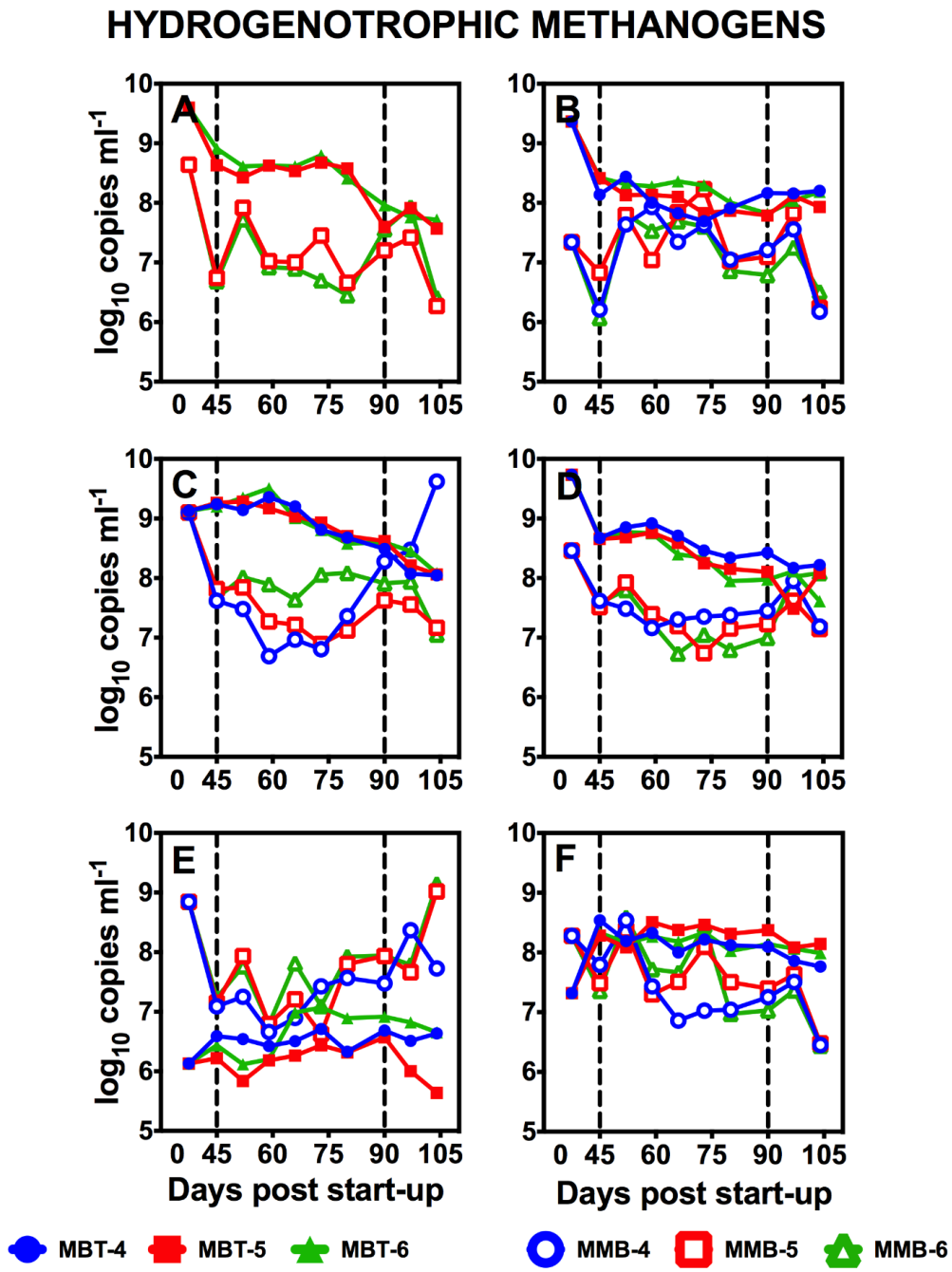

Figure 3.11: Quantification of hydrogenotrophic methanogens in six different reactor sets. : (A): Set A, (B): Set B, (C): Set C, (D): Set D, (E): Set E, and (F): Set F. Triplicate reactors within each set are shown in blue, red and green. MBT= Methanobacteriales, MMB= Methanomicrobiales

3.4 Discussion

3.4.1 Quantitative Significance of Syntrophic Microbial Communities in Reactor Stability During Organic Overload Perturbations

3.4.1.1 Propionate Degradation

Reactors [A,F] with lower numbers of SPOB (~10^7 gene copies mL^{-1}) took 2-3 times longer to degrade propionate than reactors [B-E] that harbored 10-50 times more SPOB. Reactors with these low SPOB numbers were less effective in countering the sudden increase in propionate (due to organic overload), which resulted in its buildup. VFA (esp. acetate and propionate) accumulation resulted in reduced pH (6.3-6.6; Fig. 3.4) in these reactor sets, which most likely affected SPOB growth. Boone and Xun (1987) demonstrated that the fastest growth of propionate enrichment cultures occurred between a pH of 6.8 and 8.5. Propionate degradation is inhibited at lower pH due to an increase in the undissociated forms of acetate and propionate (Fukuzaki et al., 1990). These authors proposed that increased levels of undissociated acids accelerated their entry into cells and caused a drop in intracellular pH. Proton extrusion from the cell would require the hydrolysis of ATP, which would reduce the amount available for growth and metabolism.

A drop in propionate levels occurred only after reactor pH increased to 7.3-7.5, which corresponded to drop in acetate levels (Fig. 3.1, 3.3, 3.4). This finding relates well to previous studies that reported that propionate degradation was inhibited at high acetate levels (Gorris et al., 1989; Mawson et al., 1991; Lier et al., 1993). Similar results have been previously reported where propionate was found to persist longer than other intermediates after a perturbation (Smith and McCarty, 1990). The onset of favorable environmental conditions resulted in a significant increase in SPOB abundance (Fig. 3.8 A,F), which perfectly corresponded to specific periods of enhanced propionate degradation (Fig. 3.1 A,F). Moreover, reactor sets A and F were

much more resilient to the second overload (90 d) when compared to the first overload (45 d). Faster propionate degradation (5-6 fold) was linked to the increased abundance of propionate degraders in these reactor sets. These results correspond well to Tale et al. (2011) who reported faster recovery of overloaded reactors when they were bioaugmented with propionate enrichment cultures. In addition, loss of propionate degraders resulted in its accumulation as observed with reactors C4, C6, E5 and E6. Propionate levels decreased in these reactors only if degraders increased in abundance (e.g., C6). Overall, our results suggest that a higher abundance of propionate degraders (≥ 0.1% relative abundance) improves the resilience (recovery time) of anaerobic reactors when exposed to organic overload perturbations.

All three genera involved in propionate degradation, i.e. *Syntrophobacter*, *Smithella* and *Pelotomaculum*, were detected in all reactor samples throughout the course of this experiment. This result is not surprising, as the coexistence of these phylogenetically diverse but functionally redundant bacteria has been previously documented (Ariesyady et al., 2007b; Ito et al., 2012; Narihiro et al., 2012). It is likely that physiological differences between SPOB species is utilized to maintain stable reactor function under fluctuating environmental conditions. Specific growth rates of SPOB species in co-culture with the methanogen *Methanospirillum hungatei* have been reported as follows: *S. fumaroxidans*: 0.17 d^{-1} (Harmsen et al., 1998), *S. wolinii*: 0.1 d^{-1} (Boone and Bryant, 1980), *S. pfennigii*: 0.07 d^{-1} (Wallrabenstein et al., 1995), *P. schinkii*: 0.1 d^{-1} (de Bok et al., 2005) and *P. propionicum*: 0.2 d^{-1} (Imachi et al., 2007). On the other hand, substrate affinity for total propionate has been reported to range from 0.1 to 5mM (Kaspar and Wuhrnann, 1978; Heyes and Hall, 1983; Lawrence and McCarty, 1969; Kus and Weismann 1995; Fukuzaki et al., 1990). Using propionate-fed chemostats, Shigematsu et al. (2006) reported that *Syntrophobacter* dominated at low dilution rates while *Pelotomaculum* dominated at high dilution rates, which is also suggested by our results. This relates well to our finding that *Pelotomaculum* and *Smithella* were the most responsive SPOB during specific periods of enhanced propionate degradation. Our results

suggest that *Pelotomaculum* spp. have high growth rates while *Syntrophobacter* spp. have high substrate affinity. It should be noted that SPOB-specific qPCR assays used in this study are much more inclusive and sensitive than hybridization-based detection techniques (Chapter 2; Mathai et al., 2015). Thus, it is highly likely that the abundance data presented here also includes that of uncultured propionate degraders within those genera.

3.4.1.2 Butyrate Degradation

Unlike propionate, no significant lag in butyrate degradation was observed as it was completely degraded in all reactor sets within two weeks of the first shock overload. Butyrate degradation was not a rate-limiting step in this study, which was attributed to the high abundance of butyrate degraders in all reactor sets (Fig. 3.9). Butyrate buildup in all reactors was tightly linked to acetate concentrations (Fig. 3.7). This relates well to previous findings that increase in hydrogen and acetate levels inhibited butyrate utilization (Labib et al., 1992; Schmidt and Ahring, 1993).

Butyrate levels could be linked to the population dynamics of butyrate degraders. Loss of SMS resulted in butyrate buildup as observed with reactors C4, C6 and E6. Butyrate levels declined in these reactors only after SMS increased in abundance. Interestingly, reactor sets [A, F] with a higher pre-overload abundance of butyrate degraders were not able to degrade butyrate faster than any other reactor sets. It should be noted that these reactor sets A and F underwent a more difficult startup period when compared to all other reactor sets. Though not quantified in this study, it is likely that higher chain fatty acids (C5-C18) were formed during this period. The fact that most species within SMS (e.g. *S. wolfei*, *S. palmitatica*, *S. zehnderi*) can utilize the majority of these acids as substrates (in addition to butyrate) could explain their high abundance in the stressed reactor sets. SMS numbers subsequently reduced in these reactors after they reached stable operation.

3.4.1.3 Acetate Degradation

Reactor sets with a higher abundance of MSC were better able to tolerate elevated acetate levels formed as a result of the shock overload. In contrast, all MST-dominated reactors (except C5) became functionally unstable after the perturbation. These reactors [C4, C6, E5, E6] stabilized only with the emergence of MSC, which increased in abundance to counter high acetate levels. It is interesting to note that a rapid growth of MSC in MST-dominated reactor sets was observed only after acetate levels crossed 3 g L^{-1}, which is considered to be the maximum acetate tolerance limit for MST (De Vrieze et al., 2012). The dynamic transition of MSC to elevated acetate levels has been previously documented (Delbes et al., 2001; Hori et al., 2006). In addition, Yu et al. (2006) showed that MST dominated at low acetate levels, whereas MSC outcompeted MST at high acetate levels.

MSC has several other physiological advantages over MST that could be utilized during stressed conditions (De Vrieze et al., 2012). MSC spp. are tolerant to sudden changes in pH (0.8-1.0 units) and elevated acetate levels (up to 15 g L^{-1}), while MST spp. tend to be affected by a pH shock of 0.5 units or less and can tolerate acetate up to 3 g L^{-1} (Conklin et al., 2006; Yu et al., 2006). Interestingly, MSC was able to maintain its dominance in most reactor sets even after the acetate levels declined. It is possible that operating these reactors for a much longer period of time (without perturbation) would have resulted in a shift in the acetoclastic structure because species within MST (e.g. *Methanosaeta concilii*) are reported to have long doubling times (~3 days) (Patel and Sprott, 1990). Overall, our results suggest that the pre-perturbation abundance of MSC contributes reactor resilience to acetate buildup during overload perturbations.

3.4.2 Influence of Inoculum on the Performance of Replicate Reactors Operated Under Identical Conditions

Biomass acclimation to the model substrate and operating conditions resulted in much

faster reactor startup times, as observed with reactor sets C and E. In contrast, all reactor sets that underwent a difficult startup period were inoculated with biomass from full-scale industrial reactors fed different substrates. Previous studies have reported that AD microbial structure is strongly influenced by factors such as substrate type and operating conditions (Karakashev et al., 2005; Krakat et al., 2010; Krakat et al., 2011; Sundberg et al., 2013). Results from this study suggest that biomass obtained from full-scale reactors were not optimized to deal with the new conditions and (or resources) as substantial shifts in microbial structure was observed in these reactors during the startup period. In contrast, reactor sets [C, E] inoculated with pre-acclimated biomass maintained a similar microbial structure throughout the startup period. Our results relate well with Pagaling et al. (2014) who reported that when microbial communities are faced with a novel environment, the final structure and function are unpredictable, while they were more reproducible when the source communities were pre-acclimated to their new habitat.

Our findings suggest that reactor sets with a stable operational history were functionally less so when perturbed than those that underwent a turbulent startup period. We observed that process stability and functional resilience post overload were dependent upon the pre-perturbation abundance of propionate degraders and *Methanosarcinaceae*. The data suggests that the abundance of these populations is linked to the frequency and intensity of previous perturbations, which needs to be determined. In addition, replicates within MST-dominated reactor sets were not reproducible as replicate microbial communities diverged in both structure and function. It is likely that reproducibility of these reactor sets [C, E] was affected due to the low abundance of MSC, which (unlike MST) can tolerate high acetate levels. On similar lines, Hashsham et al. (2000) reported that under perturbed conditions significant deviations within replicate reactors are possible and speculated that this was due to the presence of numerically minor but important populations.

3.5 Conclusions

The abundance of total SPOB and acetoclastic methanogens (esp. *Methanosarcinaceae*) determined the functional resilience of shock-overloaded reactors. Reactor sets with high SPOB numbers degraded propionate much faster (3-4×) than those with lower numbers. Subsequent increases in SPOB abundance resulted in enhanced propionate degradation In contrast, loss of propionate degraders led to propionate accumulation. Functional redundancy was observed within all genera (*Syntrophobacter*, *Smithella* and *Pelotomaculum*) involved in propionate degradation. Reactor sets with high numbers of *Methanosarcinaceae* were better able to deal with elevated acetate concentrations than those dominated by *Methanosaetaceae*. A shift in acetoclastic structure from *Methanosaetaceae* to *Methanosarcinaceae* drastically increased acetate utilization, thus, improving reactor stability. Though pre-acclimation of source inoculum hugely reduced reactor startup times, only those reactors that maintained or developed key syntrophic populations (both propionate-degraders and Methanosarcinaceae) were able to efficiently deal with the overload perturbation.

CHAPTER IV

THE EFFECT OF DIFFERENT ORGANIC LOADING RATES ON SYNTROPHIC MICROBIAL COMMUNITIES IN LAB-SCALE DIGESTERS

4.1 Introduction

Anaerobic digestion (AD) is an effective method for treating high-strength organic wastes. Among its advantages over aerobic processes include lower energy requirements and amounts of sludge generated, as well as production of methane that can be used as renewable source of energy. However, extensive application of AD has been hampered due to operational and stability issues. One important operational parameter that is linked to reactor stability is the organic loading rate (OLR), which combines both substrate concentration and flow rate. AD reactor performance is usually stable for organic wastes with a consistent composition and steady flow rate; however, in practice, the inflow of wastes into a reactor is often subjected to fluctuations in quality and quantity, resulting in OLR variation. High OLRs could trigger process instability as the rates of the early steps in AD of hydrolysis and acidogenesis could be faster than the later steps of acetogenesis and methanogenesis. The resultant buildup of VFA can eventually lead to a very slowly reversible acidification (Nagao et al., 2012). Previous studies have mainly focused on the aspects of process control and monitoring to improve process stability and efficiency without including information on the microbes. As a consequence, the capacity to control and predict system disturbance is somewhat restricted, and can lead to sudden failure.

Microorganisms are at the core of digesters as AD is a biochemical process mediated by a variety of microbial groups. Hence, understanding the microbial community is crucial for improving efficiency and process stability in AD. Numerous studies have looked into the influence of process parameters and environmental conditions on the composition of AD microbial communities (Karakashev et al, 2005; Krakat et al, 2010; Krakat et al, 2011; Lee et al,

2011; Bocher et al, 2015). The effect of OLR on microbial community structure has been previously studied (Jang et al., 2014; Gou et al., 2014; Kundu et al., 2013; Razaviarani and Buchanan, 2014) though all studies focused on a snapshot of steady state structure, and not on what happened during the stages of process deterioration. Few studies have examined the effect of acidification (i.e., transition from stable to deteriorative function) on reactor microbial structure (Blume et al, 2010; Lerm et al, 2012; Hori et al, 2006; Delbes et al, 2001). However, these studies did not continuously monitor changes in the microbial community structure during the transition period, instead, microbial analysis was done before and after process failure. Moreover, traditional microbial community fingerprinting methods such as single-strand conformation polymorphism (SSCP) and denaturing gradient gel electrophoresis (DGGE) were used, and these can only provide insight into the dominant microorganisms. Monitoring the transition phase is important as it could provide insight into key indicators of process stability and/or instability. The advent of high-throughput sequencing has enabled an in-depth analysis of microbial communities, which can be used to identify and track microbes with low abundance that are functionally important in these reactors.

The major focus of this study was to investigate the effect of increasing OLR on the microorganisms involved in fatty acid degradation as VFA accumulation is often reported to result in process deterioration. Despite the importance of these bacteria, no analysis has been done before to track them at different OLRs and during transition from a stable to process failure, as characterized by inhibition of methanogenesis. The VFAs propionate and butyrate are degraded to acetate, H_2 and CO_2 in syntrophic association with H_2-utilizing methanogens. Formation of CH_4 from H_2/CO_2 is performed by hydrogenotrophic methanogens, whereas acetate utilization can occur via two pathways: acetoclastic methanogenesis or syntrophic acetate oxidation (SAO). SAO is a two step reaction in which acetate is oxidized to H_2/CO_2 by syntrophic acetate oxidizing bacteria, followed by subsequent reduction of CO_2 to methane via

hydrogenotrophic methanogens. Under mesophilic conditions, it has been shown that high ammonia concentrations can trigger SAO (Schnurer et al., 1999).

The objective of this study was to investigate the effect of different OLRs on (1) reactor function, (2) overall microbial community structure and (3) syntrophic microbial communities, during stable and deteriorative phases of reactor operation. To complete this study, physicochemical and molecular (high-throughput sequencing and qPCR) analyses were performed on lab-scale reactors operated at different OLRs.

4.2 Materials and Methods

4.2.1 Reactor Set-Up and Operation

Five triplicate reactor sets (OLR-1, OLR-2, OLR-3, OLR-4 and OLR-5) were established in 160 ml serum bottles using a single homogenous blend of biomass samples collected from seven mesophilic ADs (that treated food/beverage, ethanol, yogurt, brewery, municipal, propionate and non-fat dry milk waste) as the starting culture. All reactors were sparged with N_2:CO_2 gas mixture (7:3 ratio v/v) and fed synthetic wastewater, composed of non-fat dry milk (Roundy's; Milwaukee, WI) in basal nutrient medium. The basal nutrient medium contained [mg/L]: $NaHCO_3$ [5000]; NH_4Cl [400]; $MgSO_4 \cdot 6H_2O$ [250]; KCl [400]; $CaCl_2 \cdot 2H_2O$ [120]; $(NH_4)_2HPO_4$ [80]; $FeCl_3 \cdot 6H_2O$ [55]; $CoCl_2 \cdot 6H_2O$ [10]; KI [10] and trace metal salts ($MnCl_2 \cdot 4H_2O$, NH_4VO_3, $CuCl_2 \cdot 2H_2O$, $Zn(C_2H_3O_2)_2 \cdot 2H_2O$, $AlCl_3 \cdot 6H_2O$, $NaMoO_4 \cdot 2H_2O$, H_3BO_3, $NiCl_2 \cdot 6H_2O$, $NaWO_4 \cdot 2H_2O$, and Na_2SeO_3) [each at 0.5]. All reactors were incubated on a shaker table (100 rpm) at 37±1°C.

Biogas production was measured daily (24±1 h cycle) using a glass syringe. Each day, 4 ml effluent was discarded and replaced with 4 ml feed to maintain a 15 d hydraulic retention time (HRT). Reactor set OLR-1 was fed non-fat dry milk at 1 g COD L_R^{-1} day^{-1}, whereas the loading

rate for all other reactor sets (OLR-2, OLR-3, OLR-4, and OLR-5) started at 1 g COD $L_R^{-1}day^{-1}$ and was increased by 1 g COD $L_R^{-1}day^{-1}$ every 15 days until the desired OLR was attained (2-, 3-, 4- and 5 g COD $L_R^{-1}day^{-1}$, respectively). Each reactor set was then operated at the desired OLR for at least 4 HRTs (i.e., 60 d). On 120 d, the loading rate for reactor set OLR-5 was increased from 5 g COD $L_R^{-1}day^{-1}$ to 6 g COD $L_R^{-1}day^{-1}$ and operated for an additional 2 HRTs (30 d).

4.2.2 Analytical Methods

Effluent samples were collected approximately once a week from each reactor for physicochemical analysis. Samples for volatile fatty acids (VFA) (acetic acid, propionic acid, iso-butyric acid, butyric acid, iso-valeric acid and valeric acid) and soluble COD (SCOD) concentration analysis were centrifuged at 10,000 g for 10 minutes. The supernatant was filtered through a 0.45 μM syringe filter (Bonna-Agela Technologies Inc., DE, USA) and immediately acidified with phosphoric acid (1%) for VFA analysis. VFA concentrations were measured using a gas chromatograph (7890A GC system; Agilent Technologies, CA, USA) equipped with a flame ionization detector (FID). SCOD was measured in the filtrate as described in Standard Methods (APHA et al., 1998). Biogas methane content was measured using a GC equipped with a thermal conductivity detector (TCD). Effluent pH was measured using a bench-top pH meter and a general-purpose pH electrode (Orion; Thermo Fisher Scientific, Inc, Waltham, MA) as described in Standard Methods (APHA et al., 1998).

4.2.3 Molecular Analysis

4.2.3.1 DNA Extraction

For molecular analysis, effluent samples were collected from the starter inoculum (0 d) and from triplicate reactor sets OLR-1 to OLR-4 after four HRTs (60 d) at the desired OLR

(OLR-1: 60 d; OLR-2: 75 d; OLR-3: 90 d; OLR-4: 105 d). In addition, effluent samples were periodically collected from the reactor set OLR-5 each HRT (15-, 30-, 45-, 60-, 75-, 90-, 105-, 120-, 135-, and 150 d) throughout the course of the experiment. DNA was extracted from 1 ml effluent sample with the PowerSoil Total RNA Isolation Kit (steps 1-10; MO BIO, Carlsbad, CA) followed by the PowerSoil DNA Isolation Kit (steps 8-13; MO BIO). DNA integrity was confirmed on 0.8% agarose gels stained with ethidium bromide (10 $\mu g\ mL^{-1}$) and quantified spectrophotometrically (Nanodrop ND-1000; ThermoScientific, Waltham, MA). The extracted DNA was stored in 10 mM Tris buffer (pH: 8) at -80°C until subsequent analysis.

4.2.3.2 High-Throughput Sequencing and Analysis

Twenty-five DNA samples were selected for high-throughput sequencing, which included: seed inoculum (0 d) and triplicate reactor sets: OLR-1 (60 d), OLR-2 (75 d), OLR-3 (90 d), OLR-4 (105 d) after 4 HRTs at desired OLR, and OLR-5: (90-, 105-, 120- and 135 d). DNA samples were sent to Molecular Research DNA Lab (Texas, USA) for sequencing, with universal primers: 515f (5'-GTGCCAGCMGCCGCGGTAA) and 806r (5'-GGACTACHVGGGTWTCTAAT) targeting the V4 region of the 16S rRNA gene, on Illumina MiSeq platform using a 2×300-bp paired end protocol. Sequences were preprocessed and analyzed using mothur v.1.35.1 (Schloss et al., 2009) following the MiSeq standard operating procedure (Kozich et al., 2013). In brief, paired-end reads were merged, depleted of barcodes and primers, sequences <150 bp and ambiguous base calls removed. PCR chimeras were screened using UCHIME (Edgar et al., 2011). A naïve Bayesian classifier was used to classify sequences against the Ribosomal Database Project (RDP) 16S rRNA gene training set (version 9) at 80% bootstrap confidence score (Wang et al., 2007). Sequences were classified into operational taxonomic units (OTUs) at 3% dissimilarity levels. Shannon indices were used to characterize diversity and evenness, and Chao I was used to provide estimates of species richness (Fig. 4.3)

and principal coordinates analysis was performed using Bray-Curtis dissimilarity (Fig 4.4).

4.2.3.3 Quantitative PCR (qPCR)

Quantitative PCR (qPCR) was carried out on a CFX Connect Real-Time PCR Detection System (Bio-Rad; Hercules, CA) according to the recommendations of Smith et al. (2006) and Smith and Osborn (2009). Minimum Information for Publication of Quantitative Real-Time PCR Experiments (MIQE) guidelines (Bustin et al., 2009) as applicable to environmental samples were followed. Target groups included: hydrogenotrophic- (orders: Methanobacteriales and Methanomicrobiales) and acetoclastic- (families: Methanosarcinaceae and Methanosaetaceae) methanogens, syntrophic propionate- (genera: *Syntrophobacter*, *Smithella* and *Pelotomaculum*), butyrate- (genus: *Syntrophomonas*), and acetate- (species: *Clostridium ultunense*, *Syntrophaceticus schinkii* and *Tepidanaerobacter acetatoxydans*) oxidizing bacteria (Table 4.1). Standard curves (linear dynamic range: 10^2-10^8 gene copies per reaction) were constructed for each target group using 16S rRNA gene-based PCR products, derived from either pure culture DNA or environmental clones, using the group-specific primers used in this study (Table 4.1). qPCRs were performed in duplicate in a total volume of 20µl and the final reaction mixture contained: 1×iTaq Universal SYBR Green Supermix (Bio-Rad), 500 nM of each primer, 1:10 dilution of extracted DNA and PCR-grade water. Each qPCR run included no-template controls. Amplification was performed as a two-step cycling procedure: initial denaturation at 95°C for 3 min, followed by 40 cycles at 95°C for 10 s and 55-63°C for 30 s (Table 4.1). Melt-curve analysis was performed after each run to confirm reaction specificity. Baseline and threshold calculations were determined with CFX Manager™ software (Bio-Rad).

Table 4.1: Primer sets used for quantification purposes in this study

Target Group	Primer	Sequence (5'-3')	T_m (°C)	Reference
Syntrophobacter	SBC-695F SBC-844R	ATTCGTAGAGATCGGGAGGAATACC TGRKTACCCGCTACACCTAGTGMTC	60	Chapter 2; Mathai et al. (2015)
Smithella	SMI-732F SMI-831R	GRCTTTCTGGCCCDATACTGAC CACCTAGTGAACATCGTTTACA	60	
Pelotomaculum	PEL-622F PEL-877R	CYSDBRGMSTRCCTBWGAAACYG GGTGCTTATTGYGTTARCTAC	55	
Syntrophomonas	SMS-637F SMS-757R	TGAAACTGDDDDTCTTGAGGGCAG CAGCGTCAGGGDCAGTCCAGDMA	60	
C. ultunense	Cultf Cultr	CCTTCGGGTGGAATGATAAA TCATGCGATTGCTAAGTTTCA	57	Westerholm et al. (2011a)
S. schinkii	THACf HACr	ATCAACCCCATCTGTGCC CAGAATTCGCAGGATGTC	61	
T. acetatoxydans	Tpf Tpr	AGGTAGTAGAGAGCGGAAAC TGTCGCCCAGACCATAAA	63	
Methanobacteriales	MBT857F MBT1196R	CGWAGGGAAGCTGTTAAGT TACCGTCGTCCACTCCTT	60	Yu et al. (2005)
Methanomicrobiales	MMB282F MMB832R	ATCGRTACGGGTTGTGGG CACCTAACGCRCATHGTTTAC	60	
Methanosarcinaceae	Msc380F Msc828R	GAAACCGYGATAAGGGGA TAGCGARCATCGTTTACG	60	
Methanosaetaceae	Mst702F Mst862R	TAATCCTYGARGGACCACCA CCTACGGCACCRACMAC	60	
Methanoculleus	298F 586R	GGAGCAAGAGCCCGGAGT CCAAGAGACTTAACAACCCA	58	Franke-Whittle et al. (2009)

4.3 Results and Discussion

4.3.1 Influence of OLR on Reactor Function

Reactor sets OLRs 1-4 were functionally stable and highly efficient throughout the operational period (105 d), with no VFAs detected and stable methane production (Fig 4.1). Replicate reactors within each reactor set were highly reproducible. Reactor set OLR 5 was functionally stable for three HRTs (60 d to 105 d) at an OLR of 5 g COD L^{-1}, following which a 10-14% reduction in biogas production was observed between 106 d and 120 d (Fig. 4.2 A). Acetate was detected for the first time on day 114, which corresponded with a drop in methane content and reactor pH (Fig. 4.2 B). A further OLR increase on 121 d from 5 g

COD L^{-1} to 6 g COD L^{-1} triggered acidification, which resulted in process deterioration (Fig. 4.2 A,B). A substantial increase in VFA concentrations (acetate: 0.32 to 19 g L^{-1}; propionate: 0.0 to 2.4 g L^{-1}; butyrate: 0.0 to 3.7 g L^{-1}) was observed during this period (Fig. 4.2 B). VFA accumulation could have occurred either due to kinetic uncoupling between acid producers and consumers and/or via direct inhibition of acid utilizers. Reactor acidification resulted in a pH drop from 7.2 to 5.6 and an 80% reduction in methane production (Figure 4.2 A,B). This result suggests that acetate buildup negatively affected methanogenesis because acetate is considered to be the major precursor (~70%) in methane production (Gujer and Zehnder, 1983). Other VFAs, such as propionate and butyrate, were detected only after acetate concentrations reached ~7 g L^{-1} (day 126). This relates well to previous reports where propionate and butyrate degradation was inhibited at elevated acetate concentrations and high H_2 partial pressure (Ahring and Westermann, 1988; Fukuzaki et al., 1990; Mawson et al., 1991; Labib et al., 1992; Lier et al., 1993; Schmidt and Ahring, 1993; Amani et al., 2011)

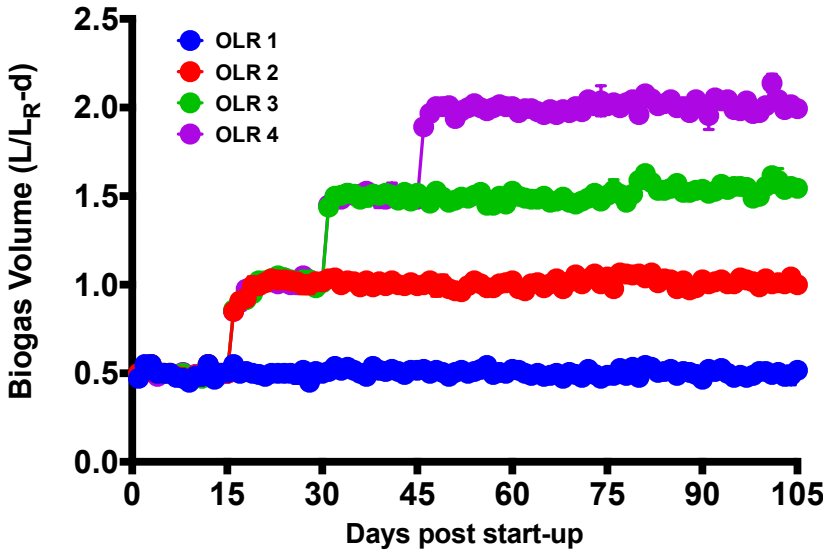

Figure 4.1: Biogas production in reactor sets OLR 1-, 2-, 3-, and 4

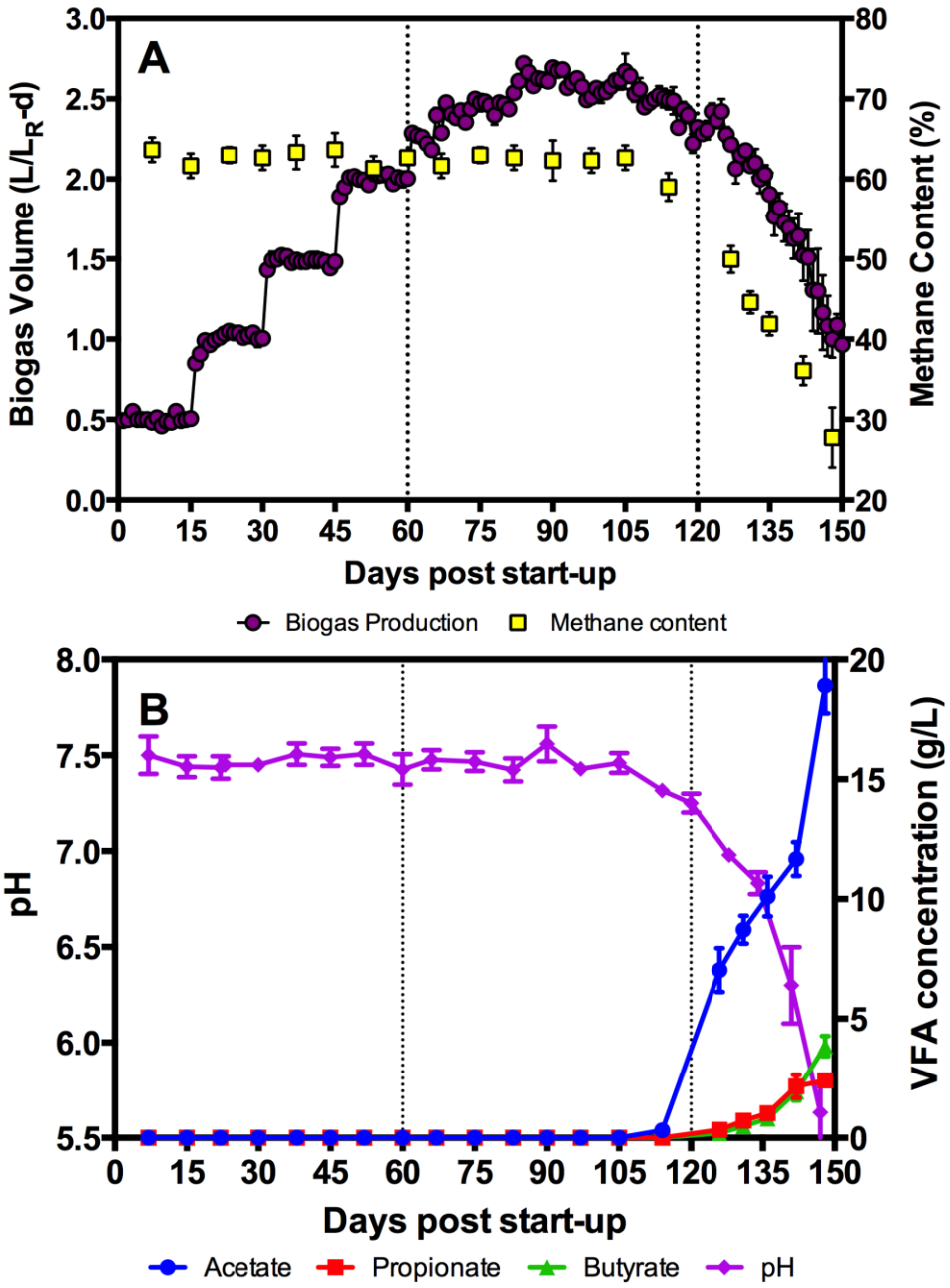

Figure 4.2: Physicochemical data of reactor set OLR 5: (A) biogas production (L $L_R^{-1}d^{-1}$) and methane content (%); (B) pH and volatile fatty acids (acetate, propionate, butyrate) concentrations (g L^{-1}). OLR was increased by 1 g COD L^{-1} day^{-1}every 15 d till day 60, and finally on day 120 (from 5 g to 6 g COD L^{-1} day^{-1}).

4.3.2 Influence of OLR on Microbial Community Structure

Dominant OTUs within each reactor set were placed under *Thermovirga* (24-46%) and *Petrimonas* (6-32%) (Fig. 4.5). Species within *Thermovirga* (phylum: Synergistetes) and *Petrimonas* (phylum: Bacteroides) are known to be involved in amino acid- and carbohydrate fermentation, respectively. Interestingly, type strains for both these genera (*T. lienii* and *P. sulfuriphila*) have been isolated from oil reservoirs (Dahle and Birkeland, 2006; Gabroski et al., 2005). In addition, OTUs within the families Anaerolineaceae (phylum: Chloroflexi) and Clostridiales Incertae Sedis XI (phylum: Firmicutes) were identified as dominant members. Other identified primary fermenters include: *Porphyromonas*, *Lutispora*, *Atopobium*, *Olsenella*, *Trichococcus*, *Aminobacterium*, *Longilinea*, *Bacteroides* and *Sedimentibacter*. The presence of multiple groups that perform the same function (i.e., amino acid and carbohydrate fermentation) indicated a high degree of functional redundancy within these reactors. This finding relates well with Hashsham et al. (2000) who proposed that parallel substrate processing promotes greater functional stability in methanogenic reactors.

Bacteria involved in syntrophic propionate- (*Syntrophobacter*, *Smithella* and Peptococcaceae 2), butyrate- (*Syntrophomonas*), glycolate- (*Syntrophobotulus*), benzoate- (*Syntrophus*), and phenol- (*Syntrophorhabdus*) degradation were detected (Fig. 4.5). Syntrophic microorganisms metabolize substrates in association with hydrogenotrophic methanogens (Schink et al., 1997; McInerney et al., 2008). The acetoclastic methanogen, *Methanosaeta*, dominated the archaeal community structure, while hydrogenotrophic methanogens (e.g., *Methanobacterium*) were underrepresented. This result indicated that acetoclastic methanogenesis represented the primary route of methane production in these reactors during stable reactor performance.

Though primary fermenters constituted >95% classified sequences, their relative

abundance was influenced at higher loading rates (3-5 g COD L^{-1}). While the OTUs within *Petrimonas*, *Porphyromonas*, *Sedimentibacter*, *Bacteroides*, *Atopobium*, *Olsenella*, Ruminococcaceae and *Aminobacterium* increased in abundance, those within *Thermovirga* and Clostridiales Incertae Sedis XI remained stable. Meanwhile, the relative abundance of functional specialists, especially those involved in syntrophic metabolism (*Syntrophobacter, Smithella, Syntrophobotulus, Syntrophus, Syntrophorhabdus*) decreased with increasing OLR (Fig. 4.2), which could be linked to the decline in hydrogenotrophic methanogens or vice versa.

Significant changes were observed in the microbial structure within the reactor set OLR 5 between 105 d (OLR 5-45 d) and 120 d (OLR 5-60 d). The relative abundance of *Aminobacterium*, *Sedimentibacter*, *Bacteroides*, *Psychrobacter*, *Desulfovibrio*, *Shewanella*, *Syntrophomonas*, *Tepidanaerobacter* and *Methanoculleus* increased. Though OTUs within *Aminobacterium*, *Sedimentibacter* and *Bacteroides* were previously detected in significant numbers within these reactors, the emergence of *Psychrobacter*, *Desulfovibrio* and *Shewanella* was intriguing.

Interestingly, the presence of *Psychrobacter* in anaerobic reactors has only been reported once (Li et al., 2013). *Psychrobacter* spp. have been defined as aerobic mesophilic bacteria, though evidence suggests that a few strains (*P. aquimaris*, *P. namhaensis* and *P. celer*) could grow anaerobically (Yoon et al., 2005a; Yoon et al., 2005b). Species within this genus often produce lipases (Yumoto et al., 2003) and hence, could play an important role in fat hydrolysis during anaerobic digestion (Joseph et al., 2008). *Desulfovibrio* spp. and *Shewanella* spp. can utilize a wide variety of organic substrates such as lactate, pyruvate and ethanol (Muyzer and Stams, 2008; Hau and Gralnick, 2007). *Syntrophomonas* spp. can degrade butyrate and higher fatty acids (e.g., palmitate, oleate) in association with hydrogenotrophic methanogens. An increase in its abundance could be indicative increased substrate availability. The relative abundance of *Tepidanaerobacter* and *Methanoculleus* increased

dramatically at this time point. It has been reported that *T. acetatoxydans* is involved in syntrophic acetate oxidation in association with *Methanoculleus* sp. at high ammonia concentrations (Westerholm et al., 2011b).

An increase in loading rate from 5 to 6 g COD L^{-1} on day 121 resulted in process deterioration, which was characterized by VFA (esp. acetate) buildup and pH decline and decreased methane production (Fig. 4.2 A,B). *Thermovirga* (37-42%), Clostridiales Incertae Sedis XI (8-9%), *Atopobium* (31-39%) and *Aminobacterium* (3-6%) dominated the microbial community structure. Moreover, OTUs within the order Clostridiales (Lachnospiraceae and Ruminococcaceae) and *Tepidanaerobacter* increased (~4 fold) in relative abundance, whereas all other OTUs declined (Fig. 4.5)

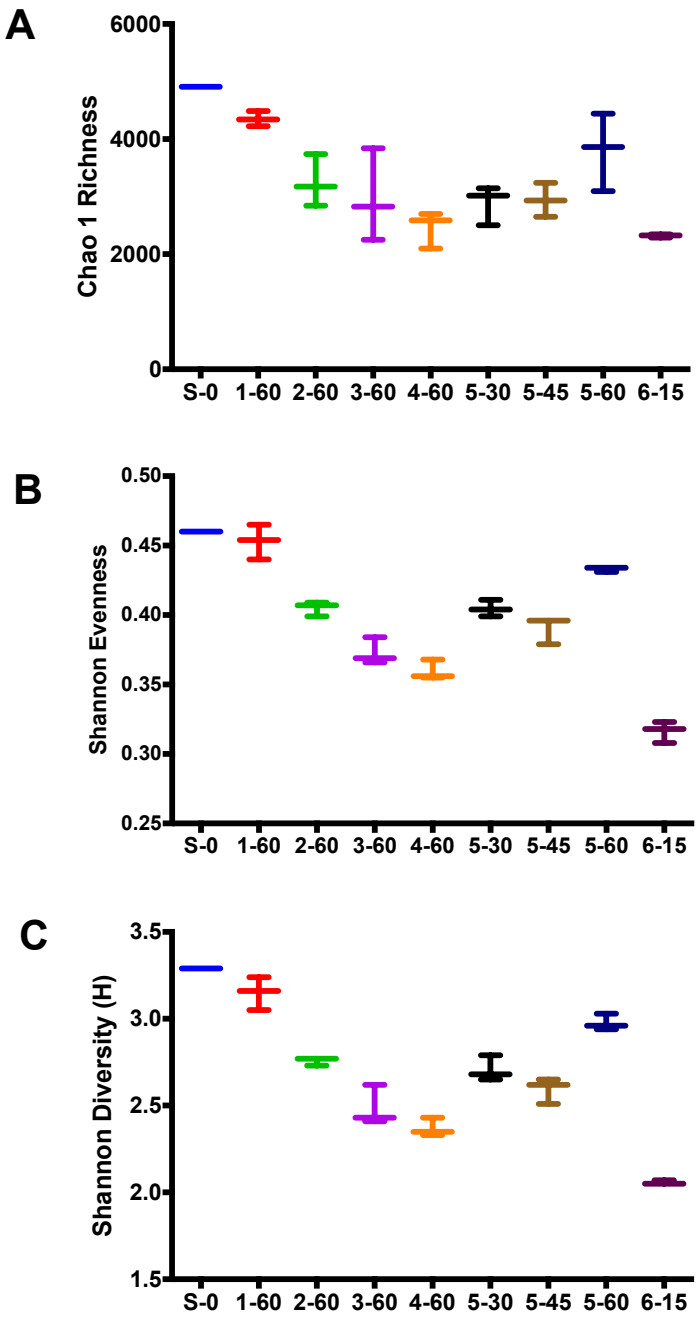

Figure 4.3: Ecological Indices: (A) Chao 1 Richness, (B) Shannon Evenness, and (C) Shannon Diversity

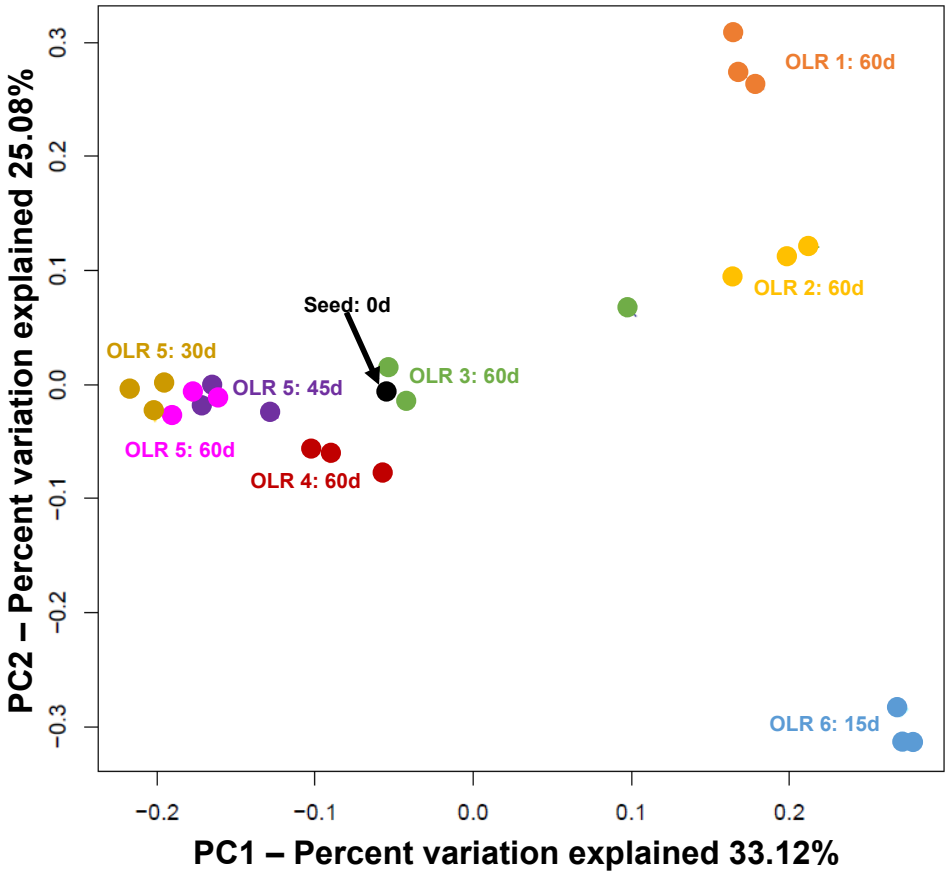

Figure 4.4: Principal coordinates analysis of microbial community based on high-throughput sequencing data

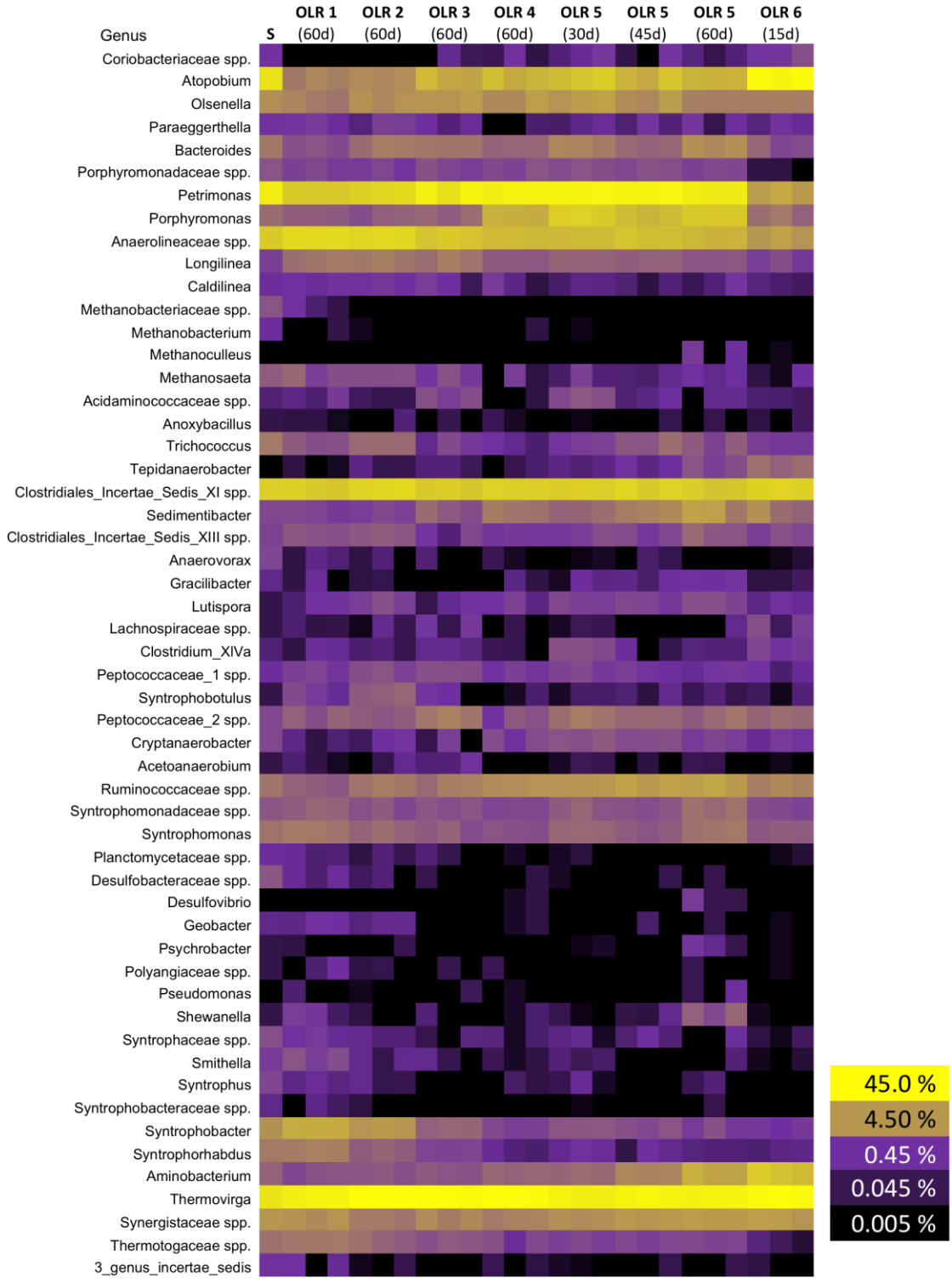

Figure 4.5: Heat map of high-throughput sequencing data showing relative abundance at genus level/unclassified family level

4.3.3 Effect of Increased OLR on Syntrophic Microbial Communities

Within reactor set OLR 5, *Syntrophobacter* decreased in abundance whereas *Pelotomaculum* increased when the OLR was stepped up each HRT (Fig. 4.6). Steady state (60 d) data at different OLRs confirmed this observation as *Syntrophobacter* was the dominant propionate degrader at OLRs 1 and 2, while *Pelotomaculum* became dominant from OLR 3 onward (Fig. 4.7 A-C). High-throughput sequencing analysis also supported this observation (Fig. 4.5). Data suggest that *Syntrophobacter* is not able to maintain numbers at high dilution rates, which agrees with the observation by Shigematsu et al. (2006). *Smithella* was at least two orders of magnitude lower in abundance than the dominant propionate degrader. *Syntrophobacter* numbers did not change during the transition to the deteriorative phase (105-120 d), whereas *Smithella* and *Pelotomaculum* increased 2-3 fold. This finding relates well to those presented in chapter 3 where *Smithella* and *Pelotomaculum* grew faster than *Syntrophobacter* during propionate buildup. Similar results were observed for *Syntrophomonas*, which increased in abundance (2-3 fold) prior to process deterioration (Fig. 4.7). All syntrophic fatty acid degraders (SFAB) drastically declined in abundance after the loading rate was raised to 6 g COD L^{-1}, which was characterized by sudden VFA accumulation (Fig. 4.2). Despite increased substrate availability, it is likely that the onset of unfavorable conditions such as elevated acetate (>7g L^{-1}) levels and low pH inhibited the SFAB growth (Schmidt and Ahring, 1993; Fukuzaki et al., 1990; Lier et al., 1993; Labib et al., 1992; Ahring and Westermann, 1988; Boone and Xun, 1987; Mawson et al., 1991). Acid-tolerant SFAB have not been identified to this date.

Methanosaetaceae was the dominant acetoclastic methanogen group and was 3-4 orders of magnitude higher in abundance than Methanosarcinaceae (Fig. 4.6; Fig. 4.7). The dominance of Methanosaetaceae could be explained as acetate was not detected in reactor

set OLR 5 until day 114. Previous studies have reported that Methanosaetaceae outcompete Methanosarcinaceae at low acetate concentrations (Yu et al., 2006; Conklin et al., 2006). Nevertheless, a gradual reduction in Methanosaetaceae numbers was observed 75 d onward, which was 15 days post OLR increase from 4 g to 5 g COD L^{-1}. A substantial decrease in Methanosaetaceae numbers was observed after further OLR increase (120 d). It is interesting that Methanosarcinaceae numbers did not increase between 121-150 d despite increased acetate concentrations. Koster et al. (1988) reported that methanogenesis was more sensitive than acidogenesis to ammonia inhibition. In particular, methane production via the acetoclastic route is considered more sensitive to elevated ammonia concentrations (Koster and Lettinga, 1984; Sprott and Patel, 1986; Robbins et al., 1989; Bhattacharya and Parkin, 1989; Angelidaki and Ahring, 1993). Though hydrogenotrophic methanogens (Methanobacteriales, Methanomicrobiales) decreased with increased OLR, a drastic increase in Methanomicrobiales numbers (~3 orders of magnitude) was observed between 105-120 d. Further analysis using genus-specific primers (Franke-Whittle et al., 2009) revealed this group to be *Methanoculleus* (data not shown).

The gradual decline in Methanosaetaceae and sudden increase in *Methanoculleus* led to an evaluation of whether a shift in acetate utilization pathways occurred from acetoclastic methanogenesis to syntrophic acetate oxidation. It has been previously suggested that acetate oxidation could be the major route of methanogenesis in the absence of Methanosaetaceae (Karakashev et al., 2006). A remarkable increase (~6 orders of magnitude) in *Tepidanaerobacter acetatoxydans* abundance was observed between 75 d and 150 d, which corresponded well with the increase in *Methanoculleus* (Fig. 4.6 E). High-throughput sequencing also confirmed this finding (Fig. 4.5). *T. acetatoxydans* was first isolated from ammonia-enriched methanogenic systems and was able to oxidize acetate only when co-cultured with

Methanoculleus sp. (Westerholm et al., 2011b). Elevated ammonia levels (>3 g L^{-1} total ammonia nitrogen, TAN) are reported to inhibit acetoclastic more than hydrogenotrophic methanogens (Koster and Lettinga, 1984; Sprott and Patel, 1986; Robbins et al., 1989; Bhattacharya and Parkin, 1989; Angelidaki and Ahring, 1993). Moreover, Schnurer et al. (2008) reported that increased ammonia levels selects for syntrophic acetate oxidation. Theoretical calculation of feedstock showed that ammonia levels reached 3.3 g L^{-1} at 4 g COD L^{-1}, 4.1 g L^{-1} at 5 g COD L^{-1} and 5 g L^{-1} at 6 g COD L^{-1}. Thus, TAN levels generated at OLR 4 g COD L^{-1} and higher is more that those previously reported to be inhibitory. It should be noted that *T. acetatoxydans* was not detected in reactors operated below an OLR of 4 g COD L^{-1}, which further strengthen the conclusion that syntrophic acetate oxidation was triggered at high OLRs due to ammonia buildup. On similar lines, abundance of *Syntrophaceticus schinkii* (Westerholm et al., 2010) increased 4-10 fold when OLR was raised from 4 to 5 g COD L^{-1} and overall, 10-20 times between 60-120 d (Fig. 4.6 E). However, *Clostridium ultunense*, another mesophilic syntrophic acetate oxidizer (Schnurer et al., 1996) was not detected in all samples analyzed. It should be noted that the shift in acetate utilization did not help mitigate acetate levels, which could be attributed to the relatively slow growth rates of syntrophic acetate oxidizers. In addition, Schnurer et al. (1999) proposed that SAO route of acetate utilization is 10-800 times less efficient than acetoclastic methanogenesis.

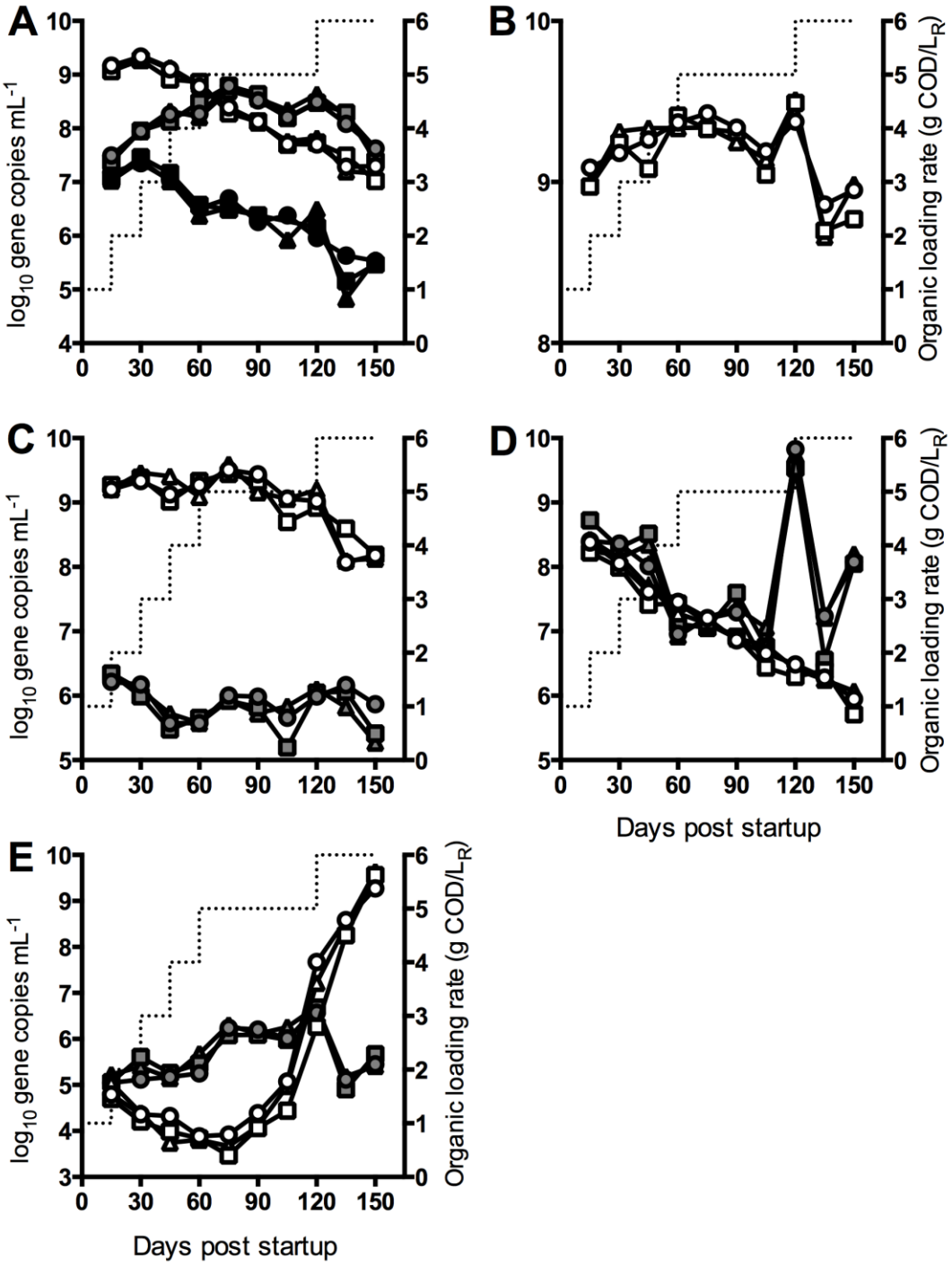

Figure 4.6: Quantification of syntrophic microbial communities in reactor set OLR 5. Legend: (A) grey: *Syntrophobacter*, white : *Pelotomaculum*, black: *Smithella* ; (B) white : *Syntrophomonas*, (C) white : Methanosaetaceae, grey : Methanosarcinaceae ; (D) white : Methanobacteriales, grey : Methanomicrobiales ; (E) white : *Tepidanaerobacter acetatoxydans*, grey : *Syntrophaceticus schinkii*

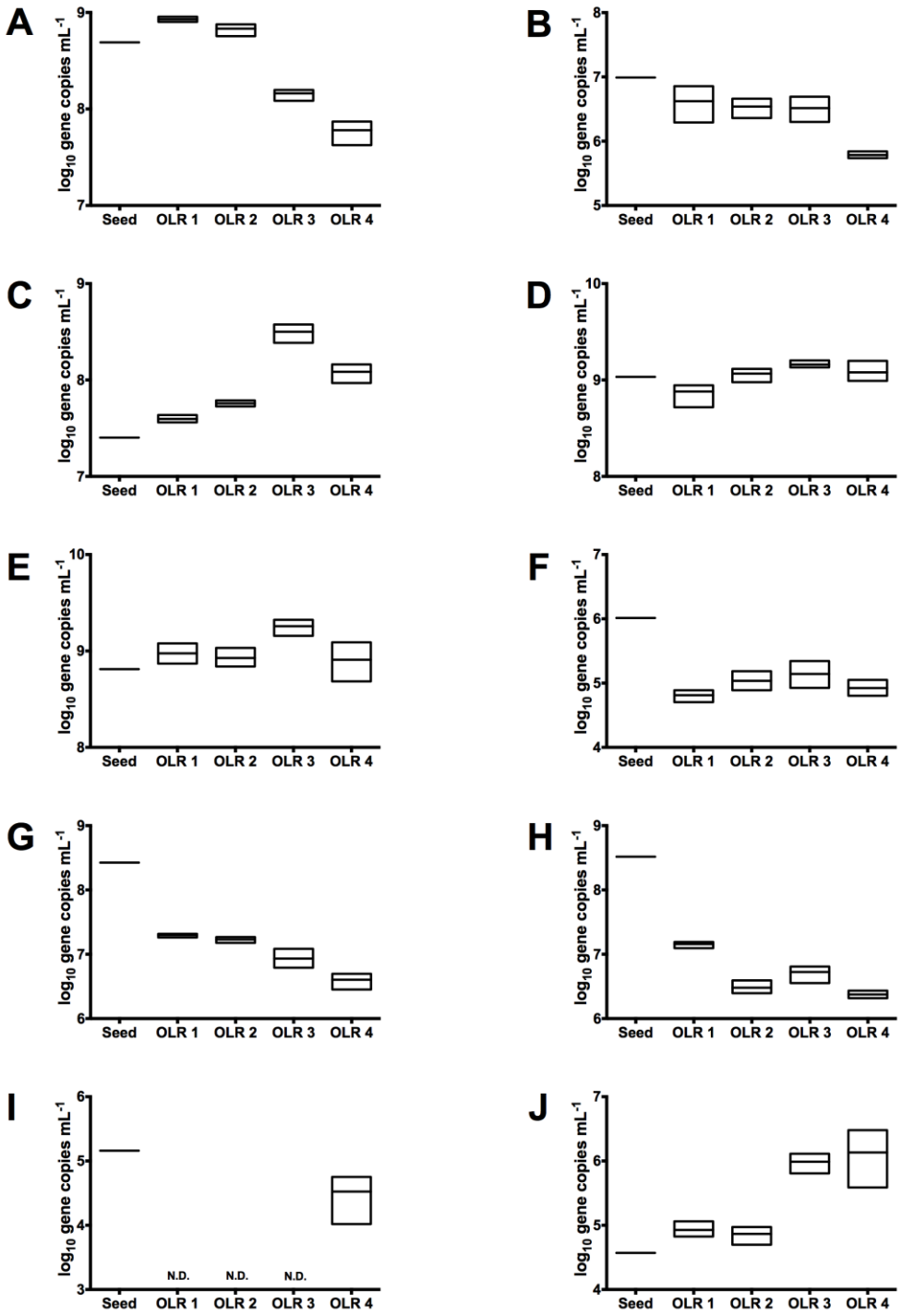

Figure 4.7: Quantification of syntrophic microbial communities at steady state (60 d at desired OLR) in reactor sets OLR 1, OLR 2, OLR 3 and OLR 4. Seed inoculum also depicted. (A) *Syntrophobacter*, (B) *Smithella*, (C) *Pelotomaculum*, (D) *Syntrophomonas*, (E) Methanosaetaceae, (F) Methanosarcinaceae, (G) Methanobacteriales, (H) Methanomicrobiales, (I) *Tepidanaerobacter acetatoxydans*, and (J) *Syntrophaceticus schinkii*.

4.4 Conclusions

In summary, increased organic loading rate resulted in functional and microbial community structural changes in AD. Increases in OLR resulted in reduction in richness, evenness and diversity, though these indices increased prior to system collapse. Acidogens increased in relative abundance with increasing OLR, while syntrophic microbial communities decreased. Microbial community structure shifted during the transition from stable to deteriorative phase. A decline in acetoclastic methanogens was followed by a drastic increase in syntrophic acetate oxidizers and hydrogenotrophic methanogens. In addition, the abundance of VFA degraders increased during the transitionary phase between stable reactor performance and failure. Results from this study indicate that the monitoring syntrophic fatty-acid degrading microbial communities could help improve process stability.

.

CONCLUDING REMARKS

Volatile fatty acids are major intermediates in anaerobic digestion and account for a significant proportion of the total methane produced. However, due to the dynamic nature of waste production, the composition and volume of digester influent may change regularly. Such fluctuations could result in process imbalance and even failure when VFA production exceeds its degradation, leading to reactor acidification. Process stability can be improved by developing a greater understanding of the dynamics of the key microbial players involved in VFA degradation. Despite their indispensible role in VFA degradation, little information exists on the microbial communities involved. A detailed insight on structure-function relationships of SMC is essential to comprehend AD processes. The overall goal of this dissertation was to understand the contribution of SMC to anaerobic digestion function and stability.

To facilitate ecological studies, four quantitative PCR assays based on the 16S rRNA gene were developed targeting genera of propionate- and butyrate-degrading bacteria. These were applied to a variety of natural and engineered methanogenic environments. The highest SFAB abundance was observed in propionate enrichment cultures and anaerobic reactors. In addition, SFAB and methanogen abundance varied with reactor configuration and substrate identity. The importance of developing these assays is that it will enable investigators to monitor these bacteria in both natural and artificial engineered habitats and provide data that will elucidate how they respond to fluctuating resources and conditions. This represents the first report of qPCR assays that are applicable to investigating these bacteria in the laboratory and the field.

The contribution of SMC to AD function and stability was investigated in lab-scale

reactors, using the above designed assays, exposed to two forms of disturbance: shock overload (pulse disturbance) and increased OLR (press disturbance). SMC dynamics were linked to AD function using physicochemical and molecular techniques.

First, the effect of shock overloads on SMC structure and function was examined. Results showed that functional resilience to the pulse disturbance in reactors was linked to the abundance of propionate-degraders and Methanosarcinaceae (acetoclastic methanogens). Reactors with reduced numbers of these microorganisms displayed increased VFA buildup, however, there was a subsequent increase in the abundance of propionate-degraders and Methanosarcinaceae which improved the functional resilience in these reactors to the next perturbation. These results indicate that SMC drive the functional resilience of anaerobic reactors in response to organic overload perturbations.

Second, the effect of increased OLRs on SMC structure and function was examined. SMC steadily decreased in abundance with increasing OLR. Prior to system collapse, a decrease in acetoclastic methanogens was observed which corresponded to an increase in syntrophic acetate oxidizers and hydrogenotrophic methanogens. These results indicate that monitoring SMC could help improve predict process imbalance.

Overall, the results of these two experiments demonstrated that an increased abundance of syntrophic fatty acid degrading microbial communities were essential in AD during stressed conditions, such as organic overload and high OLRs.

Future work should examine the application of these assays in at least two broad aspects of research. Although the assays were demonstrated to be useful in measuring the abundance of these bacteria in the natural environment, this area of research was not pursued further in this dissertation. It is hoped that the primer sets will be valuable to investigators working in habitats with biological methane production in the environment and

help them further understand the processes and microbial interactions involved. Additionally, in engineered habitats, the assays should be employed to determine the effect of different operational conditions (e.g., temperature, retention time) on the dynamics of syntrophic communities, and consequently identify conditions that could either maintain or promote these communities. As demonstrated here, these communities play important roles in digester function when confronted with at least two forms of perturbation. How these microbial communities respond to other forms of disturbance also needs to be investigated. Results from these studies could change how digesters are monitored and aid in the design of better anaerobic treatment processes.

BIBLIOGRAPHY

Ahring BK, Westermann P (1988) Product inhibition of butyrate metabolism by acetate and hydrogen in a thermophilic coculture. *Appl Environ Microbiol* 54:2393-2397.

Amani T, Nosrati M, Mousavi SM, Kermanshahi RK (2011) Study of syntrophic anaerobic digestion of volatile fatty acids using enriched cultures at mesophilic conditions. *Int J Environ Sci Tech* 8:83–96.

American Public Health Association (APHA), American Water Works Association (AWWA), Water Environment Federation (WEF), et al. (1998) Standard Methods for the Examination of Water and Wastewater (twentieth ed)

Angelidaki I, Ahring BK (1993) Thermophilic digestion of livestock waste: the effect of ammonia. *Appl Microbiol Biotechnol* 38:560–564.

Angenent LT, Zheng D, Sung S, Raskin L (2002) Microbial community structure and activity in a compartmentalized, anaerobic bioreactor. *Water Environ Res* 74:450-461.

Ariesyady HD, Ito T, Okabe S (2007a) Functional bacterial and archaeal community structures of major trophic groups in a full-scale anaerobic sludge digester. Water Res 41:1554-1568.

Ariesyady HD, Ito T, Yoshiguchi K, Okabe S (2007b) Phylogenetic and functional diversity of propionate-oxidizing bacteria in an anaerobic digester sludge. *Appl Microbiol Biotechnol* 75:673-683.

Barredo MS, Evison LM (1991) Effect of propionate toxicity on methanogen-enriched sludge, *Methanobrevibacter smithii*, and *Methanospirillum hungatii* at different pH values. *Appl Environ Microbiol* 57:1764–1769.

Bergman EN (1990) Energy contributions of volatile fatty acids from the gastrointestinal tract in various species. *Physiol Rev* 70:567-590.

Bhattacharya SK, Parkin GF (1989) The effect of ammonia on methane fermentation process. *J Water Pollut Control Fed* 61:55–59.

Blume F, Bergmann I, Nettmann E, Schelle H, Rehde G, Mundt K, Klocke M (2010) Methanogenic population dynamics during semi-continuous biogas fermentation and acidification by overloading. *J Appl Microbiol* 109:441-450.

Bocher BT, Cherukuri K, Maki JS, Johnson M, Zitomer DH (2015) Relating methanogen community structure and anaerobic digester function. *Water Res* 70:425-435.

Boone DR (1982) Terminal reactions in the anaerobic digestion of animal waste. *Appl Environ Microbiol* 43:57-64.

Boone DR, Bryant MP (1980) Propionate-degrading bacterium, *Syntrophobacter wolinii sp.* nov. gen. nov., from methanogenic ecosystems. *Appl Environ Microbiol* 40:626-632.

Boone DR, Xun L (1987) Effects of pH, temperature, and nutrients on propionate degradation by a methanogenic enrichment culture. *Appl Environ Microbiol* 53:1589-1592.

Boonyakitsombut S, Kim MI, Ahn YH, Speece RE (2002) Degradation of propionate and its precursors: The role of nutrient supplementation. *KSCE J Civ Eng* 6:379-387.

Borja R, Banks CJ (1995) Response of an anaerobic fluidized-bed reactor treating ice-cream waste-water to organic, hydraulic, temperature and pH shocks. *J Biotechnol* 39:251–259.

Bouvier T, del Giorgio PA (2003) Factors influencing the detection of bacterial cells using fluorescence in situ hybridization (FISH): A quantitative review of published reports. *FEMS Microbiol Ecol* 44:3-15.

Bustin SA, Benes V, Garson JA, Hellemans J, Huggett J, Kubista M, Mueller R, Nolan T, Pfaffl MW, Shipley GL, Vandesompele J, Wittwer CT (2009) The MIQE guidelines: minimum information for publication of quantitative real-time PCR experiments. *Clin Chem* 55:611-622.

Chauhan A, Ogram A (2006) Fatty acid-oxidizing consortia along a nutrient gradient in the Florida Everglades. *Appl Environ Microbiol* 72:2400–2406.

Chauhan A, Ogram A, Reddy KR (2004) Syntrophic-methanogenic associations along a nutrient gradient in the Florida Everglades. *Appl Environ Microbiol* 70:3475-3484.

Chen S, Liu X, Dong X (2005). *Syntrophobacter sulfatireducens sp.* nov., a novel syntrophic, propionate-oxidizing bacterium isolated from UASB reactors. *Int J Syst Evol Microbiol* 55:1319-1324.

Cole JR, Wang Q, Fish JA, Chai B, McGarrell DM, Sun, Y, Brown CT, Porras-Alfaro A, Kuske CR, Tiedje JM (2014) Ribosomal Database Project: data and tools for high throughput rRNA analysis. *Nucleic Acids Res* 42:D633-642.

Conklin A, Stensel HD, Ferguson J (2006) Growth kinetics and competition between *Methanosarcina* and *Methanosaeta* in mesophilic anaerobic digestion. *Water Environ Res* 78:486-496.

Couras CS, Louros VL, Grilo AM , Leitão JH, Capela MI, Arroja LM, Nadais MH (2014) Effects of operational shocks on key microbial populations for biogas production in UASB (Upflow Anaerobic Sludge Blanket) reactors. *Energy* 73:866–874.

Dahle H, Birkeland NK (2006) *Thermovirga lienii* gen. nov., sp. nov., a novel moderately thermophilic, anaerobic, amino-acid-degrading bacterium isolated from a North Sea oil well. *Int J Syst Evol Microbiol* 56:1539-1545.

de Bok FA, Harmsen HJ, Plugge CM, de Vries MC, Akkermans AD, de Vos WM, Stams AJ (2005) The first true obligately syntrophic propionate-oxidizing bacterium, *Pelotomaculum schinkii sp.* nov., co-cultured with *Methanospirillum hungatei*, and emended description of the genus *Pelotomaculum*. *Int J Syst Evol Microbiol* 55:1697-1703.

de Bok FA, Stams AJ, Dijkema C, Boone DR (2001) Pathway of propionate oxidation by a syntrophic culture of *Smithella propionica* and *Methanospirillum hungatei*. *Appl Environ Microbiol* 67:1800-1804.

De Vrieze J, Hennebel T, Boon N, Verstraete W (2012) *Methanosarcina*: the rediscovered methanogen for heavy duty biomethanation. *Bioresour Technol* 112:1-9.

Delbès C, Moletta R, Godon J (2001) Bacterial and archaeal 16S rDNA and 16S rRNA dynamics during an acetate crisis in an anaerobic digestor ecosystem. *FEMS Microbiol Ecol* 35:19-26.

Dhaked RK, Waghmare CK, Alam SI, Kamboj DV, Singh L (2003) Effect of propionate toxicity on methanogenesis of night soil at phychrophilic temperature. *Bioresour Technol* 87:299-303.

Dupla M, Conte T, Bouvier JC, Bernet N, Steyer JP (2004) Dynamic evaluation of a fixed bed anaerobic digestion process in response to organic overloads and toxicant shock loads. *Water Sci Technol* 49:61-68.

Edgar RC, Haas BJ, Clemente JC, Quince C, Knight R (2011) UCHIME improves sensitivity and speed of chimera detection. *Bioinformatics* 27:2194-2200.

Espinosa A, Rosas L, Ilangovan K, Noyola A (1995) Effect of trace metals on the anaerobic degradation of volatile fatty acids in molasses stillage. *Water Sci Technol* 32:121–129.

Fernandez AS, Hashsham SA, Dollhopf SL, Raskin L, Glagoleva O, Dazzo FB, Hickey RF, Criddle CS, Tiedje JM (2000) Flexible community structure correlates with stable community function in methanogenic bioreactor communities perturbed by glucose. *Appl Environ Microbiol* 66:4058-4067.

Fernández N, Díaz EE, Amils R, Sanz JL (2008) Analysis of microbial community during biofilm development in an anaerobic wastewater treatment reactor. *Microb Ecol* 56:121-132.

Franke-Whittle IH, Goberna M, Insam H (2009) Design and testing of real-time PCR primers for the quantification of *Methanoculleus*, *Methanosarcina*, *Methanothermobacter*, and a group of uncultured methanogens. *Can J Microbiol* 55:611-616.

Fukuzaki S, Nishio N, Shobayashi M, Nogai S (1990) Inhibition of the fermentation of propionate to methane by hydrogen, acetate and propionate. *Appl Environ Microbiol* 56:719–723.

Gallert C, Winter J (2008) Propionic acid accumulation and degradation during restart of a full-scale anaerobic biowaste digester. *Bioresour Technol* 99:170-178.

Gan Y, Qiu Q, Liu P, Rui J, Lu Y (2012) Syntrophic oxidation of propionate in rice field soil at 15 and 30°C under methanogenic conditions. *Appl Environ Microbiol* 78:4923–4932.

Glissmann K, Conrad R (2000) Fermentation pattern of methanogenic degradation of rice straw in anoxic paddy soil. *FEMS Microbiol Ecol* 31:117-126.

Gorris LGM, van Deursen JMA, van der Drift C, Vogels GD (1989) Inhibition of propionate degradation by acetate in methanogenic fluidized bed reactors. *Biotechnol Lett* 11:61-66.

Gou C, Yang Z, Huang J, Wang H, Xu H, Wang L (2014) Effects of temperature and organic loading rate on the performance and microbial community of anaerobic co-digestion of waste activated sludge and food waste. *Chemosphere* 105:146-151.

Grabowski A, Tindall BJ, Bardin V, Blanchet D, Jeanthon C (2005) *Petrimonas sulfuriphila* gen. nov., sp. nov., a mesophilic fermentative bacterium isolated from a biodegraded oil reservoir. *Int J Syst Evol Microbiol* 55:1113-1121.

Grimm V, Schmidt E, Wissel C (1992) On the application of stability concepts in ecology. *Ecol Model* 63:143–161.

Gujer W, Zehnder AJB (1983) Conversion processes in anaerobic digestion. *Water Sci Technol* 15:127–167.

Hajarnis SR, Ranade DR (1994) Effect of propionate toxicity on some methanogens at different pH values and in combination with butyrate. Proc. 7th International Symposium on Anaerobic Digestion pp:46–49

Han SK, Kim SH, Shin HS (2005) UASB treatment of wastewater with VFA and alcohol generated during hydrogen fermentation of food waste. *Proc Biochem* 40:2897–2905.

Hansen KH, Ahring BK, Raskin L (1999) Quantification of syntrophic fatty acid-beta-oxidizing bacteria in a mesophilic biogas reactor by oligonucleotide probe hybridization. *Appl Environ Microbiol* 65:4767-4774.

Harmsen HJ, Akkermans AD, Stams AJ, de Vos WM (1996a) Population dynamics of propionate-oxidizing bacteria under methanogenic and sulfidogenic conditions in anaerobic granular sludge. *Appl Environ Microbiol* 62:2163-2168.

Harmsen HJ, Kengen HM, Akkermans AD, Stams AJ, de Vos WM (1996b) Detection and localization of syntrophic propionate-oxidizing bacteria in granular sludge by *in situ* hybridization using 16S rRNA-based oligonucleotide probes. *Appl Environ Microbiol* 62:1656-1663.

Harmsen HJ, Van Kuijk BL, Plugge CM, Akkermans AD, De Vos WM, Stams AJ (1998)

Syntrophobacter fumaroxidans sp. nov., a syntrophic propionate-degrading sulfate-reducing bacterium. *Int J Syst Bacteriol* 48:1383-1387.

Harmsen HJM, Kengen HMP, Akkermans ADL, Stams, AJM (1995) Phylogenetic analysis of two syntrophic propionate-oxidizing bacteria in enrichments cultures. *Syst Appl Microbiol* 18:67-73.

Hashsham SA, Fernandez AS, Dollhopf SL, Dazzo FB, Hickey RF, Tiedje JM, Criddle CS (2000) Parallel processing of substrate correlates with greater functional stability in methanogenic bioreactor communities perturbed by glucose. *Appl Environ Microbiol* 66:4050-4057.

Hatamoto M, Imachi H, Fukayo S, Ohashi A, Harada H (2007a) *Syntrophomonas palmitatica sp.* nov., an anaerobic, syntrophic, long-chain fatty-acid-oxidizing bacterium isolated from methanogenic sludge. *Int J Syst Evol Microbiol* 57:2137-2142.

Hatamoto M, Imachi H, Ohashi A, Harada H (2007b) Identification and cultivation of anaerobic, syntrophic long-chain fatty acid-degrading microbes from mesophilic and thermophilic methanogenic sludges. *Appl Environ Microbiol* 73:1332–1340.

Hatamoto M, Imachi H, Yashiro Y, Ohashi A, Harada H (2008) Detection of active butyrate-degrading microorganisms in methanogenic sludges by RNA-based stable isotope probing. *Appl Environ Microbiol* 74:3610-3614.

Hau HH, Gralnick JA (2007) Ecology and biotechnology of the genus *Shewanella*. *Ann Rev Microbiol* 61:237-258.

Heyes RH, Hall RJ (1983) Kinetics of two subgroups of propionate-using organisms in anaerobic digestion. *Appl Environ Microbiol* 46:710–715.

Hori T, Haruta S, Ueno Y, Ishii M, Igarashi Y (2006) Dynamic transition of a methanogenic population in response to the concentration of volatile fatty acids in a thermophilic anaerobic digester. *Appl Environ Microbiol* 72:1623-1630.

Houwen FP, Plokker J, Stams AJM, Zehnder AJB (1990) Enzymatic evidence for involvement of the methylmalonyl-CoA pathway in propionate oxidation by *Syntrophobacter wolinii*. *Arch Microbiol* 155:52-55.

Imachi H, Sakai S, Ohashi A, Harada H, Hanada S, Kamagata Y, Sekiguchi Y (2007) *Pelotomaculum propionicicum sp.* nov., an anaerobic, mesophilic, obligately syntrophic, propionate-oxidizing bacterium. *Int J Syst Evol Microbiol* 57:1487-1492.

Imachi H, Sekiguchi Y, Kamagata Y, Hanada S, Ohashi A, Harada H (2002) *Pelotomaculum thermopropionicum* gen. nov., sp. nov., an anaerobic, thermophilic, syntrophic propionate-oxidizing bacterium. *Int J Syst Evol Microbiol* 52:1729-1735.

Imachi H, Sekiguchi Y, Kamagata Y, Loy A, Qiu YL, Hugenholtz P, Kimura N, Wagner M, Ohashi A, Harada H (2006) Non-sulfate-reducing, syntrophic bacteria affiliated with

Desulfotomaculum cluster I are widely distributed in methanogenic environments. *Appl Environ Microbiol* 72:2080-2091.

Ito T, Yoshiguchi K, Ariesyady HD, Okabe S (2012) Identification and quantification of key microbial trophic groups of methanogenic glucose degradation in an anaerobic digester sludge. *Bioresour Technol* 123:599-607.

Jackson BE, Bhupathiraju VK, Tanner RS, Woese CR, McInerney MJ (1999) *Syntrophus aciditrophicus* sp. nov., a new anaerobic bacterium that degrades fatty acids and benzoate in syntrophic association with hydrogen-using microorganisms. *Arch Microbiol* 171:107-114.

Jang HM, Kim JH, Ha JH, Park JM (2014) Bacterial and methanogenic archaeal communities during the single-stage anaerobic digestion of high strength food wastewater. *Bioresour Technol* 165:174-182.

Joseph B, Ramteke PW, Thomas G (2008) Cold active microbial lipases: some hot issues and recent developments. *Biotechnol Adv* 26:457-470.

Juottonen H, Galand PE, Tuittila ES, Laine J, Fritze H, Yrjälä, K (2005) Methanogen communities and Bacteria along an ecohydrological gradient in a northern raised bog complex. *Environ Microbiol* 7:1547-1557.

Karakashev D, Batstone DJ, Angelidaki I (2005) Influence of environmental conditions on methanogenic compositions in anaerobic biogas reactors. *Appl Environ Microbiol* 71: 331-338.

Karakashev D, Batstone DJ, Trably E, Angelidaki I (2006) Acetate oxidation is the dominant methanogenic pathway from acetate in the absence of Methanosaetaceae. *Appl Environ Microbiol* 72:5138-5141.

Kaspar HF, Wuhrnann K (1978) Kinetic parameters and relative turnovers of some important catabolic reactions in digesting sludge. *Appl Environ Microbiol* 36:1–7.

Kendall MM, Liu Y, Boone DR (2006) Butyrate- and propionate-degrading syntrophs from permanently cold marine sediments in Skan Bay, Alaska, and description of *Algorimarina butyrica* gen. nov., sp. nov. *FEMS Microbiol Lett* 262:107-114.

Kosaka T, Uchiyama T, Ishii S, Enoki M, Imachi H, Kamagata Y, Ohashi A, Harada H, Ikenaga H, Watanabe K (2006) Reconstruction and regulation of the central catabolic pathway in the thermophilic propionate-oxidizing syntroph *Pelotomaculum thermopropionicum*. *J Bacteriol* 188:202–210.

Koster IW, Lettinga G (1984) The influence of ammonium-nitrogen on the specific activity of pelletized methanogenic sludge. *Agric Wastes* 9:205–216.

Koster IW, Lettinga G. (1988) Anaerobic digestion at extreme ammonia concentrations. *Biol Wastes* 25:51–59.

Kozich JJ, Westcott SL, Baxter NT, Highlander SK, Schloss PD (2013) Development of a dual-index sequencing strategy and curation pipeline for analyzing amplicon sequence data on the MiSeq Illumina sequencing platform. *Appl Environ Microbiol* 79:5112-5120.

Krakat N, Schmidt S, Scherer P (2010) Mesophilic fermentation of renewable biomass: does hydraulic retention time regulate methanogen diversity? *Appl Environ Microbiol* 76: 6322-6326.

Krakat N, Schmidt S, Scherer, P (2011) Potential impact of process parameters upon the bacterial diversity in the mesophilic anaerobic digestion of beet silage. *Bioresour Technol* 102:5692-5701.

Krylova NI, Janssen PH, Conrad R (1997) Turnover of propionate in methanogenic paddy soil. *FEMS Microbiol Ecol* 23:107-117.

Kundu K, Sharma S, Sreekrishnan TR (2013) Changes in microbial communities in a hybrid anaerobic reactor with organic loading rate and temperature. *Bioresour Technol* 129:538-547.

Kus F, Wiesmann U (1995) Degradation kinetics of acetate and propionate by immobilized anaerobic mixed cultures. *Water Res* 29:1437–1443.

Labib F, Ferguson JF, Benjamin MM, Merigh M, Ricker NL (1992) Anaerobic butyrate degradation in a fluidized-bed reactor: effects of increased concentrations of hydrogen and acetate. *Environ Sci Technol* 26:369–376.

Larkin MA, Blackshields G, Brown NP, Chenna R, McGettigan PA, McWilliam H, Valentin F, Wallace IM, Wilm A, Lopez R and other authors (2007) Clustal W and Clustal X version 2.0. *Bioinformatics* 23:2947-2948.

Lawrence AW, McCarty PL (1969) Kinetics of methane fermentation in anaerobic treatment. *Res J Water Pollut Control Fed* 41:R1–R17.

Lee IS, Parameswaran P, Rittmann BE (2011) Effects of solids retention time on methanogenesis in anaerobic digestion of thickened mixed sludge. *Bioresour Technol* 102:10266-10272.

Lerm S, Kleyböcker A, Miethling-Graff R, Alawi M, Kasina M, Liebrich M, Würdemann H (2012) Archaeal community composition affects the function of anaerobic co-digesters in response to organic overload. *Waste Manag* 32:389-399.

Li A, Chu Y, Wang X, Ren L, Yu J, Liu X, Yan J, Zhang L, Wu S, Li S (2013) A pyrosequencing-based metagenomic study of methane-producing microbial community in solid-state biogas reactor. *Biotechnol Biofuels* 6:3.

Li C, Mörtelmaier C, Winter J, Gallert C (2014) Effect of moisture of municipal biowaste on start-up and efficiency of mesophilic and thermophilic dry anaerobic digestion. *Bioresour Technol* 168:23-32.

Li C, Mörtelmaier C, Winter J, Gallert C (2015) Co-digestion of wheat and rye bread suspensions with source-sorted municipal biowaste. *Waste Manag* 40:63-71.

Li J, Ban Q, Zhang L, Kumar AK (2012) Syntrophic propionate degradation in anaerobic digestion: a review. *Int J Agric Biol* 14:843-850.

Li L, He Q, Ma Y, Wang X, Peng X (2015) Dynamics of microbial community in a mesophilic anaerobic digester treating food waste: Relationship between community structure and process stability. *Bioresour Technol* 189:113-120.

Lier JVB, Grolle KC, Frijters CT, Stams AJ, Lettinga G (1993) Effects of acetate, propionate, and butyrate on the thermophilic anaerobic degradation of propionate by methanogenic sludge and defined cultures. *Appl Environ Microbiol* 59:1003-1011.

Liu P, Qiu Q, Lu Y (2011) Syntrophomonadaceae-affiliated species as active butyrate-utilizing syntrophs in paddy field soil. *Appl Environ Microbiol* 77:3884–3887.

Liu RR, Tian Q, Yang B, Chen JH (2010) Hybrid anaerobic baffled reactor for treatment of desizing wastewater. *Int J Environ Sci Tech* 7:111–118.

Liu Y, Balkwill DL, Aldrich HC, Drake GR, Boone DR (1999) Characterization of the anaerobic propionate-degrading syntrophs *Smithella propionica* gen. nov., sp. nov. and *Syntrophobacter wolinii*. *Int J Syst Bacteriol* 49:545-556.

Liu Y, Zhang Y, Quan X, Li Y, Zhao Z, Meng X, Chen S (2012) Optimization of anaerobic acidogenesis by adding Fe0 powder to enhance anaerobic wastewater treatment. *Chem Eng J* 192:179–185.

Lorowitz WH, Zhao H, Bryant MP (1989) *Syntrophomonas wolfei subsp. saponavida subsp.* nov., a long-chain fatty-acid-degrading, anaerobic, syntrophic bacterium; *Syntrophomonas wolfei subsp. wolfei subsp.* nov.; and emended descriptions of the genus and species. *Int J Syst Bacteriol* 39:122-126.

Lovley DR, Klug MJ (1982) Intermediary metabolism of organic matter in the sediments of a eutrophic lake. *Appl Environ Microbiol* 43:552-560.

Lueders T, Pommerenke B, Friedrich MW (2004) Stable-isotope probing of microorganisms thriving at thermodynamic limits: syntrophic propionate oxidation in flooded soil. *Appl Environ Microbiol* 70:5778–5786.

Mackie RI, Wilkins CA (1988) Enumeration of anaerobic bacterial microflora of the equine gastrointestinal tract. *Appl Environ Microbiol* 54:2155-2160.

Marchain U, Krause C (1993) Propionic to acetic acid ratios in overloaded anaerobic digestion. *Biores Technol* 43:195-203.

Mathai PP, Zitomer DH, Maki JS (2015) Quantitative detection of syntrophic fatty acid degrading bacterial communities in methanogenic environments. *Microbiol* 161:1169-1177.

Mawson AJ, Earle RL, Larsen VF (1991) Degradation of acetic and propionic acids in the methane fermentation. *Water Res* 12:1549–1554.

McCarty PL, Brosseau MH (1963) Effect of high concentrations of individual volatile acids on anaerobic treatment. Industrial Waste Conference Proceedings, Purdue University, Lafayette, Indiana 18:283-296.

McCarty PL, Smith DP (1986). Anaerobic wastewater treatment. *Environ Sci Technol* 20:1200–1206.

McInerney MJ, Bryant MP, Hespell RB, Costerton JW (1981a) *Syntrophomonas wolfei* gen. nov. sp. nov., an anaerobic, syntrophic, fatty acid-oxidizing bacterium. *Appl Environ Microbiol* 41:1029-1039.

McInerney MJ, Mackie RI, Bryant MP (1981b) Syntrophic association of a butyrate-degrading bacterium and methanosarcina enriched from bovine rumen fluid. *Appl Environ Microbiol* 41:826-828.

McInerney MJ, Struchtemeyer CG, Sieber J, Mouttaki H, Stams AJ, Schink B, Rohlin L, Gunsalus RP (2008) Physiology, ecology, phylogeny, and genomics of microorganisms capable of syntrophic metabolism. *Ann N Y Acad Sci* 1125:58-72.

McMahon KD, Stroot PG, Mackie RI, Raskin L (2001) Anaerobic codigestion of municipal solid waste and biosolids under various mixing conditions--II: Microbial population dynamics. *Water Res* 35:1817-1827.

McMahon KD, Zheng D, Stams AJ, Mackie RI, Raskin L (2004) Microbial population dynamics during start-up and overload conditions of anaerobic digesters treating municipal solid waste and sewage sludge. *Biotechnol Bioeng* 87:823-834.

Menes RJ, Travers D (2006) Detection of fatty acid beta-oxidizing syntrophic bacteria by fluorescence in situ hybridization. *Water Sci Technol* 54:33-39.

Moertelmaier C, Li C, Winter J, Gallert C (2014) Fatty acid metabolism and population dynamics in a wet biowaste digester during re-start after revision. *Bioresour Technol* 166:479-484.

Morris R, Schauer-Gimenez A, Bhattad U, Kearney C, Struble CA, Zitomer DH, Maki JS (2014) Methyl coenzyme M reductase (mcrA) gene abundance correlates with activity measurements of methanogenic H_2 /CO_2 -enriched anaerobic biomass. *Microb Biotechnol* 7:77-84.

Muyzer G, de Waal EC, Uitterlinden AG (1993) Profiling of complex microbial populations

by denaturing gradient gel electrophoresis analysis of polymerase chain reaction-amplified genes coding for 16S rRNA. *Appl Environ Microbiol* 59:695-700.

Muyzer G, Stams AJM (2008) The ecology and biotechnology of sulphate reducing bacteria. *Nature Rev Microbiol* 6:441-454.

Nagao N, Tajima N, Kawai M, Niwa C, Kurosawa N, Matsuyama T, Yusoff FM, Toda T (2012) Maximum organic loading rate for the single-stage wet anaerobic digestion of food waste. *Bioresour Technol* 118:210-218.

Narihiro T, Nobu MK, Kim NK, Kamagata Y, Liu WT (2015) The nexus of syntrophy-associated microbiota in anaerobic digestion revealed by long-term enrichment and community survey. *Environ Microbiol* 17:1707-1720.

Narihiro T, Terada T, Ohashi A, Kamagata Y, Nakamura K, Sekiguchi Y (2012) Quantitative detection of previously characterized syntrophic bacteria in anaerobic wastewater treatment systems by sequence-specific rRNA cleavage method. *Water Res* 46:2167-2175.

Neubert MG, Caswell H (1997) Alternatives to resilience for measuring the responses of ecological systems to perturbation. *Ecology* 78:653–665.

Nilsen RK, Torsvik T, Lien T (1996) *Desulfotomaculum thermocisternum sp.* nov., a sulfate reducer isolated from a hot north sea oil reservoir. *Int J Syst Bacteriol* 46:397-402.

Pagaling E, Strathdee F, Spears BM, Cates ME, Allen RJ, Free A (2014) Community history affects the predictability of microbial ecosystem development. *ISME J* 8:19-30.

Patel GB, Sprott GD (1990) *Methanosaeta concilii* gen. nov., sp. nov. (*'Methanothrix concilii'*) and *Methanosaeta thermoacetophila* nom. rev., comb. nov. *Int J Syst Bacteriol* 40:79-82.

Peng J, Song Y, Yuan P, Liu R (2015) Re-activation and succession of functional microbial communities during long-term storing sludge granulation. *Environmental Earth Sciences* 73: 5037-5046.

Peng JF, Song YH, Wang YL, Peng Y, Liu R (2013) Spatial succession and metabolic properties of functional microbial communities in an anaerobic baffled reactor. *Int Biodeterior Biodegr* 80: 60–65.

Plugge CM, Balk M, Stams AJ (2002) *Desulfotomaculum thermobenzoicum subsp. thermosyntrophicum subsp.* nov., a thermophilic, syntrophic, propionate-oxidizing, spore-forming bacterium. *Int J Syst Evol Microbiol* 52:391-399.

Power ME, Tilman D, Estes JA, Menge BA, Bond WJ, Mills LS, Daily G, Castilla JC, Lubchenco J, Paine R (1996) Challenges in the quest for keystones. *BioScience 46*:609-620.

Pullammanppallil PC, Chynoweth DP, Lyberatos G, Svoronos SA (2001) Stable

performance of anaerobic digestion in the presence of a high concentration propionic acid. *Bioresour Technol* 78:165–169.

Razaviarani V, Buchanan ID (2014) Reactor performance and microbial community dynamics during anaerobic co-digestion of municipal wastewater sludge with restaurant grease waste at steady state and overloading stages. *Bioresour Technol* 172:232-240.

Regueiro L, Veiga P, Figueroa M, Alonso-Gutierrez J, Stams AJ, Lema JM, Carballa M (2012) Relationship between microbial activity and microbial community structure in six full-scale anaerobic digesters. *Microbiol Res* 167:581-589.

Robbins JE, Gerhard SA, Kappel TJ (1989) Effects of ammonia in anaerobic digestion and an example of digestor performance from cattle manure protein mixtures. *Biol Wastes* 27:1–14.

Roy F, Samain E, Dubourguier HC, Albagnac G (1986) *Synthrophomonas sapovorans sp.* nov., a new obligately proton reducing anaerobe oxidizing saturated and unsaturated long chain fatty acids *Arch Microbiol* 145:142-147.

Russell JB, Hespell RB (1981) Microbial rumen fermentation. *J Dairy Sci* 64:1153-1169.

Schauer-Gimenez AE, Zitomer DH, Maki JS, Struble CA (2010) Bioaugmentation for improved recovery of anaerobic digesters after toxicant exposure. *Water Res* 44:3555-3564.

Scheid D, Stubner S (2001) Structure and diversity of Gram-negative sulfate-reducing bacteria on rice roots. *FEMS Microbiol Ecol* 36:175-183.

Schink B (1997) Energetics of syntrophic cooperation in methanogenic degradation. *Microbiol Mol Biol Rev* 61:262-280.

Schink B, Stams AJM (2002) Syntrophism among Prokaryotes. *The Prokaryotes* 2:309-335.

Schink B, Thauer RK (1988) Energetics of syntrophic methane formation and the influence of aggregation, p. 5-17. In G. Lettinga, A. J. B. Zehnder, J. T. C. Grotenhuis, and L. W. Hulshoff-Pol (ed.), Granular anaerobic sludge, microbiology and technology. Pudoc, Wageningen, The Netherlands.

Schloss PD, Westcott SL, Ryabin T, Hall JR, Hartmann M, Hollister EB, Lesniewski RA, Oakley BB, Parks DH, Robinson CJ, Sahl JW, Stres B, Thallinger GG, Van Horn DJ, Weber CF (2009) Introducing mothur: open-source, platform-independent, community-supported software for describing and comparing microbial communities. *Appl Environ Microbiol* 75:7537-7541.

Schmidt JE, Ahring BK (1993) Effects of hydrogen and formate on the degradation of propionate and butyrate in thermophilic granules from an upflow anaerobic sludge blanket reactor. *Appl Environ Microbiol* 59:2546-2551.

Schnürer A, Nordberg A (2008) Ammonia, a selective agent for methane production by syntrophic acetate oxidation at mesophilic temperature. *Water Sci Technol* 57:735-740.

Schnurer A, Schink B, Svensson BH (1996) *Clostridium ultunense sp*. nov., a mesophilic bacterium oxidizing acetate in syntrophic association with a hydrogenotrophic methanogenic bacterium. *Int J Syst Bacteriol* 46:1145-1152.

Schnürer A, Zellner G, Svensson BH (1999) Mesophilic syntrophic acetate oxidation during methane formation in biogas reactors. *FEMS Microbiol Ecol* 29:249-261.

Scholten JC, Stams AJ (1995) The effect of sulfate and nitrate on methane formation in a freshwater sediment. *Antonie Van Leeuwenhoek* 68:309-315.

Sekiguchi Y, Kamagata Y, Nakamura K, Ohashi A, Harada H (2000) *Syntrophothermus lipocalidus* gen. nov., sp. nov., a novel thermophilic, syntrophic, fatty-acid-oxidizing anaerobe which utilizes isobutyrate. *Int J Syst Evol Microbiol* 50:771-779.

Shah BA, Shah AV, Singh RR (2009) Sorption isotherms and kinetics of chromium uptake from wastewater using natural sorbent material. *Int J Environ Sci Technol* 6:77–90.

Shigematsu T, Era S, Mizuno Y, Ninomiya K, Kamegawa Y, Morimura S, Kida K (2006) Microbial community of a mesophilic propionate-degrading methanogenic consortium in chemostat cultivation analyzed based on 16S rRNA and acetate kinase genes. *Appl Microbiol Biotechnol* 72:401-415.

Sieber JR, McInerney MJ, Plugge CM, Schink B, Gunsalus RP (2010) Methanogenesis: Syntrophic Metabolism Handbook of Hydrocarbon and Lipid Microbiology pp 337-355

Siegert I, Banks C (2005) The effect of volatile fatty acid additions on the anaerobic digestion of cellulose and glucose in batch reactors. *Process Biochemistry* 40:3412–3418.

Smith CJ, Nedwell DB, Dong LF, Osborn AM (2006) Evaluation of quantitative polymerase chain reaction-based approaches for determining gene copy and gene transcript numbers in environmental samples. *Environ Microbiol* 8:804-815.

Smith CJ, Osborn AM (2009) Advantages and limitations of quantitative PCR (Q-PCR)-based approaches in microbial ecology. *FEMS Microbiol Ecol* 67:6-20.

Smith DP, McCarty PL (1990) Factors governing methane fluctuations following shock loading of digesters. *Res J Water Pollut Control Fed* 62:58-64.

Sorensen AH, Ahring BK (1993) Measurements of the specific methanogenic activity of anaerobic digestor biomass. *Appl Microbiol Biotechnol* 40: 427–443.

Sousa DZ, Pereira MA, Stams AJ, Alves MM, Smidt H (2007b) Microbial communities involved in anaerobic degradation of unsaturated or saturated long-chain fatty acids.

Appl Environ Microbiol 73:1054-1064.

Sousa DZ, Smidt H, Alves MM, Stams AJ (2007a) *Syntrophomonas zehnderi sp.* nov., an anaerobe that degrades long-chain fatty acids in co-culture with *Methanobacterium formicicum*. *Int J Syst Evol Microbiol* 57:609-615.

Sousa DZ, Smidt H, Alves MM, Stams AJ (2009) Ecophysiology of syntrophic communities that degrade saturated and unsaturated long-chain fatty acids. *FEMS Microbiol Ecol* 68:257-272.

Speece R (2008) Anaerobic Biotechnology and Odor/Corrosion Control for Municipalities and Industries. Archae Press. Nashville, TN.

Sprott GD, Patel GB (1986) Ammonia toxicity in pure cultures of methanogenic bacteria. *Syst Appl Microbiol* 7:358–363.

Stams AJ, Sousa DZ, Kleerebezem R, Plugge CM (2012a) Role of syntrophic microbial communities in high-rate methanogenic bioreactors. *Water Sci Technol* 66:352-362.

Stams AJM, Plugge CM (2009) Electron transfer in syntrophic communities of anaerobic bacteria and archaea. *Nat Rev Microbiol* 7:568–577.

Stams AJM, Worm P, Sousa DZ, Alves MM, Plugge CM (2012b) Syntrophic Degradation of Fatty Acids by Methanogenic Communities. Microbial Technologies in Advanced Biofuels Production pp 127-142.

Steinberg LM, Regan JM (2011) Response of lab-scale methanogenic reactors inoculated from different sources to organic loading rate shocks. *Bioresour Technol* 102:8790-8798.

Stieb M, Schink B (1985) Anaerobic oxidation of fatty acids by *Clostridium bryantii sp.* nov., a spore forming, obligately syntrophic bacterium. *Arch Microbiol* 140:387-390.

Sundberg C, Al-Soud WA, Larsson M, Alm E, Yekta SS, Svensson BH, Sørensen SJ, Karlsson A (2013) 454 pyrosequencing analyses of bacterial and archaeal richness in 21 full-scale biogas digesters. *FEMS Microbiol Ecol* 85:612-626.

Svetlitshnyi V, Rainey F, Wiegel J (1996) *Thermosyntropha lipolytica* gen. nov., sp. nov., a lipolytic, anaerobic, alkalitolerant, thermophilic bacterium utilizing short- and long-chain fatty acids in syntrophic coculture with a methanogenic archaeum. *Int J Syst Bacteriol* 46:1131-1137.

Tale VP, Maki JS, Struble CA, Zitomer DH (2011) Methanogen community structure-activity relationship and bioaugmentation of overloaded anaerobic digesters. *Water Res* 45:5249-5256.

Tang YQ, Shigematsu T, Morimura S, Kida K (2007) Effect of dilution rate on the microbial structure of a mesophilic butyrate-degrading methanogenic community during continuous cultivation. *Appl Microbiol Biotechnol* 75:451-465.

Thauer RK, Jungermann K, Decker K (1977) Energy conservation in chemotrophic anaerobic bacteria. *Bacteriol Rev* 41:100-180.

Wallrabenstein C, Hauschild E, Schink B (1995) *Syntrophobacter pfennigii* sp. nov., new syntrophically propionate-oxidizing anaerobe growing in pure culture with propionate and sulfate. *Arch Microbiol* 164:346-352.

Wang Q, Garrity GM, Tiedje JM, Cole JR (2007) Naive Bayesian classifier for rapid assignment of rRNA sequences into the new bacterial taxonomy. *Appl Environ Microbiol* 73:5261-5267.

Wang Q, Kuninobu M, Ogawa H, Katoa Y (1999) Degradation of volatile fatty acids in highly efficient anaerobic digestion. *Biomass Bioenerg* 16:407–416.

Wang Y, Zhang Y, Wang J, Meng L (2009) Effects of volatile fatty acid concentrations on methane yield and methanogenic bacteria. *Biomass Bioenergy* 33:848-853.

Westerholm M, Dolfing J, Sherry A, Gray ND, Head IM, Schnürer A (2011a) Quantification of syntrophic acetate-oxidizing microbial communities in biogas processes. *Environ Microbiol Rep* 3:500-505.

Westerholm M, Roos S, Schnürer A (2010) *Syntrophaceticus schinkii* gen. nov., sp. nov., an anaerobic, syntrophic acetate-oxidizing bacterium isolated from a mesophilic anaerobic filter. *FEMS Microbiol Lett* 309:100-104.

Westerholm M, Roos S, Schnürer A (2011b) *Tepidanaerobacter acetatoxydans sp.* nov., an anaerobic, syntrophic acetate-oxidizing bacterium isolated from two ammonium-enriched mesophilic methanogenic processes. *Syst Appl Microbiol* 34:260-266.

Wofford NQ, Beaty PS, McInerney MJ (1986) Preparation of cell-free extracts and the enzymes involved in fatty acid metabolism in *Syntrophomonas wolfei. J Bacteriol* 167:179-185.

Wu C, Dong X, Liu X (2007) *Syntrophomonas wolfei subsp. methylbutyratica subsp.* nov., and assignment of *Syntrophomonas wolfei subsp. saponavida* to *Syntrophomonas saponavida sp.* nov. comb. nov. *Syst Appl Microbiol* 30:376-380.

Wu C, Liu X, Dong X (2006) *Syntrophomonas cellicola sp.* nov., a spore-forming syntrophic bacterium isolated from a distilled-spirit-fermenting cellar, and assignment of *Syntrophospora bryantii* to *Syntrophomonas bryantii comb.* nov. *Int J Syst Evol Microbiol* 56:2331-2335.

Wu WM, Jain MK, Hickey RF, Zeikus JG (1996) Perturbation of syntrophic isobutyrate and butyrate degradation with formate and hydrogen. *Biotechnol Bioeng* 52:404-411.

Xing J, Criddle C, Hickey R (1997a) Effects of a long-term periodic substrate perturbation on an anaerobic community. *Water Res* 31:2195–2204.

Xing J, Criddle C, Hickey R (1997b) Long-term adaptive shifts in anaerobic community structure in response to a sustained cyclic substrate perturbation. *Microb Ecol* 33:50-58.

Yoon JH, Lee CH, Kang SJ, Oh TK (2005b) *Psychrobacter celer* sp. nov., isolated from sea water of the South Sea in Korea. *Int J Syst Evol Microbiol* 55:1885-1890.

Yoon JH, Lee CH, Yeo SH, Oh TK (2005a) *Psychrobacter aquimaris* sp. nov. and *Psychrobacter namhaensis* sp. nov., isolated from sea water of the South Sea in Korea. *Int J Syst Evol Microbiol* 55:1007-1013.

Yu Y, Kim J, Hwang S (2006) Use of real-time PCR for group-specific quantification of aceticlastic methanogens in anaerobic processes: population dynamics and community structures. *Biotechnol Bioeng* 93:424-433.

Yu Y, Lee C, Kim J, Hwang S (2005) Group-specific primer and probe sets to detect methanogenic communities using quantitative real-time polymerase chain reaction. *Biotechnol Bioeng* 89:670-679.

Yumoto I, Hirota K, Sogabe Y, Nodasaka Y, Yokota Y, Hoshino T. (2003). *Psychrobacter okhotskensis sp.* nov., a lipase-producing facultative psychrophile isolated from the coast of the Okhotsk Sea. *Int J Syst Evol Microbiol* 53:1985-1989.

Zahedi S, Sales D, Romero LI, Solera R (2013a) Optimisation of single-phase dry-thermophilic anaerobic digestion under high organic loading rates of industrial municipal solid waste: population dynamics. *Bioresour Technol* 146:109-117.

Zahedi S, Sales D, Romero LI, Solera R (2013b) Optimisation of the two-phase dry-thermophilic anaerobic digestion process of sulphate-containing municipal solid waste: population dynamics. *Bioresour Technol* 148:443-452.

Zahedi S, Sales D, Romero LI, Solera R (2014) Dark fermentation from real solid waste. Evolution of microbial community. *Bioresour Technol* 151:221-226.

Zhang C, Liu X, Dong X (2004) *Syntrophomonas curvata sp.* nov., an anaerobe that degrades fatty acids in co-culture with methanogens. *Int J Syst Evol Microbiol* 54:969-973.

Zhang C, Liu X, Dong X (2005) *Syntrophomonas erecta sp.* nov., a novel anaerobe that syntrophically degrades short-chain fatty acids. *Int J Syst Evol Microbiol* 55:799-803.

Zhang F, Liu X, Dong X (2012) *Thermosyntropha tengcongensis sp.* nov., a thermophilic bacterium that degrades long-chain fatty acids syntrophically. *Int J Syst Evol Microbiol* 62:759-763.